Politecnico di Torino

Politecnico di Torino

Master's Degree in Biomedical Engineering

Interactive video-guided patient positioning system for the flat panel Walk-Through PET

Candidate: Marta Savioli

Supervisors:
Prof. Filippo Molinari
Prof. Massimo Salvi
Prof. dr. Stefaan Vandenberghe
Prof. dr. Christian Vanhove
Dr. ir. Jens Maebe
Ir. Rabia Aziz

Academic Year 2025/2026

A project in collaboration with Ghent University

Acknowledgment

I’m truly happy to dedicate this section to all the people who have supported me throughout this thesis project. First and foremost, my heartfelt thanks go to Prof. Stefaan Vandenberghe and to my supervisors, Rabia and Jens, for welcoming me into the team from the very beginning and making me feel like a true part of it. Thank you for your continuous guidance throughout this journey and for always being available, especially during the final stages of writing and revising my thesis. Rabia, I am especially grateful to you for your support during the long hours of experimental work in the lab with participants, and above all, for the genuine human connection we developed.

A special thank you also goes to all the people who have been part of my life for years, as well as to those who entered it just ten months ago. Martina and Anna, thank you for every moment we have shared over these months, for allowing me to be completely myself, and for making me feel at home even miles away. Matteo, I thanked you in my first thesis, and I want to do so again. Sharing the university journey with you has been one of the most meaningful and beautiful parts of this experience. You have always encouraged me to give my best. Despite the distance, you’ve never stopped being there for me and I will always be grateful to you.

Finally, I would like to express my sincere gratitude to my family. Reaching this milestone has also been possible thanks to your constant support. Thank you for always believing in me and being present throughout this journey, even if only through a video call. I am grateful to you for be present for such an important moment in my life.

Thank you all.

Marta Savioli, March 2026

Permission for Use of Content

Marta Savioli, Torino, March 2026

Contact: martii.savioli@gmail.com

Disclaimer

This master's dissertation is part of an exam. Any comments formulated by the assessment committee during the oral presentation of the master's dissertation are not included in this text.

Declaration on the Use of AI Tools

During the writing of this master's thesis, generative AI tools were employed to improve the linguistic quality of the text and to ensure a style more consistent with the required academic tone. These tools were also utilized for paraphrasing and translating certain concepts, exclusively in specific sections where the concepts were initially easier to express in my native language. Specifically, ChatGPT by OpenAI was employed to generate stylistic suggestions and improve consistency in academic language; DeepL Translator was utilised for translation; and DeepL Write was employed to refine and rephrase certain sentences. These tools were not used to generate technical and scientific content, nor to replace the critical thinking necessary to develop the thesis argument and conduct the analysis. All technical and scientific content in this thesis has been developed autonomously, based on reliable academic sources such as scientific articles and reference texts, listed in the References section. Moreover, the description of the audiovisual tools created and the motion study conducted, which formed the thesis project, the analysis of the results, their discussion and the final conclusion are my own original work.

Abstract

The MEDISIP research group at Ghent University has introduced an innovative flat panel, patient-centered PET system that redefines scanner geometry and clinical workflow. The design offers notable benefits, including improved spatial resolution and sensitivity, shorter acquisition times (30 seconds), and increased patient throughput. Despite these advances, two limitations persist: the continued need for medical personnel assistance during patient positioning and the increased upper body motion during upright scanning, even with ergonomic supports already integrated in the mock-up design. To address these aspects, this thesis proposes two interactive audiovisual tools: an animated 3D video guide to facilitate patient self-positioning (prototype stage), and a 30-second timer video aimed at improving postural stability and attentional focus during scanning. The video guide was developed using *Blender*, an open-source platform for 3D modeling and animation, while the timer video was produced using video editing software including *Wave.video* and *FlexClip*. The effectiveness of the 30-second timer video was subsequently evaluated through a motion study involving 31 healthy adult volunteers, implemented across two experimental conditions (Study Design 1 and Study Design 2). Findings indicate that the timer video with audio track integrated, particularly when presented first, significantly reduced head and shoulder motion, outperforming even breath-hold techniques reported in a comparable study [1]. Reductions included a 47% decrease in head movement and 36% and 32% reductions in right and left shoulder displacement, respectively. While residual respiratory-induced motion was observed at the chest and abdomen, it remained below the system's 2 mm spatial resolution threshold, suggesting minimal impact on image quality. These results support the integration of the 30-second timer video in terms of audiovisual guidance as a non-invasive, effective strategy to enhance scan quality and workflow efficiency in upright PET imaging.

Keywords: Walk-Through PET, Audiovisual Instructional Tools, Upper Body Motion, Postural Stabilization Strategies, Kinematic Metrics.

Interactive video-guided patient positioning system for the flat panel Walk-Through PET

Marta Savioli, Rabia Aziz, Jens Maebe, Stefaan Vandenberghe, Christian Vanhove

Abstract - **The MEDISIP research group at Ghent University has introduced an innovative flat panel, patient-centered PET system that redefines scanner geometry and clinical workflow. The design offers notable benefits, including improved spatial resolution and sensitivity, shorter acquisition times (~30 seconds), and increased patient throughput. Despite these advances, two limitations persist: the continued need for medical personnel assistance during patient positioning and the increased upper body motion during upright scanning, even with ergonomic supports already integrated in the mock-up design. To address these aspects, this thesis proposes two interactive audiovisual tools: an animated 3D video guide to facilitate patient self-positioning (prototype stage), and a 30-second timer video aimed at improving postural stability and attentional focus during scanning. The video guide was developed using *Blender*, an open-source platform for 3D modeling and animation, while the timer video was produced using video editing software including *Wave.video* and *FlexClip*. The effectiveness of the 30-second timer video was subsequently evaluated through a motion study involving 31 healthy adult volunteers, implemented across two experimental conditions (Study Design 1 and Study Design 2). Findings indicate that the timer video with audio track integrated, particularly when presented first, significantly reduced head and shoulder motion, outperforming even breath-hold techniques reported in a comparable study [7]. Reductions included a 47% decrease in head movement and 36% and 32% reductions in right and left shoulder displacement, respectively. While residual respiratory-induced motion was observed at the chest and abdomen, it remained below the system's 2 mm spatial resolution threshold, suggesting minimal impact on image quality. These results support the integration of the 30-second timer video in terms of audiovisual guidance as a non-invasive, effective strategy to enhance scan quality and workflow efficiency in upright PET imaging.**

Keywords - **Walk-Through PET, Audiovisual Instructional Tools, Upper Body Motion, Postural Stabilization Strategies, Kinematic Metrics.**

I. Introduction

Positron emission tomography (PET) is one of the most advanced imaging modalities in nuclear medicine, as it provides real-time visualization of metabolic processes within the body at high spatial resolution. By administering specific radiotracers tailored to the biological function under investigation, PET enables the detection, visualization, and quantification of tracer distribution within the body. This property makes PET an essential tool for diagnosis and clinical evaluation of disease. Its main applications extend to a wide range of medical fields, including neurology, cardiology, and oncology, where it plays a central role in early diagnosis, treatment planning, patient monitoring and clinical research. Over the past three decades, PET technology has undergone significant advancements, primarily driven by innovations in detector instrumentation aimed at addressing conventional scanners' limitations, such as low sensitivity, limited spatial resolution, and long acquisition times. Among the most impactful innovations is *Time-of-Flight* (TOF) technology, which enables more accurate localization of the annihilation event along the *Line Of Response* (LOR) by precisely measuring the arrival time of coincident photons at the detector ring [1]. Current TOF resolution ranges between 200 and 300 ps, largely due to the introduction of silicon photomultiplier tubes (SiPMs), which have also contributed to improvements in spatial resolution [2]. These developments, combined with increased system sensitivity achieved through extended *axial field-of-view* (AFOV), ranging from 64 to 194 cm in current PET scanners, have led to substantial enhancements in *signal-to-noise ratio* (SNR) and significant reductions in image noise, resulting in higher image quality and diagnostic accuracy [3].

Conventional PET scanners use pixelated detectors arranged in a cylindrical geometry, where the patient lies down on a bed that moves through the gantry during the scan. While LAFOV systems offer high performance, the large number of detectors required to cover the patient volume for a single scan acquisition results in high development and maintenance costs, often unaffordable for many hospitals and research centers. Moreover, patient positioning remains time-consuming, limiting patient throughput and resulting in higher workload on medical personnel needed to support and assist the patients during the clinical procedure.

To address these limitations, the MEDISIP research group at Ghent University has introduced a novel, patient-centered PET design that redefines scanner geometry and workflow [4]. In the *Walk-Through PET* (WT-PET) scanner, patients are scanned in an upright position between two flat detector panels that are placed 50 cm apart and cover 106 cm axially, as illustrated in Figure 1. This facilitates enhanced patient throughput, reducing personnel demands. By replacing conventional pixelated crystals with monolithic detectors equipped with depth-of-interaction (DOI) capabilities, parallax error is significantly reduced, allowing detector panels to be positioned closer to the patient. This configuration enhances system sensitivity and allows for reductions in both radiotracer dose and acquisition time. Moreover, it enables the same AFOV to be achieved with fewer detectors, contributing to a notable cost reduction. The system's compact footprint (measuring 2.3 meters high, 2 meters wide, and 1.5 meters deep) facilitates more efficient hospital setup. As a result, the estimated selling price is approximately half that of current systems with comparable AFOV, offering a highly cost-effective solution for medical centers [5].

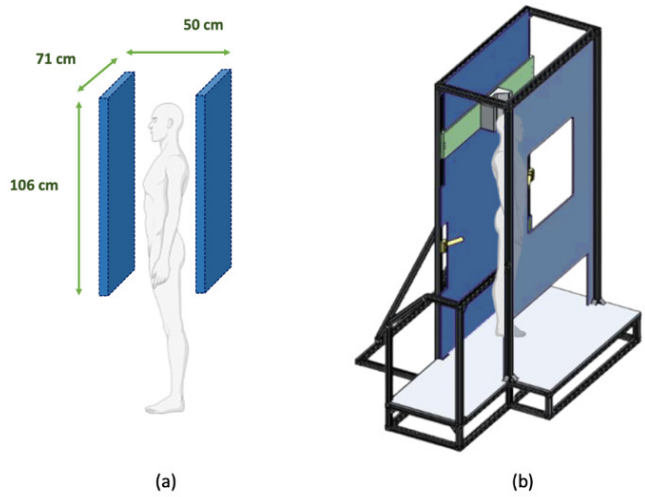

Figure 1: (a) the Walk-Through PET concept with panel dimensions, (b) current design of the Walk-Through PET mock-up, including ergonomic components such as headrest and handlebars to provide enhanced patient support.

Although the novel design concept offers promising advantages, several aspects still require further investigation. Medical personnel is still involved in patient assistance during the positioning phase within the scanner. Furthermore, recent studies have shown increased upper body motion due to the reduced stability in maintaining an upright position for the entire scan duration (estimated at approximately 30 seconds), despite the inclusion of ergonomic supports, such as a headrest and handlebars in the current mock-up design, as shown in Figure 1b. These supports were specifically introduced to improve postural stability. This thesis aims to investigate and address these two primary aspects targeted by the novel Walk-Through PET scanner by developing two interactive videos. The first is an animated 3D video guide designed to serve as a concise yet effective audiovisual product capable of clearly guiding patients through the four key steps of the positioning procedure, making the overall process more autonomous and less dependent on medical personnel. The second tool is a 30-second timer video, designed to maintain the patient's visual attention and improve postural stability during scanning procedure, thereby reducing upper body motion and enhancing image quality. To evaluate its effectiveness, a motion study was conducted involving thirty-one healthy volunteers.

A. Animated 3D video guide

The development process of this instructional video began with the identification of the four key steps identified as most essential for patient preparation and positioning. These include proper initial positioning on the platform by following the marked footprints, adjustment of the headrest, correct grip of the handlebars (steps requiring assistance from the medical technician), and finally, the start of the scan. In line with this framework, a first script was drafted to define the tone, language, and pacing of the narration, aiming to communicate the message in clear, direct, and effective manner. British English was selected for this first version due to its wide international comprehensibility. The script was subsequently converted into a storyboard using the *Microsoft OneNote* platform, thereby facilitating the planning of visual content and camera angles. The core of the 3D animated production was carried out in *Blender*, an open-source platform that supports the entire 3D design pipeline, from modelling to post-production. Starting with the WT-PET scanner, the design was progressively refined to accurately replicate the envisioned model, including the trapezoidal side geometries and adjustable ergonomic supports. The scene was then divided into two distinct spatial areas: a scanning and a technician's room. The integration of human figures represented a pivotal step in the final development of the working environment. The characters used were created using the *MakeHuman* plugin for *Blender* (MPFB), which offers extensive customization options for appearance and automatic rigging to facilitate posture control via mesh nodes. Given the complexity of animating realistic human movement, static scenes were employed, and subsequently made dynamic through the implementation of selected camera movements, such as panoramically shots and zooms, to optimize clarity and production efficiency. The rendering phase was executed employing the *Extra Easy Virtual Environment Engine* (EEVEE), chosen for its balance between visual quality and shorter rendering times compared to the initially tested *Cycles* rendering engine. The final video editing was completed using the *CapCut* editing software, where titles, smooth transitions, and explanatory graphics (e.g. icons, arrows, and visual cues) were added. To guarantee accessibility for users with hearing impairments, auto-generated subtitles were synchronized with the voice-over narration, which was produced using *Voicebooking*, an online platform for creating AI-generated audio tracks. The result is a 1-minute and 49-second instructional video titled "*Walk-Through PET: an Intuitive Video Guide for the Scan*."

B. 30-second Timer video

The 30-second timer video represents an innovative visual aid designed to maintain concentration and stability among patients during the 30 second scan, making the experience more pleasant, controlled and less noticeable in terms of duration. In addition to the timer, introductory and concluding scenes with text instructions have been included to make the content more autonomous and self-sufficient. The initial phase of the project entailed the drafting of the script for these scenes. The original version was produced in English (with British accent and male voice) and then translated into French and Dutch, using the *Voicebooking* platform for the generation of the audio tracks. The graphic design process began with the creation of the 30-second timer, for which the online tool *Wave.video*, well known in the field of video editing, was utilized. A circular layout rotating clockwise was chosen. The selection of colors was crucial, considering that the video would be projected onto a vertical metallic grey panel. Regarding this aspect, several combinations of timer/background colors were tested until the final version was achieved. It exhibits a dark grey background (for visual continuity with the metallic panel), a circular blue timer with a light blue element at the bottom (for contrast and to further evoke the healthcare setting) and a red dot in the center (for focused attention). The size of the elements has been designed to ensure readability even from ~30 cm, taking into account possible visual impairments in patients. The instructional text scenes, set up in the script, were then graphically created on *FlexClip*, where the text was inserted on colored circular backgrounds, consistent with the timer design already defined. Furthermore, a 3-second countdown accompanied by a beeping sound was inserted between the initiation of the video and the timer display to optimize the patient's preparation for the scan. All content was then imported into the *iMovie* software for the video editing process.

C. Motion Study

The motion study explored the effect of the 30-second timer video, presented both with and without audio, on participant stability during a simulated WT-PET scan. Two main hypotheses were tested: whether the timer could improve participant concentration and stability, and whether the addition of audio, as a form of multisensory stimulation, could further reduce upper body motion. Thirty-one healthy volunteers were divided into two groups, each following a different sequence of recording conditions. In *Study Design 1*, twenty participants completed four 30-second trials: without video display, with video only, with video and audio, and again without video, to assess potential adaptation to the stimulus. In *Study Design 2*, eleven participants underwent the same conditions but in a different order (video with audio, video without audio, no video display), to examine whether the sequence of presentation influenced the results. Body motion was tracked using five infrared markers placed on the head, shoulders, chest, and abdomen, captured by an *Orbbec Femto Mega* depth camera [6]. Simultaneously, the video timer was projected onto the front panel using Samsung's *The Freestyle – Second Generation* projector. After adjusting the ergonomic supports, participants were asked to maintain a stable position throughout each session. At the end of every trial, brief subjective feedback was collected from each participant to support a qualitative analysis of the experience. The recorded RGB, infrared (IR), and depth images were then processed using *thresholding* and *connected component analysis* to detect and track the marker positions over time [7]. The full image processing pipeline is illustrated in Figure 2.

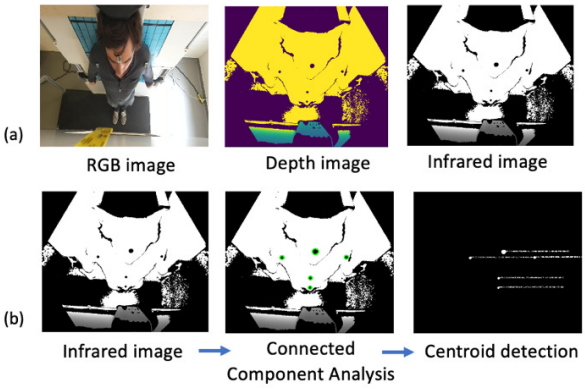

Figure 2: Image processing pipeline: (a) extraction of RGB, Depth, and Infrared images, and (b) pre-processing of the IR image and 2D centroid detection.

The 2D centroid of each marker was identified by calculating image moments. Specifically, the centroid coordinates were computed as:

$$c_x = \frac{M_{12}}{M_{zero}}$$

$$c_y = \frac{M_{21}}{M_{zero}}$$

where the zero-order moment M_0 represents the total area of the binary region, and the first-order moments M_{12} and M_{21} correspond to the intensity-weighted coordinates along the x and y axes, respectively. These 2D centroids were then projected into 3D space using the average depth values collected around each centroid. By applying the intrinsic parameters of the camera, namely, the focal lengths and the coordinates of the principal point, it was possible to reconstruct the 3D spatial positions of the markers. These 3D points were then transformed from the camera reference system to a global one using a homogeneous transformation matrix T, which combines a rotation matrix R and a translation vector t. To apply this transformation, each point was extended with a homogeneous coordinate. To quantitatively assess motion, two statistical parameters were used: the average absolute deviation (AAD) and the average Euclidean distance. AAD was computed separately along each spatial axis (x, y, z) to capture directional variability, while the Euclidean distance was used to quantify the overall displacement in 3D space. This was calculated as the distance between the marker's current position (x, y, z) and its mean position (μ_x, μ_y, μ_z), averaged across the entire recording duration:

$$d = \sqrt{(x-\mu_x)^2 + \left(y-\mu_y\right)^2 + (z-\mu_z)^2}$$

This approach enabled a consistent comparison of motion levels across different experimental conditions for each participant.

II. RESULTS AND DISCUSSION

A. Animated 3D video guide

The animated 3D video guide is currently in the prototyping stage. Further validation studies involving healthy volunteers will evaluate the clarity and effectiveness of the audiovisual product in helping patients to better understand the clinical procedure in a more autonomous way. The primary objective is to reduce the reliance on constant medical assistance in nuclear medicine departments and to streamline the scanning procedure. This, in turn, may further enhance patient throughput, already improved by the novel flat panel design. Figure 3 highlights the high visual quality achieved through EEVEE rendering, presenting selected scenes from the current version of the video guide.

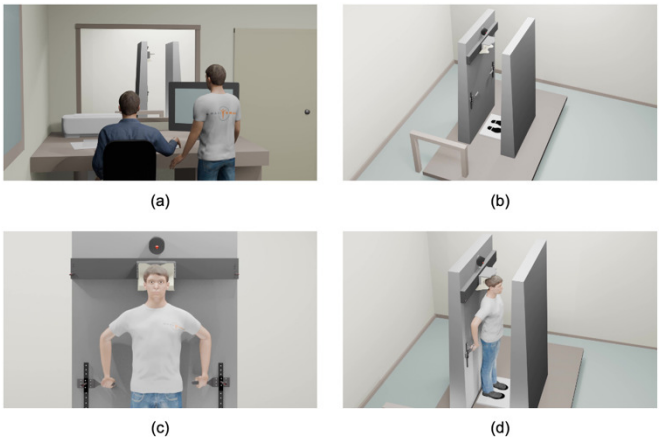

Figure 3: Selected final scenes rendered with EEVEE: (a) introductory scene, (b) initial overview of the WT-PET scanner, (c) final patient positioning, and (d) concluding scene prior to the scan.

B. 30-second Timer video

The 30-second timer video was developed to enhance the performance of the WT-PET scans by promoting patient focus and sustained attention throughout the 30-second scanning period, with the addition of a focal red dot in the central screen. The primary aim was to improve participant postural stability, particularly in upper body motion, thereby optimizing image quality and diagnostic accuracy. Figure 4 presents a selection of key frames included into the final version of the video.

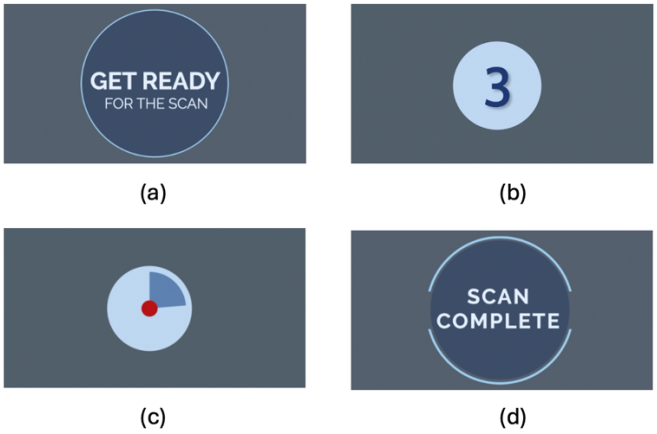

Figure 4: (a) English version of the introductory instruction scene, (b) 3-second countdown inserted to optimize patient's preparation for the scan, (c) final 30-second timer video design, (d) English version of the concluding instruction scene.

C. Motion Study

The results analysis was structured into two main categories. The first involved a quantitative assessment based on the kinematic metrics previously computed. The analysis of the 3D motion profiles in Study Design 1 (see Figure 5) revealed significant variability in motion, with the chest and abdomen displaying the most pronounced fluctuations, predominantly along the y-axis.

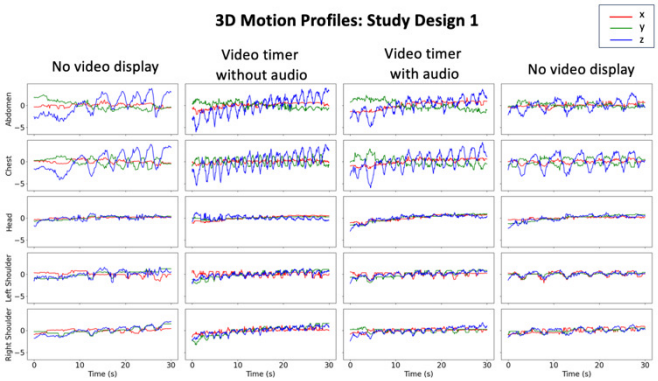

Figure 5: 3D motion profiles from Study Design 1. Columns correspond to different video configurations, while rows indicate specific marker positions. Movements along the x, y, and z axes represent lateral, anteroposterior, and vertical directions, respectively.

These displacements exhibit a cyclical pattern consistent with diaphragmatic breathing, characterised by antero-posterior expansion and contraction of the abdomen during respiration. A comparable motion pattern was observed at the same anatomical landmarks in Study Design 2. This finding is further supported by the analysis of mean Euclidean distance and average absolute deviation (AAD) metrics, which consistently identified the chest and abdomen as the regions exhibiting the greatest displacement and inter-subject variability. Figures 6 and 7 illustrate the highest mean Euclidean distances in these regions, accompanied by wide standard error bands, indicating substantial variability among participants. Consequently, Tables 1 and 2 present the maximum AAD values along the y-axis for the chest and abdomen, reinforcing the conclusion that these anatomical points are subject to the most pronounced respiratory-related motion.

Marker	Coordinate	No video display (mm)	Video timer without audio (mm)	Video timer with audio (mm)	No video display again (mm)
Head	X	0.24 ± 0.2	0.31 ± 0.1	0.40 ± 0.4	0.34 ± 0.3
	Y	0.44 ± 0.2	0.49 ± 0.2	0.52 ± 0.3	0.49 ± 0.3
	Z	0.26 ± 0.1	0.33 ± 0.1	0.39 ± 0.2	0.36 ± 0.3
Left Shoulder	X	0.32 ± 0.2	0.34 ± 0.2	0.40 ± 0.2	0.37 ± 0.2
	Y	0.38 ± 0.2	0.44 ± 0.2	0.46 ± 0.1	0.43 ± 0.2
	Z	0.54 ± 0.5	0.60 ± 0.3	0.74 ± 0.5	0.60 ± 0.2
Right Shoulder	X	0.28 ± 0.1	0.33 ± 0.2	0.43 ± 0.2	0.35 ± 0.1
	Y	0.39 ± 0.2	0.49 ± 0.3	0.46 ± 0.3	0.41 ± 0.2
	Z	0.51 ± 0.3	0.72 ± 0.6	0.77 ± 0.5	0.66 ± 0.7
Chest	X	0.44 ± 0.3	0.49 ± 0.4	0.55 ± 0.3	0.55 ± 0.6
	Y	1.12 ± 0.7	1.02 ± 0.5	1.18 ± 0.7	1.01 ± 0.4
	Z	0.62 ± 0.3	0.60 ± 0.2	0.66 ± 0.3	0.55 ± 0.2
Abdomen	X	0.44 ± 0.2	0.60 ± 0.3	0.68 ± 0.4	0.56 ± 0.4
	Y	0.92 ± 0.4	0.90 ± 0.3	0.93 ± 0.4	0.87 ± 0.3
	Z	0.93 ± 0.4	0.93 ± 0.4	1.08 ± 0.9	0.91 ± 0.4

Table 1: Average Absolute Deviation (mm) for each anatomical marker and spatial coordinate (X, Y, Z) across the four recording conditions evaluated in Study Design 1.

Marker	Coordinate	Video timer with audio (mm)	Video timer without audio (mm)	No video display (mm)
Head	X	0.22 ± 0.1	0.26 ± 0.1	0.30 ± 0.2
	Y	0.34 ± 0.1	0.43 ± 0.3	0.45 ± 0.1
	Z	0.27 ± 0.2	0.28 ± 0.3	0.37 ± 0.3
Left Shoulder	X	0.25 ± 0.1	0.34 ± 0.1	0.29 ± 0.1
	Y	0.32 ± 0.1	0.33 ± 0.1	0.36 ± 0.1
	Z	0.48 ± 0.2	0.54 ± 0.3	0.50 ± 0.3
Right Shoulder	X	0.21 ± 0.1	0.30 ± 0.1	0.28 ± 0.0
	Y	0.37 ± 0.2	0.46 ± 0.3	0.36 ± 0.1
	Z	0.50 ± 0.3	0.57 ± 0.2	0.48 ± 0.2
Chest	X	0.29 ± 0.1	0.39 ± 0.2	0.35 ± 0.2
	Y	1.09 ± 0.4	1.13 ± 0.4	1.17 ± 0.4
	Z	0.50 ± 0.1	0.53 ± 0.1	0.56 ± 0.2
Abdomen	X	0.41 ± 0.2	0.51 ± 0.2	0.47 ± 0.3
	Y	1.13 ± 0.4	1.13 ± 0.4	1.14 ± 0.6
	Z	0.94 ± 0.5	0.93 ± 0.4	1.00 ± 0.4

Table 2: Average Absolute Deviation (mm) for each anatomical marker and spatial coordinate (X, Y, Z) across the three recording conditions evaluated in Study Design 2.

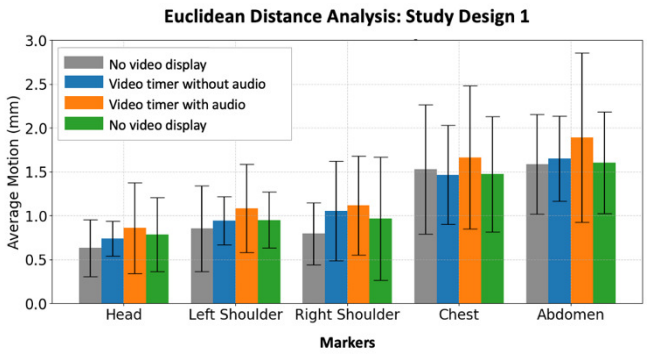

Figure 6: Average Euclidean distance (mm) for each marker across four recording conditions in Study Design 1. Each anatomical point shows four color-coded bars representing stimuli: grey (no video), blue (video timer without audio), orange (video timer with audio), and green (no video display).

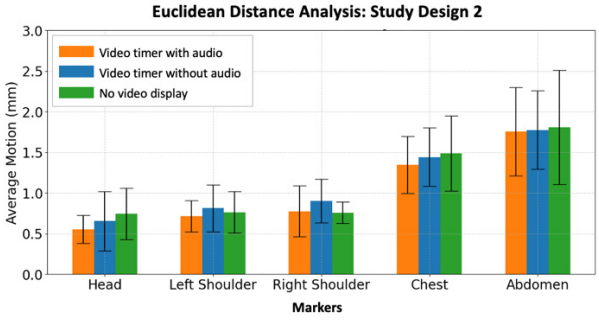

Figure 7: Average Euclidean distance (mm) for each marker across three recording conditions in Study Design 2. Each anatomical point shows three color-coded bars representing stimuli: orange (video timer with audio), blue (video timer without audio), and green (no video display).

The assessment of mean Euclidean distance, measured using five passive infrared markers in Study Design 1, indicated that the visual stimulus alone did not significantly enhance postural stability. Moreover, the addition of an audio track resulted in a noticeable increase in marker displacement, as shown in Figure 6. All anatomical markers exhibited greater movement, with increases ranging from +0.07 mm to +0.24 mm, particularly at the thoracic and abdominal levels. Despite these quantitative results, qualitative feedback revealed that most participants preferred the audiovisual condition, describing it as clearer and more engaging. A critical consideration in interpreting these findings is the potential bias introduced by the order of stimulus presentation. In Study Design 1, the audiovisual condition was consistently administered as third, following at least two minutes of upright standing, including instructional time and breaks between recordings. It is hypothesized that presenting the audiovisual condition later in the sequence may have led to participant fatigue, reduced attention, or postural adaptation, ultimately compromising performance.

In contrast, Study Design 2 presented the audiovisual condition first, resulting in significantly different outcomes. As shown in Figure 7, participants demonstrated improved postural stability, evidenced by reductions in mean Euclidean distances (ranging from 0.07 mm to 0.13 mm) and decreased inter-subject variability. These findings suggest that earlier exposure to the audiovisual stimulus may enhance attentional focus and minimize the effects of fatigue, thereby improving overall postural control.

To validate this hypothesis, a direct comparison was conducted between the first recordings from Study Designs 1 and 2 (see Figure 8). The results showed that four out of five anatomical markers exhibited reduced movement in the audiovisual condition, with decreases ranging from –0.06 mm to –0.18 mm. A slight increase in displacement was observed only at the abdominal marker (+0.16 mm). These findings confirm that the order in which stimuli are presented has a significant influence on the results and should be recognized as a major source of potential bias in this type of studies.

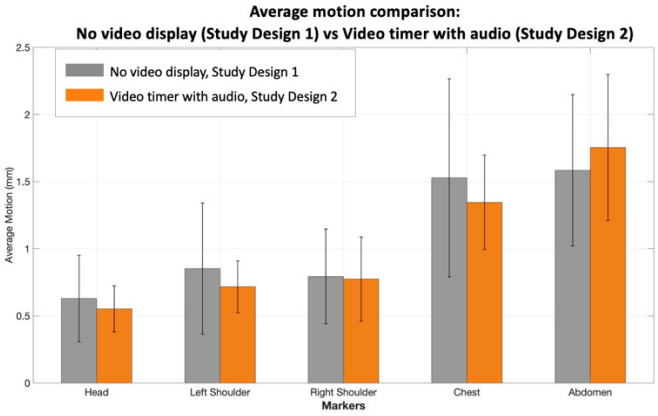

Figure 8: Comparison of Average Motion (mm) for each anatomical marker between the first recordings of Study Design 1 and Study Design 2. Each marker is represented by two bars, corresponding to different stimulus conditions: grey for the baseline condition (no video display, Study Design 1), and orange for the audiovisual condition (video timer with audio, Study Design 2), highlighting the stimulus effect on initial postural stability.

To quantify the reduction in upper body motion achieved in this study, a final comparative analysis was performed using data from a previously published study involving 20 healthy volunteers [7]. This study assessed participants under both normal and breath-hold conditions across three PET scanner systems, including the same WT-PET mock-up used in the current work [7]. The comparison specifically focused on the *video timer with audio* condition from Study Design 2 in the present study and equivalent data from the earlier work. As shown in Table 3, the audiovisual stimulus led to clear improvements in postural stability across most anatomical markers. Average head motion was reduced by 47% (from 1.03 mm to 0.55 mm), while left and right shoulder motion decreased by 36% and 32%, respectively. Standard deviations were also lower, indicating greater consistency among participants. It is important to note, however, that some variation in accuracy between the current and previous studies may be attributable to differences in experimental conditions, such as lighting, infrared camera angle, or camera-to-subject distance, which could influence marker detection and tracking precision. Even when compared to the breath-hold condition, the audiovisual condition appeared to outperforme it in reducing motion at the head and shoulders. This suggests that the attentional focus elicited by the audiovisual stimulus can equal, or even exceed, the biomechanical benefits of temporary respiratory suspension in certain upper body areas. However, improvements at the chest and abdomen were less pronounced, likely due to persistent effect of diaphragmatic breathing, which breath-hold protocols more effectively mitigate.

Study condition	Head	Left Shoulder	Right Shoulder	Chest	Abdomen
Normal breathing	1.03 ± 0.6	1.12 ± 0.4	1.15 ± 0.5	1.99 ± 0.8	2.42 ± 1.1
Breath-hold	0.81 ± 0.4	1.04 ± 0.4	0.92 ± 0.3	**1.33 ± 0.7**	**1.67 ± 1.1**
Video timer with audio	**0.55 ± 0.2**	**0.72 ± 0.2**	**0.78 ± 0.3**	1.35 ± 0.4	1.75 ± 0.5

Table 3: Comparison of Average motion (mm) ± Standard Deviation between video timer with audio experimental condition in Study Design 2 and experimental measurements conducted at normal breathing and breathold conditions taken

from [6]. For each marker position, the best result in terms of average motion is shown in bold.

Overall, these findings support the hypothesis that the use of an audiovisual timer can significantly improve upper body stability during PET scans. This non-invasive strategy presents a promising alternative to traditional breath-hold techniques, enhancing patient compliance and comfort without compromising effectiveness.

This statement is further supported by qualitative findings' evaluation based on comments and impressions collected from 31 participants at the conclusion of each final recording, providing a subjective insight into their experience. As illustrated in Figure 9, 78% of the participants preferred the video timer with audio, considering it as a valid support to enhance the sense of guidance, through a simple, effective, and immediately impactful communication. Conversely, 19% favored the timer without audio, experienced it as a potential source of stress and anxiety during the scanning. Only 3% of participants expressed a preference for the traditional scanning procedure without any additional external cues.

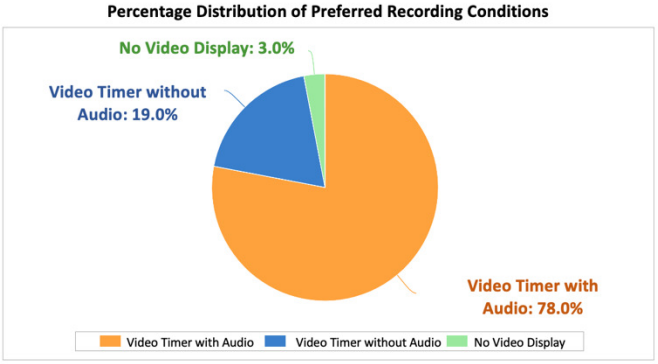

Figure 9: Percentage distribution of participants' preferences across different recording conditions in Study Design 1 and Study Design 2.

III. CONCLUSION

This thesis investigated two primary aspects targeted by the novel Walk-Through PET scanner: the need for constant medical assistance during patient positioning and significant upper body motion during upright scanning procedure. To address these issues, two interactive audiovisual tools were developed: a 3D animated video guide and a 30-second timer video with and without audio. The timer video was validated through a motion study involving 31 healthy volunteers. Although the order in which the stimuli were administered influenced the experimental results, this factor does not represent a limitation in clinical practice, which requires only a single scan. Results showed that the *video timer with audio* is the most effective in enhancing postural stability during simulated upright scans, particularly when administered as the first condition. This outcome was further supported by comparisons with the data reported in the following study [7], especially under normal breathing condition. The timer video with audio led to substantial reductions in upper body motion, including a 47% decrease in average head motion and a 36% and 32% reduction in right and left shoulder mobility, respectively. It also outperformed conventional breathing control methods, highlighting its potential as a non-invasive alternative to techniques such as breath-holding and apnea. Despite these improvements, residual motion remained in the chest and abdomen due to respiratory artifacts (1.35 mm and 1.75 mm, respectively), even under the best condition tested. As a result, integrating audiovisual stimuli with established breathing control protocols could offer combined benefits across all anatomical regions. To further reduce motion artifacts, especially in the abdomen, the study suggests enhancements to the WT-PET system, including the integration of motion correction algorithms and new ergonomic support structures. One proposed solution involves a customizable support structure with a cavity to accommodate patient's torso designed for upright use, similar to the existing headrest, although this would require an additional manual adjustment step and could affect patient throughput. In conclusion, the 30-second timer video represents a significant contribution toward improving the usability and efficiency of the current WT-PET scanner. The outcomes lay the foundation for future system optimization, promoting its large-scale adoption in clinical settings. Future research should assess the usability of the animated 3D video guide in helping patients complete the preparation and positioning phase more independently, though some manual assistance for ergonomic adjustments will likely remain necessary.

REFERENCES

[1] R. Lecomte, "Novel detector technology for clinical pet," European journal of nuclear medicine and molecular imaging, vol. 36, pp. 69–85, 2009.

[2] S. Vandenberghe, P. Moskal, and J. S. Karp, "State of the art in total body pet," EJNMMI physics, vol. 7, pp. 1–33, 2020.

[3] J. van Sluis, R. Borra, C. Tsoumpas, J. H. van Snick, M. Roya, D. Ten Hove, A. H. Brouwers, A. A. Lammertsma, W. Noordzij, R. A. Dierckx et al., "Extending the clinical capabilities of short-and long-lived positron-emitting radionuclides through high sensitivity pet/ct," Cancer Imaging, vol. 22, no. 1, p. 69, 2022.

[4] S. Vandenberghe, F. M. Muller, N. Withofs, M. Dadgar, J. Maebe, B. Vervenne, M. A. Akl, S. Xue, K. Shi, G. Sportelli et al., "Walk-through flat panel total-body pet: a patient-centered design for high throughput imaging at lower cost using doi-capable high-resolution monolithic detectors," European journal of nuclear medicine and molecular imaging, vol. 50, no. 12, pp. 3558–3571, 2023.

[5] M. Dadgar, J. Maebe, and S. Vandenberghe, "Evaluation of lesion contrast in the walk-through long axial fov pet scanner simulated with xcat anthropomorphic phantoms," EJNMMI physics, vol. 11, no. 1, p. 44, 2024.

[6] M. Dadgar, J. Maebe, M. Abi Akl, B. Vervenne, and S. Vandenberghe, "A simulation study of the system characteristics for a long axial fov pet design based on monolithic bgo flat panels compared with a pixelated lso cylindrical design," EJNMMI physics, vol. 10, no. 1, p. 75, 2023.

[7] R. Aziz, J. Maebe, F. M. Muller, Y. D'Asseler, and S. Vandenberghe, "Quantitative analysis of patient motion in walk-through pet scanner and standard axial field of view pet scanner using infrared-based tracking," EJNMMI physics, vol. 11, no. 1,p. 99, 2024.

Table of Contents

List of Figures

List of Tables

List of Acronyms

AAD Average Absolute Deviation.

AFOV Axial-Field-of-View.

BGO Bismuth Germanate Oxide.

CAGR Compound Annual Growth Rate.

CBM Continuous Bed Motion.

CT Computed Tomography.

DOI Depth of Interaction.

EEVEE Extra Easy Virtual Environment Engine.

FBP Filtered Back Projection.

FDG Fluorodeoxyglucose.

FWHM Full Width at Half Maximum.

GSO Gadolinium Oxyorthosilicate.

LAFOV Long Axial-Field-of-View.

LOR Line of Response.

LYSO Lutetium Yttrium Oxyorthosilicate.

MRI Magnetic Resonance Imaging.

NKI-AVL Netherlands Cancer Institute.

PET Positron Emission Tomography.

PET/CT Positron Emission Tomography–Computed Tomography.

PET/MRI Positron Emission Tomography–Magnetic Resonance Imaging.

PMT Photomultiplier Tube.

ROI Region of Interest.

SAFOV Short Axial-Field-of-View.

SiPM Silicon Photomultiplier.

SNR Signal-to-Noise Ratio.

SPECT Single-Photon Emission Computed Tomography.

SS Step-and-Shoot.

SUV Standardised Uptake Value.

TB-PET Total-Body PET.

TOF Time-of-Flight.

TOF-PET Time-of-Flight PET.

WHO World Health Organization.

WT-PET Walk-Through PET.

WT-PET-CT Walk-Through PET–Computed Tomography.

WT-TB-PET Walk-Through Total-Body PET.

1

Introduction

1.1 Background

Positron emission tomography (PET) is one of the most advanced imaging techniques in the field of nuclear medicine. The employment of specific radiotracers enables the visualisation of metabolic processes in vivo with high spatial resolution, thus establishing it as a fundamental tool for diagnosis and clinical evaluation. Its applications extend to a wide range of medical disciplines, from neurology (where it's used in the early diagnosis of diseases such as Alzheimer's, Parkinson's and epilepsy) to cardiology and oncology, where PET plays a central role in lesion detection, patient treatment monitoring, follow-up and clinical research.

Despite considerable technological advances over the last three decades, conventional PET scanners still exhibit critical limitations. These include high operation and acquisition costs, which prevent their widespread adoption in clinical and research settings. Moreover, the conventional cylindrical geometry with patient bed integrated, introduces a further level of complexity to the patient positioning procedure. Particularly, this process is both time-consuming and demanding in terms of patient position accuracy, represented a possible limitation in the number of examinations that can be conducted on a daily basis and increasing the workload for healthcare personnel.

In order to address these issues, the Medical Imaging and Signal Processing (MEDISIP) research group at Ghent University has developed an innovative prototype: the Walk-Through PET (WT-PET) scanner. This novel system, which is currently under development, is based on a vertical panel geometry inspired by airport flat panel scanners. This design has been proven to enhance patient positioning phase, with the main aim of reducing operational costs, and potentially increasing spatial resolution and daily patient throughput.

The axial field of view of this novel scanner is comparable to that of current long axial-field-of view (LAFOV) PET scanners, but at a significantly lower estimated cost. However, despite the numerous advantages, several operational limitations still need to be adressed. In particular, medical personnel is still required to assist patients in correct positioning between the two vertical panels. Moreover, the requirement for patients to mantain an upright position for 30 seconds, the estimated time required for image acqusition, can accentuate upper body motion, which can negatively affect image quality.

1.2 Research Objectives and Methodology

This thesis aims to address these limitations by developing two interactive videos. The first is a 3D animated video guide. It has been specifically designed to instruct patients in a clear, concise and almost autonomous manner on the key steps involved in positioning procedure within the scanner. The main aim is to reduce the operational workload on medical personnel during this phase. The second tool is a 30-second video timer, which can be integrated within the scanner via a projector. This video is designed to maintain the patient's visual attention and improve postural stability during the scan, thereby reducing upper body motion. Various software tools were employed in the design and development of both videos. *Blender* was used for 3D graphic modelling, while *Wave.video*, *CapCut* and *Flexclip* were utilized for video editing. The voiceovers integrated into both videos were generated using *Voicebooking*, an AI platform for voice tracks production. To evaluate the effectiveness of the timer video in reducing upper body motion, an experimental study was conducted on 31 participants, divided into two groups. Each group was exposed to different video sequences in order to minimise potential bias and obtain reliable results. The video was projected inside the scanner mock-up using Samsung's *The Freestyle – Second Generation* projector. For motion tracking, five passive infrared markers were applied to specific anatomical points, and a *Orbbec Femto Mega* depth camera was used for 3D motion data acquisition. Both qualitative and quantitative methodologies were employed to better analyse the obtained results. Quantitative analysis was based on the computation of kinematic metrics such as average Euclidean distance, 3D motion profiles, and average absolute deviation, while qualitative analysis consisted on collecting participant feedbacks at the end of

each recording session.

1.3 Thesis Outline

The thesis is structured into eight chapters. Chapter 2 provides an introduction to PET, exploring its main features as a molecular imaging technique and the physical principles on which it is based, as well as the instrumentation empolyed for the detection. The chapter focuses also on the phenomenon of image degradation, considering both the effects related to positron physics, and artefacts induced by patient motion. The subsequent chapter provides a detailed overview of the technological evolution of PET scanners, starting from traditional models and moving on to the scanner systems most widely used in current clinical practice. It discusses the improvements achieved in terms of sensitivity and spatial resolution, as well as the main limitations, such as high costs, ethical and economic accessibility constraints, and critical operational challenges related to patient positioning and upper body motion. These limitations motivated the MEDISIP research group to propose the new WT-PET scanner model. Chapter 4 introduces the design concept of this novel scanner, with a particular focus on its strengths such as high patient throughput, a small footprint, and economic sustainability. The chapter also explores the primary limitations of the current prototype, which form the basis of the thesis.

The planning, design and implementation of the two audiovisual products developed to address these critical issues are described in Chapters 5 and 6. Chapter 5 focuses on the design of the 3D animated video guide for patient positioning, while Chapter 6 focuses on the development of the 30-second timer video designed to promote postural stability during scanning. Chapter 7 is dedicated to the experimental motion study conducted on a sample of 31 participants, with the objective to evaluate the effectiveness of the video timer in reducing participant upper body motion. Both quantitative and qualitative analyses, previously mentioned, are presented and finally discussed. The discussion of the findings includes a comparison with existing literature, an evaluation of the impact of the stimulus delivery order, and a critical analysis on the strengths and limitations of the 30-second video timer with audio based on the results obtained.

Finally, Chapter 8 concludes the thesis by providing an overview of the work carried out and the main outcomes obtained, suggesting possible strategies and future solutions for optimising patient positioning, motion control and overall scan performances in WT-PET. Chapter 9, in turn, presents ethical reflections on how the thesis project was

developed and carried out, with particular attention to the creation of the two video and the motion study involving 31 participants.

2

PET imaging

2.1 Molecular imaging

2.1.1 Functionality over morphology: a change of perspective in medical imaging

The clinical approach to the diagnosis and treatment of many diseases has been significantly affected by developments in medical imaging technologies during the last few decades. The advent of advanced imaging techniques has had a profound impact on the fields of diagnosis, treatment planning, and disease monitoring, particularly in the context of neurological diseases such as Alzheimer's disease, dementia, and mild cognitive impairment; neuromotor disorders including Parkinson's disease, tics, and dystonia; as well as in the field of oncology [5]. The evaluation of diseases has improved significantly since the advent of digitalised medical imaging, which has replaced the previous qualitative, visually-driven method with a more accurate, quantitative analysis. The enhancement of diagnostic accuracy is facilitated by this shift, which is dependent on numerical data derived from images through the application of mathematical methods.

Currently, imaging modalities are classified into two main categories: morphological and functional imaging. The transition from a morphological to a functional approach has led to a conceptual shift in the medical evaluation of disease. Traditionally, morphological imaging, in the oncology field for example, has focused on displaying the anatomical structure and characteristics of the lesion, describing its shape, size, and central or extended location in the body. However, functional imaging has introduced a new perspective in this field, interpreting structural changes in the lesion as a result of dynamic biological processes interacting with human tissues. These processes in-

duce metabolic or functional alterations at the cellular level, which can be detected and visualised long before structural changes become apparent, offering greater sensitivity in the detection. The integration of molecular biology with in vivo imaging techniques, such as positron emission tomography (PET) and single-photon emission computed tomography (SPECT), has further advanced oncological imaging. These techniques use biomarkers to visualize specific cellular functions or disrupted metabolic pathways, facilitating the identification of molecular targets and altered physiological processes. Consequently, they not only enable early diagnosis, but also improve treatment planning, particularly in radiotherapy and chemotherapy, by anticipating the progression of anatomical lesions and optimizing patient clinical management [14, 5].

2.1.2 Radiotracer principle

Positron emission tomography (PET) is one of the most widely used functional imaging techniques in nuclear medicine. It involves the use of radiotracers. Radiotracers are radioactive substances used for diagnostic purposes due to the presence of positron-emitting radionuclides bound to the tracer's molecules. The clinical areas in which PET imaging is currently most commonly applied include neurology (e.g. for the early diagnosis of diseases such as Parkinson's disease, Alzheimer's disease and epilepsy) and cardiology (e.g. for the assessment of coronary artery disease and myocardial viability) [12]. However, it is in the field of oncology that this imaging technique has seen the greatest development, not only for the diagnosis of tumour lesions but also for the staging and monitoring of cancer treatment. The radiotracer distributes itself in the body according to the metabolic activity of tissues after being supplied orally or intravenously using a radiopharmaceutical, which is made by mixing a radionuclide with a pharmaceutical agent. The choice of radiotracer depends on the biological process that is being studied. In the field of oncology, these tracers are used as markers for metabolic processes. By exploiting the differences in metabolic activity between tumour and healthy tissue, the uptake of radiotracers by human cells is used as a highly accurate lesion detection tool [12]. The most widely used radiotracer in PET is fluorodeoxyglucose (FDG). This chemical compound is characterised by a structure and chemical behaviour similar to glucose, as illustrated in Figure 2.1.

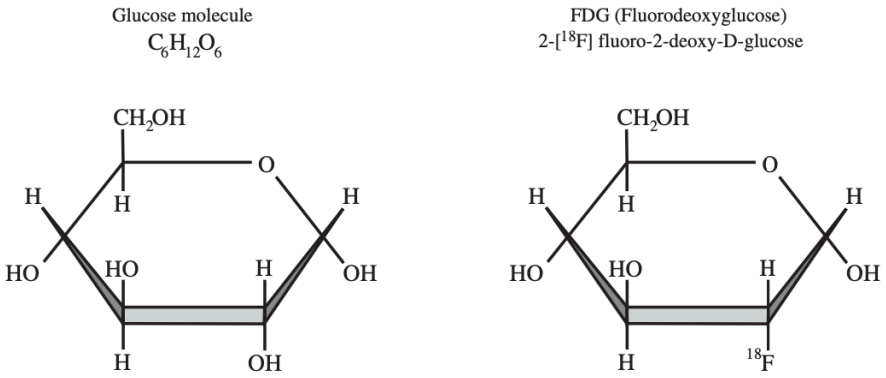

Figure 2.1: Structure of Glucose and Fluorodeoxyglucose [2].

The chemical and structural similarity between FDG and glucose underlies FDG's selective uptake and subsequent accumulation within neoplastic cells. This facilitates the identification and characterisation of tumour lesions with high density and specificity during PET scanning [2]. Its main use is in the diagnosis, staging, or restaging of colorectal, lung, head, neck, or melanoma tumours. However, there are also other radiotracers used in oncology which, because of their different chemical structure, target other aspects of cell metabolism, such as cell proliferation or protein synthesis. These include 11C-choline (for brain, oesophageal, and prostate cancer), 11C-methionine, and 18F-tyrosine (both for brain tumours and soft tissue sarcomas) [12]. Several other types of radiotracers for oncological applications are available on the market such as fluoro-dihydroxyphenylalanine ([^{18}F]FDOPA), used to diagnose neuroendocrine tumours and gallium-68-labeled PSMA-11 ligand ([^{68}Ga]PSMA-11) and fluorine-18-labeled PSMA-1007 ligand ([^{18}F]PSMA-1007) to mark prostate cancer cells [2, 5, 15, 16].

2.1.3 Injection of Radiotracer

It is crucial to emphasize the preparation of the patient for a PET scan, which involves the use of radiotracers. Since FDG is a glucose analogue, patients must avoid all caloric intake for at least 4-6 hours before the scan. To ensure optimal safety and precision, a standard protocol involves measuring the patient's serum glycemic rate and fasting glucose levels before the injection of the radiotracer. Acceptable values are generally in the range of 70-110 mg/dL. Any value in excess of this range would result in hyperglycaemia, thereby altering the natural absorption of FDG by the tumour cells. FDG is administered intravenously or orally with water, especially for the elderly, obese,

and chemotherapy patients. In order to allow the radiotracer for distribution throughout the body, patients are advised to wait 40 to 45 minutes after injection before entering the scanner. It is essential, considering the direct correlation between muscular activity and metabolic rate, and the chemical similarity of FDG to glucose, that once the radiotracer is in the body, the patient reduces any movement or stress as much as possible. In order to facilitate the uptake process and thus ensure a uniform distribution of FDG, the patient is requested to rest in a quiet room, free of noise, and to maintain a comfortable and relaxed position before the scan. It is also essential that the patient avoid any form of communication in order to reduce the physiological uptake in the skeletal muscles as much as possible [2].

2.2 Physics and detection principles

2.2.1 Positron physics

The physical principle behind PET technology is based on the detection of two annihilation photons produced when a positron is emitted by a radionuclide through radioactive decay. The instability of the radionuclide, resulting from an unbalanced ratio of protons to neutrons in the nucleus, leads the isotope to decay to reach a more stable state. There are several types of decay; however, the focus here is on $\beta+$ decay. This process occurs when a radionuclide exhibits an excess of protons [12]. When a positron is emitted, the decay process leads to the conversion of a proton into a neutron, as shown by the Equation 2.1:

$$p^+ \rightarrow n^0 + e^+ + \nu_e \tag{2.1}$$

The choice of PET tracer is determined by the specific biological process to be observed. Once the tracer is selected, it is labelled with the appropriate radioisotope corresponding to the type of radiotracer to be administered. Table 2.1 presents a list of the most frequently radionuclides used.

Radionuclide	Half-Life
Fluorine 18 (^{18}F)	110 min
Carbon 11 (^{11}C)	20 min
Nitrogen 13 (^{13}N)	10 min
Oxygen 15 (^{15}O)	122 sec
Rubidium 82	75 sec

Table 2.1: Commonly used PET radionuclides and their half-lives [12].

To illustrate this principle, we have taken the decay of 18F as a reference:

$$^{18}\text{F} \rightarrow {}^{18}\text{O} + e^{+} + \nu \tag{2.2}$$

In Equation 2.2, e^{+} denotes the positron (antimatter), and v represents the neutrino. The positron, which has the same mass as an electron but an opposite charge, travels away from the decay site. After covering a short distance (less than 1 mm for 18F in water), it loses its kinetic energy and annihilates with an electron, producing the following reaction:

$$e^{+} + e^{-} \rightarrow \gamma + \gamma \tag{2.3}$$

The annihilation process represented in Equation 2.3 results in the emission of two 511 keV gamma photons, which travel in opposite directions (about 180° apart), in accordance with the conservation of momentum and energy [12].

2.2.2 Detection principles

Colinearity and simultaneity

The scanner detection in PET is based on two fundamental physical principles that allow this system to avoid the use of a mechanical collimator to locate the source of the emitted radiation. These principles are collinearity and simultaneity. During isotope decay, two 511 keV photons are emitted from the annihilation point in opposite directions (180° apart) and detected nearly simultaneously (or within a short-defined time window) by the surrounding detector ring, as shown in Figure 2.2.

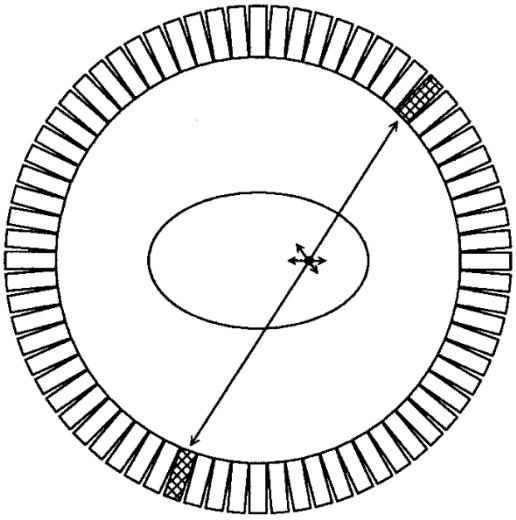

Figure 2.2: Principle of coincidence detection in ring PET scanner [3].

All the photon pairs that do not arrive at opposite points along the detector ring within a few nanoseconds' time window are ignored by the PET scanner. This principle is called 'discrimination', and it uses coincidence electronics to only detect coincidences. So, when a photon is detected, a coincidence circuit is triggered. In the event of a second photon hitting another detector within a predetermined time window, as depicted in Figure 2.3, it is assumed that both photons originate from the same annihilation event, thereby defining a line of response (LOR) for each coincidence.

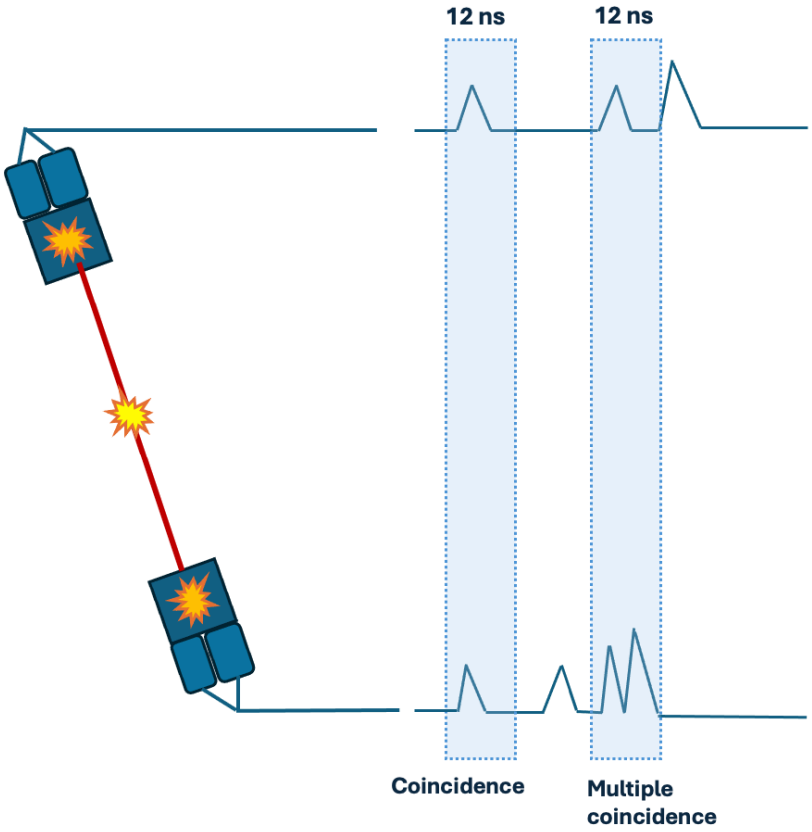

Figure 2.3: Use of a coincidence time window for LORs detection in PET imaging.

Each LOR represents a projection of the radiotracer distribution in the body. By acquiring a series of projections, it is possible to reconstruct the distribution of the injected tracer using either the traditional algorithm of filtered back projection (FBP) or iterative algorithms. Figure 2.4 illustrates the main steps of the clinical procedure that lead to the final PET imaging acquisition.

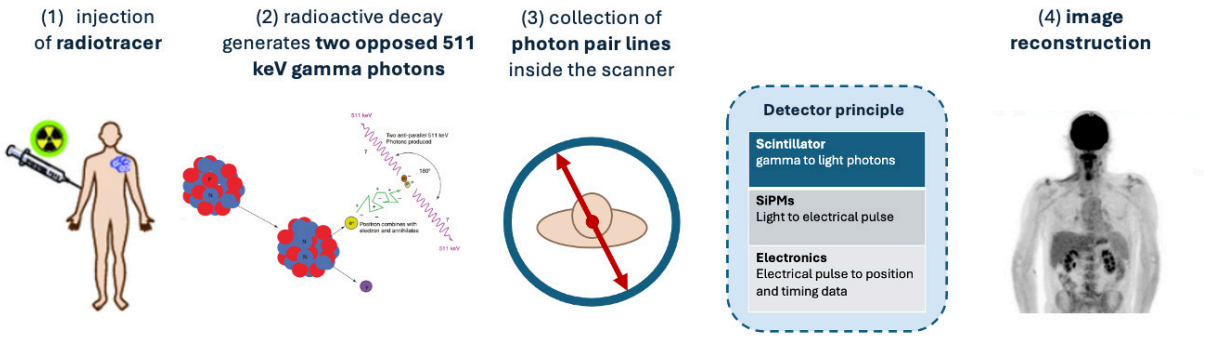

Figure 2.4: Illustration of the clinical procedure leading to PET image acquisition.

The fourth step, concerning the electronic components of the technological system for the acquisition of a PET image, will be analyzed in detail in the section 2.2.3.

The absence of a mechanical collimator in PET imaging has been shown to significantly increase detection efficiency and sensitivity compared to SPECT. However, several limitations remain, both system-intrinsic and patient-related. Interactions between positrons and biological tissue, such as attenuation, scattering, and absorption, together with technological factors intrinsic to the system, including geometric sensitivity and detector sensitivity itself, result in a reduction of detected events to less than 1% of the initial production. Due to geometric sensitivity, a significant number of photons will be ejected along a path that does not intersect the detectors. Additionally, there may be photons that pass through the detector without being fully absorbed. Furthermore, the coincidence principle requires that both photons be detected to define a LOR. The subsequent sections will discuss the problems and the technological innovations that have been proposed to improve PET sensitivity and spatial resolution [12].

2.2.3 Detection technology

The performance of PET technology in detecting events is based on a principle of coincidence detection. However, the scanner must be composed of highly specialised components in order for this principle to guarantee accurate detection. PET detectors are based on a combination of scintillators, a light conversion unit, and electronics with high spatial, energy and temporal resolution (with an accuracy in the order of hundreds of picoseconds). These components form a detector ring that surrounds the patient's bed during the scan.

Scintillators

The process of energy conversion begins in the scintillators. The initial interaction between the 511 keV gamma photons and the crystal is followed by an absorption phase during which the energy carried by the two photons is absorbed by the scintillator. Based on the scintillator's stopping power, which characterizes the likelihood of interaction between the gamma photon and the scintillating material, the absorption efficiency directly affects the sensitivity of the detector. Following this initial stage comes an energy conversion phase, during which the crystal releases a fraction of the energy absorbed, in the form of multiple visible light photons. In order to guarantee optimal performance in PET, there are certain critical parameters that must be satisfied. Specifically, a short decay time (in order to achieve good time resolution, reduce

dead time, minimize random events and provide high count rates), a high energy resolution (generally correlated with intense light emission) and a high stopping power (to increase detection efficiency) are required. The most common scintillators employed in PET commercial systems are listed in Table 2.2, with their technological characteristics [8].

Table 2.2: Overview of Scintillator Material Properties [8].

Scintillator	**Light output** (photons/MeV)	**Decay time** (ns)	**Density** (g/cm^3)	**Light attenuation length** (cm)
LYSO	32000	41	7.1	20.9
BGO	8500	300	7.13	22.8
GSO	7600	30–60	6.71	22.2
$LaBr_3$	65000	15	5.29	16.0

The performance of a PET system is highly dependent on the properties of these materials. In the early stages of PET technology development, NaI(Tl) was predominantly utilized due to its exceptional energy resolution, though it was limited by a relatively long decay time and low stopping power. The subsequent introduction of Bismuth Germanate Scintillator crystal (BGO) led to a significant improvement in the stopping power of incident photons (due to its high, effective atomic number Z and high density) though at a lower energy resolution. The most advanced materials currently are the Lutetium–yttrium oxyorthosilicate (LYSO) and Gadolinium Oxyorthosilicate (GSO), both of which are characterized by reduced decay times and intermediate properties between NaI(Tl) and BGO. These materials are regarded as the most promising candidates for PET 3D systems as they facilitate high count rates. In particular, LYSO has established itself as the new gold standard, favoring the integration of Time-of-Flight Positron Emission Tomography (TOF-PET) technology, which allows for further improvement in the system's temporal resolution (in the order of 200-300 ps) [13, 17]. As TOF technology represents a step forward in event detection accuracy by increasing the signal-to-noise ratio through estimating where along the LOR the annihilation took place, there is a move towards using this type of crystal. This shift aims to achieve better temporal resolution and, consequently, increasingly accurate detection.

Photomultiplier Tubes, Silicon Photomultipliers and Anger Logic

Once the initial energy conversion has taken place, multiple visible light photons are guided into the photodetectors, which further convert this optical energy into an electric signal. The output of each photomultiplier tube (PMT) obtained after the conversion is then used to encode the x and y coordinates required to identify the point of incidence

of the two gamma photons on the crystal. This is done using the Anger logic technique. This logic collects and encodes the signals received from each photomultiplier tube. By analysing their intensity and applying a weighted average, this logic can return the exact position and energy associated with each event [18, 4]. A significant technological advance was achieved with the introduction of silicon photomultipliers (SiPMs), which are progressively replacing traditional PMTs. These innovative devices offer high gain, comparable to that of PMTs, while also providing several key advantages such as lower operating voltage, improved spatial resolution and increased resistance to magnetic fields, that offer novel possibilities for the advancement of integrated imaging systems such as hybrid Positron emission tomography–magnetic resonance imaging (PET/MRI) scanners. From a functional point of view, each cell within the SiPM operates independently and exhibits binary behaviour (on/off). The integration of the output of all activated cells generates a digital signal that is proportional to the energy deposited in the scintillator by the incident photons, thus allowing precise quantification of the energy for each detected event. The latest generation of SiPMs further enhances performance by reducing the temperature sensitivity and improving the temporal, energy, and spatial resolution [5].

2.3 Image quality: physical and patient-induced limitations

2.3.1 Time of Flight: a great improvement in image quality

In the past 30 years, there have been significant developments in PET technology and instrumentation, with the improvements in hardware, detectors and image processing systems that have affected both the quality of the scans and the accuracy of quantification. In addition to the integration of novel scintillators that have resulted in enhanced spatial resolution and sensitivity, and the implementation of advanced fully 3D iterative reconstruction algorithms, one of the most innovative technologies introduced in the early 1990s was the *Time-Of-Flight* (TOF) technology. This technique provides a more accurate estimate of the annihilation event that has occurred along the LOR by determining the difference in arrival time $t_1 - t_2$ of the photon pair in the opposite detectors. In conventional PET systems, three parameters are typically considered: the time of incidence, the point of impact, and the photon energy. In conventional systems, temporal information is commonly used only for the 'simultaneity' principle. In this case, the moment of impact of two photons is compared with a predefined time window of the

order of nanoseconds, only to determine if the pair of photons can belong to the same event or not. Then, for each pair of photons detected, a coincidence LOR is defined on which the position of the annihilation event is spread. This process is then repeated for a series of different angles, until a sufficient number of projections are obtained that can be used to reconstruct the distribution of the radiotracer in the patient's body. In TOF-PET systems, temporal information is used to probabilistically estimate where along the LOR the annihilation event occurred. Hypothetically, with perfect TOF information, the reconstruction step could also be removed since the position of each annihilation event could be identified using only the photon pair and the time difference information. However, even with imperfect temporal information, it could be possible to reduce noise propagation along the LOR. The accuracy with which the annihilation position can be measured along the LOR is determined by the time accuracy with which the t1-t2 interval can be calculated (a factor which depends on the type of detector used). The Equation 2.4 is used to calculate this parameter [4]:

$$\Delta x = \frac{c \cdot \Delta t}{2} \tag{2.4}$$

where c is the speed of light (i.e., 30 cm/ns). The signal-to-noise ratio (SNR) gain obtainable by incorporating TOF information into the image reconstruction process has been shown to be related to the ratio of the size of the imaged object to the positional accuracy of the TOF, as shown in Equation 2.5 [4]:

$$\frac{\text{SNR}_{\text{TOF}}}{\text{SNR}_{\text{non-TOF}}} = \sqrt{\frac{D_{\text{object}}}{\Delta x}} \tag{2.5}$$

For instance, considering a temporal resolution of 500 ps would yield an accuracy of 7.5 cm along the LOR for event detection. This would result in an effective gain in sensitivity by a factor of 2.3 for whole body imaging (estimated object diameter = 40 cm), which can be translated into a reduction in dose or a reduction in imaging time. Table 2.3 illustrates the enhancement in sensitivity that can be achieved for different patient diameters and time resolutions. The diameters selected for the Table 2.3 represent thin (20 cm), average (27 cm) and heavy (30 cm) patients. These data are taken from [13].

Parameter	$\Delta t = 300$ ps	$\Delta t = 600$ ps	$\Delta t = 1000$ ps
D = 20 cm	4.4	2.2	1.3
D = 27 cm	6.0	3.0	1.8
D = 35 cm	7.8	3.9	2.3

Table 2.3: Sensitivity gain determined under uniform distribution conditions [13].

The SNR gain reveals that this enhancement is not only related to the temporal resolution, but also to the size of the patient. This is of particular relevance, as conventional PET systems are more prone to quality degradation in large patients due to greater attenuation by soft tissue, resulting in both a loss of true counts and an increment in scattered ones. The advent of novel scintillators, such as LSO and LYSO, which exhibit rapid time decay, high light emission, and photon stopping power, has enabled the development of TOF-PET technology. This innovation has facilitated more precise lesion detection, thanks to better event localisation along the LOR and reduced noise propagation.

2.3.2 Spatial resolution and Image degrading effects

The spatial resolution of a PET scanner is an intrinsic property of the detection technology, reflecting the system's ability to physically distinguish two sources as two separate peaks within the minimum distance between two points in a reconstructed image. This capability is crucial in diagnostic applications, particularly in oncology, where precise lesion detection and accurate tumour definition are essential for an effective clinical decision making. However, the spatial resolution of the acquired image is often significantly reduced, resulting in a degradation of image quality. This phenomenon is attributable to various factors, both inherent to PET technology and induced by the movement of the scanned patient. In sections 2.3.3, 2.3.4 and 2.3.5, the physical limitations and patient-induced artefacts that result in reduction in image quality will be discussed in more detail.

2.3.3 Effects related to positron physics

Acolinearity and positron range

Coincidence detection introduces two fundamental physical constraints on PET spatial resolution. The first of these is derived from the finite distance travelled by the positron before annihilation, commonly referred to as the 'positron range'. The second fundamental limit is due to the small deviation from perfect collinearity ($180° \pm 0.25°$) resulting from the residual momentum of the positron and electron before annihilation, known as 'acolinearity'. These two effects are illustrated in Figure 2.5 and represent the intrinsic limitations imposed by positron physics. Therefore, the overall spatial resolution of PET technology is determined by the combination of these two physical factors, along with the intrinsic resolution determined by the PET detection system itself.

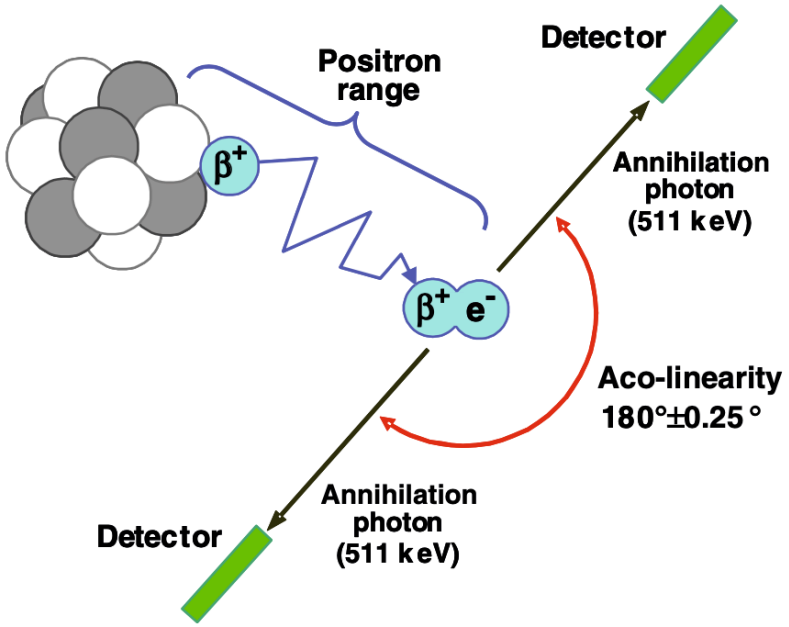

Figure 2.5: Positron emission and annihilation coincidence detection in PET [4].

The overall resolution can thus be expressed by Equation 2.6 [4]:

$$R = a\sqrt{\left(\frac{d}{2}\right)^2 + b^2 + c^2 + r^2} \tag{2.6}$$

where: 'a' accounts for tomographic reconstruction degradation ($1 \leq a \leq 1.3$), 'd/2' represents the geometric response between coincident detector pixels of size d, 'b' denotes detector positioning accuracy from crystal identification algorithms,'r' represents the mean positron range before annihilation and 'c' for the colinearity effect [4].

One of the primary consequences of the 'positron range' is the blurring effect on the acquired PET image, that results in spatial resolution degradation. This phenomenon depends on the maximum emission energy and the energy distribution of the positron ($\beta+$), and therefore on the radionuclides used to label the selected biomolecules and its surrounding tissue. The greater the energy of a positron emitted, the greater the distance it will travel in human tissue before annihilating with an electron. This results in an increase in the uncertainty about the real annihilation position, visually manifesting as image blurring. This effect can be seen in Table 2.4, which compares different radioisotopes, each with its own maximum emission energy [4].

Radioisotope	β^+ Energy (MeV)		Resolution (mm)		ρ^a
	Max	Average	FWHM	FWTM	
^{11}C	0.96	0.385	0.19	1.86	0.92
^{13}N	1.20	0.491	0.28	2.53	1.4
^{15}O	1.73	0.735	0.50	4.14	2.4
^{18}F	0.64	0.242	0.10	0.33	0.54
^{64}Cu	0.65	0.278	0.13	0.55	0.72
^{68}Ga	1.90	0.836	0.58	4.83	2.8
^{82}Rb	3.36	1.52	1.27	10.5	6.1

$^a\rho = 2.355 \times$ rms $=$ effective range

Table 2.4: Impact of positron range in soft tissue on PET spatial resolution (mm) [4].

For isotopes like ^{18}F and ^{64}Cu, which emit positrons with maximum energies of 0.64 MeV and 0.65 MeV, the positron range has a minimal effect. This is evident from their Full Width at Half Maximum (FWHM) values, which are less than 0.1 mm. In contrast, ^{82}Rb emits positrons with a much higher energy (3.4 MeV), resulting in an FWHM greater than 1 mm, indicating significantly more image blurring due to the longer positron range. A further contribution to image degradation is the effect of acolinearity. Even when the deviation is minimal, its contribution to the degradation of spatial resolution depends on the diameter of the scanner: the larger the diameter of the scanner, the greater the effect of acolinearity. This can be easily seen when comparing whole-body PET scanners with small animal scanners. In the first case, a diameter of 90 cm leads to image degradation of approximately 2 mm, while in the latter case, degradation is approximately 0.4 mm for a diameter of only 18 cm.

2.3.4 Effects related to detection system's geometry

Intrinsic resolution, Depth of Interaction and Parallax error

Another parameter that has a significant effect on the spatial resolution of the acquired image is the size of the detector, which is a purely geometric property. The typical dimensions of crystals in current use range from 3-4 mm in width and 15-30 mm in depth. In general, the smaller the detector, the greater the gain in spatial resolution. The depth of interaction (DOI) within the scintillator imposes a fundamental limit on resolution [12]. When events occur far from the centre of the scanner, the photons

produced by annihilation no longer travel perpendicularly to the detector. Rather, they hit the detector at an oblique angle. Depending on the depth of the scintillator at which the 511 keV photon interacts, an error in the determination of the correct LOR occurs, known as parallax error [5]. The process described above is clearly illustrated in Figure 2.6.

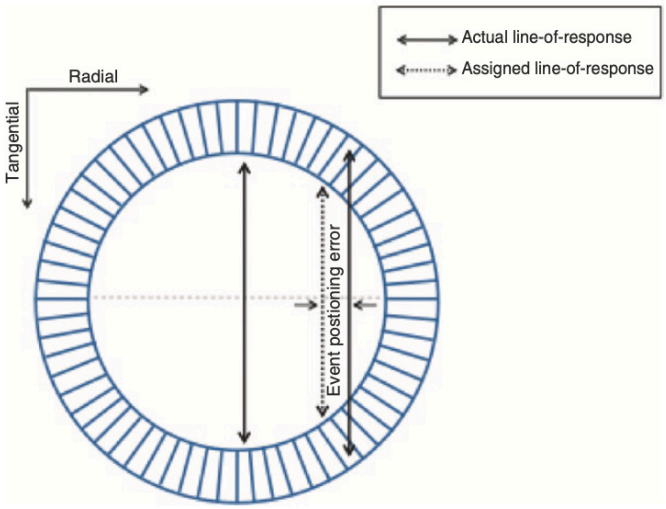

Figure 2.6: Parallax error in a PET scanner: the potential consequence is the introduction of an error in identifying the correct line of response, resulting from the imprecision of off-centre positron annihilation measurements. The scanner's overall spatial resolution may be subject to deterioration [5].

Most current PET systems based on pixelated detectors are not able to calculate the DOI, so the system associates the point of incidence to the crystal's surface, even though the actual absorption of energy occurred at a certain depth inside [3]. This error is particularly evident in scanners used for small animals, as these systems use long crystals and small diameter rings to improve sensitivity. In contrast, clinical whole-body scanners possess a total diameter of 90 cm and a field of view greater than 50 cm, that make them less prone to this type of error.

2.3.5 Patient-induced artefacts

In this section, the image degradation effects caused by subject movement during scanning will be examined. It is important to note that patient movement has the potential to negatively affect PET image acquisition, resulting in inconsistencies in the collected

data. These inconsistencies manifest as motion artefacts. It is evident that these artefacts have a significant impact on image quality, potentially compromising the accuracy of clinical evaluation and lesion interpretation. The classification of movement can generally be made into two categories: voluntary and involuntary, depending on its origin.

Voluntary movement

Voluntary movement typically arises from muscle contractions involving head, shoulders, limbs, or the entire body. This phenomenon can be induced by common actions such as mastication or deglutition; however, it can also be triggered by emotional states, including discomfort or anxiety, which are commonly experienced during a PET scan. This category of motion is often characterised as rigid, including displacements such as translations and rotations. The head is one of the anatomical regions most prone to movement during a scan. Typical displacements consist of translations of 2–5 mm and rotations of 2°–3° [19]. To mitigate these effects, the use of supports and restraint systems has become a standard practice, helping to minimise motion and improve image quality.

Involuntary movement

Involuntary motion, on the other hand, refers to the displacement of chest and abdomen primarily caused by respiration and cardiac activity. Table 2.5 illustrates the typical movements induced by breathing for different tissues and organs of the body [19].

Various strategies have been developed to limit these effects during imaging procedures. One notable example is the use of apnoea protocols, which enable data acquisition during either the end-inspiratory or end-expiratory phase, thereby reducing diaphragm movement. However, their application is restricted to short-duration scans (less than one minute). One of the most common artefacts related to breathing is ‘lesion deregistration’. This phenomenon has the potential to result in an erroneous diagnosis. Specifically, the respiratory movement can produce a visual illusion that there is a liver lesion at the base of the lung, simulating a pulmonary nodule, as shown in Figure 2.7.

Tissue/Organ/Structure	Typical Motion (mm)
Lung / Lung tumour	0–22 (10 ± 7)
Heart	4–24 (12.4 ± 6)
Liver	10–26 (15 ± 6)
Spleen	5–20 (13)
Pancreas	13–42 (20 ± 10)
Kidney	1–25 (14 ± 7)
Diaphragm	9–27 (16 ± 9)
Abdominal wall	5–19 (10 ± 4)

Table 2.5: Representative values of respiratory-induced displacement for various tissues and organs. The reported values correspond to maximal motion (mean ± standard deviation) observed along one of the main orthogonal directions, typically in the cranio-caudal axis [19].

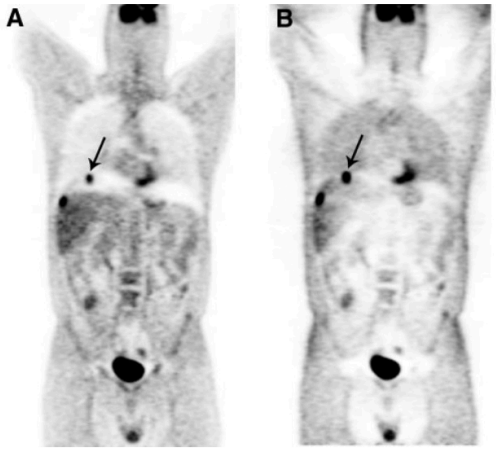

Figure 2.7: (A) 58-year-old patient with colon cancer. Lesion at the dome of the liver appears mislocalized to the right lung due to respiratory motion. (B) image without attenuation correction confirms that all lesions are actually confined to the liver [6].

Effects on the image

The artefacts associated with the types of movement described above typically manifest as image blurring, reduced contrast between organs, dispersion of activity and incorrect positioning of lesions (ghosting effect). In PET, the choice of radiopharmaceutical can also significantly influence the type and extent of motion artefacts, due to differences

in the biodistribution and kinetics of the tracer. In tumour assessment studies, patient movement has been demonstrated to result in a variation in PET quantification of up to 35% for a 5 mm tumour and up to 10% for a 10 mm tumour [19].

3

PET scanners: from Traditional Technology to the State-of-the-Art

As outlined in the previous chapter, the main applications of conventional PET scanners lie in oncological imaging. In this context, these systems are primarily employed for the detection and diagnosis of small tumor lesions, for the evaluation of their staging or restaging, and for the planning of personalised treatments tailored to each patient.

3.1 Multimodality hybrid imaging

Over the past two decades, there has been a growing interest in multimodal hybrid imaging. This evolution is attributable to the recognition that combining functional imaging with anatomical imaging modalities can yield substantial benefits from both clinical and technical perspectives. The primary objective has been to leverage the strengths of each technique to obtain the maximum amount of diagnostic information in a single acquisition session, thereby reducing the overall duration of the procedure and accelerating the therapeutic decision-making process. Functional imaging methods including SPECT and PET have been combined with morphological imaging methods such as computed tomography (CT) and magnetic resonance imaging (MRI) to provide a combination of the former's high molecular sensitivity and the latter's high spatial resolution and contrast. This development has resulted in the acquisition of images that exhibit highly precise and well-defined anatomical details of the patient's morphology [2].

PET/CT

The development of hybrid positron emission tomography-computed tomography (PET/CT) systems was guided by the primary objective of acquiring high-quality diagnostic in-

formation without compromising patient comfort or excessively prolonging scan times. Notably, the first prototype PET/CT scanner system was developed in 1998 and subsequently made commercially available in 2001. This advanced tool introduced the concept of 'anatometabolic' imaging, a term first coined in 1993 by Wahl et al. to describe the fusion of FDG PET images and CT scans [2]. Even though this technology has many advantages, it's important to take into account also its drawbacks. It is important to note that exposure to elevated levels of ionising radiation, in comparison to alternative methods, has been identified as a significant potential risk factor, particularly in cases where repeated examinations are conducted for the purpose of therapeutic monitoring. This is of particular relevance for paediatric patients, whose tissues are still developing and therefore more sensitive to the biological effects of radiation.

3.2 Short Axial Field-of-View PET scanners

While hybrid imaging modalities have expanded the diagnostic potential of PET, conventional PET scanners are still constrained by a limited short axial field-of-view (SAFOV), generally between 15 and 30 cm. This range is sufficient to cover the region of the body required for the examination, but only by adopting either sequential acquisition techniques, such as the 'step-and-shoot' (SS) mode, or by using the more recent Continuous Bed Motion (CBM) acquisition mode [9]. Among the main limitations associated with a short AFOV is the low signal collection efficiency. Approximately 85-90% of the patient's body typically lies outside the scanner's AFOV. Moreover, even within the scanned region, only about 3-5% of the available signal is effectively detected. Thereby, this technological parameter not only represents a key criterion for classifying the different PET systems currently available on the market, but also has a direct impact on both the performance of the scanner and the overall efficiency and organization of the clinical workflow.

3.2.1 Long acquisition time vs high scan demand

One of the limitations of conventional PET scanners is the prolonged acquisition time required to obtain whole-body images. This result can only be achieved by the use of sequential acquisition techniques, which not only extend the overall scanning duration but also increase the complexity of clinical workflow management. These limitations, combined with the low signal collection efficiency, make SAFOV-based PET systems poorly inadequate to meet the growing global demand for PET examinations. In this

context, a study conducted by the Netherlands Cancer Institute (NKI-AVL) revealed a continuous increase in the number of PET/CT scans performed between 2004 to 2024, reaching a peak of over 5000 scans per year in 2018.

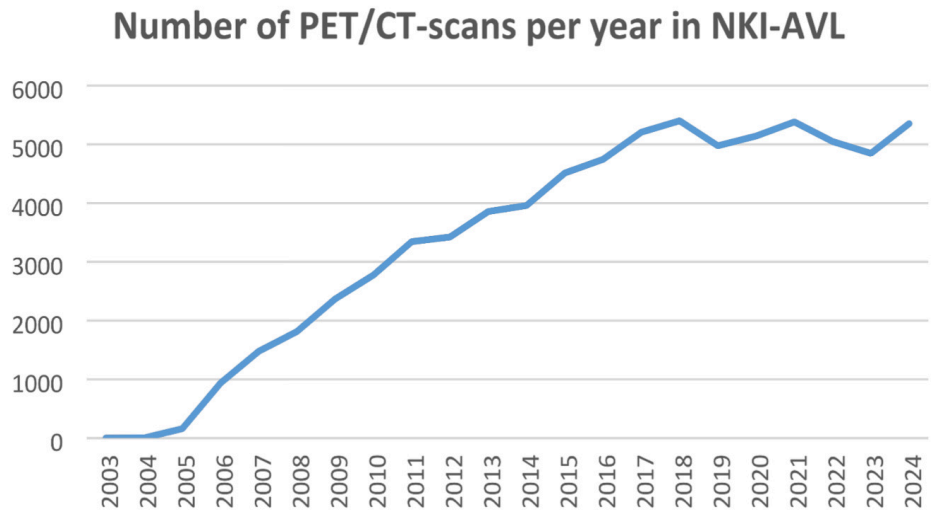

Figure 3.1: The rising use of PET/CT at Netherlands Cancer Institute – Antoni van Leeu- wenhoek Hospital (NKI-AVL) [7].

The upward trend, shown in Figure 3.1, can be attributed to several factors, including the rising incidence of oncological diseases, the development of novel radiotracers, and the implementation of increasingly extensive follow-up protocols. A temporary decline in the number of scans was observed only during the COVID-19 pandemic, mainly due to restrictions related to healthcare personnel availability and hospital operational capacity. As PET/CT imaging is progressively becoming a routine clinical tool for a growing number of patients, no longer limited to selected cases, this increase in demand has placed considerable pressure on PET centres still relying on SAFOV-based systems. A common strategy adopted to deal with this situation has often involved reducing the acquisition time per patient in order to increase the daily number of examinations, frequently at the expense of image quality [7, 9].

3.3 Long Axial Field-of-View PET scanners

In recent years, numerous technological innovations have been introduced to overcome the limitations of SAFOV technology, such as low sensitivity, reduced spatial resolution, and long acquisition times, in order to improve scanning performances. A significant

contribution to this technological evolution has come from advancements in detector design, in particular the progressive replacement of traditional PMTs with SiPMs. The integration of SiPM technology has enabled remarkable improvements in PET system performance, mainly by optimising TOF resolution, currently in the range of 210 to 300 ps, and significantly increasing system sensitivity to values approaching 20 kcps/MBq, as shown in Figure 3.2.

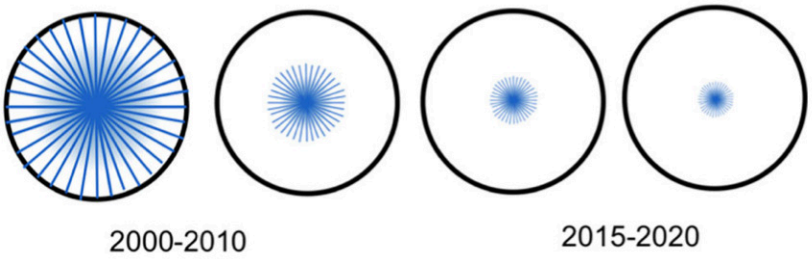

Figure 3.2: Effective sensitivity improved by TOF. This is one of the most significant developments in PET technology in the last three decades [8].

Furthermore, the compact dimensions of SiPMs have also allowed the use of scintillation crystals with cross-sections smaller than 4x4 m^2, resulting in a significant improvement in spatial resolution (see Figure 3.3).

Figure 3.3: Improvement in spatial resolution achieved by replacing 4-6 mm pixels with PMTs with 3-4 mm pixels with SiPMs [8].

The combination of enhanced TOF capabilities, increased sensitivity, and higher spatial resolution has led to a relevant improvement in SNR combined with a significant reduction in image noise. These advancements have resulted in substantial benefits in terms of image quality and diagnostic accuracy, thereby contributing to the enhancement of the effectiveness and efficiency of digital PET systems in routine clinical practice.

The most recent and revolutionary innovation in this technological landscape includes the extension of the PET scanners' AFOV. The latest generation of PET systems has

achieved an AFOV ranging from 64 to 194 cm, thereby establishing the foundation for the development of long axial field-of-view (LAFOV) PET scanners [20]. This extension of the FOV is sufficient to cover the majority of clinical studies, both oncological (e.g. lung cancer, lymphoma) and non-oncological (e.g. vasculitis), allowing images to be acquired in a single bed-position. The first LAFOV PET system was introduced in 2018 by United Imaging with uExplorer. This device provides an AFOV of 194 cm, allowing complete coverage of the body from head to toe in a single scan acquisition [21]. This technology is currently expanding and is already being used in various research centres and hospitals worldwide. The ability to acquire a total body scan within a single field of view offers a substantial reduction in acquisition time. To illustrate this point, consider the SAFOV Biograph Vision scanner (AFOV 26 cm). To cover an extension of 106 cm, it is necessary to perform several scans (multi-bed), taking approximately 16 minutes, with a time of 2 minutes per scan position. On the other hand, with a LAFOV system such as the Biograph Vision Quadra, comparable images can be acquired in just 2 minutes thanks to the extended coverage of the entire region of interest in a single bed-position.

In contrast to Total-Body (TB) PET systems, which are often characterised by considerable size and high manufacturing costs, LAFOV PET scanners represent an intermediate solution between conventional SAFOV systems and the most advanced TB PET systems. The extension of the AFOV, obtained through the addition of extra detector rings, results in a substantial increase in the volume of the patient's body that can be scanned per unit time (up to four times greater than that of conventional SAFOV systems) and also in a significant improvement in system sensitivity, which can reach values 10 to 40 times higher than those achievable with traditional SAFOV scanners. This effect is primarily related to the wider acceptance angle for 511 keV annihilation photons, leading to a more efficient collection of the emitted signal and, consequently, improved image quality and reduced acquisition times. Figure 3.4 provides a graphical representation of the different AFOVs of the main PET systems, with a qualitative and quantitative comparison in terms of body coverage.

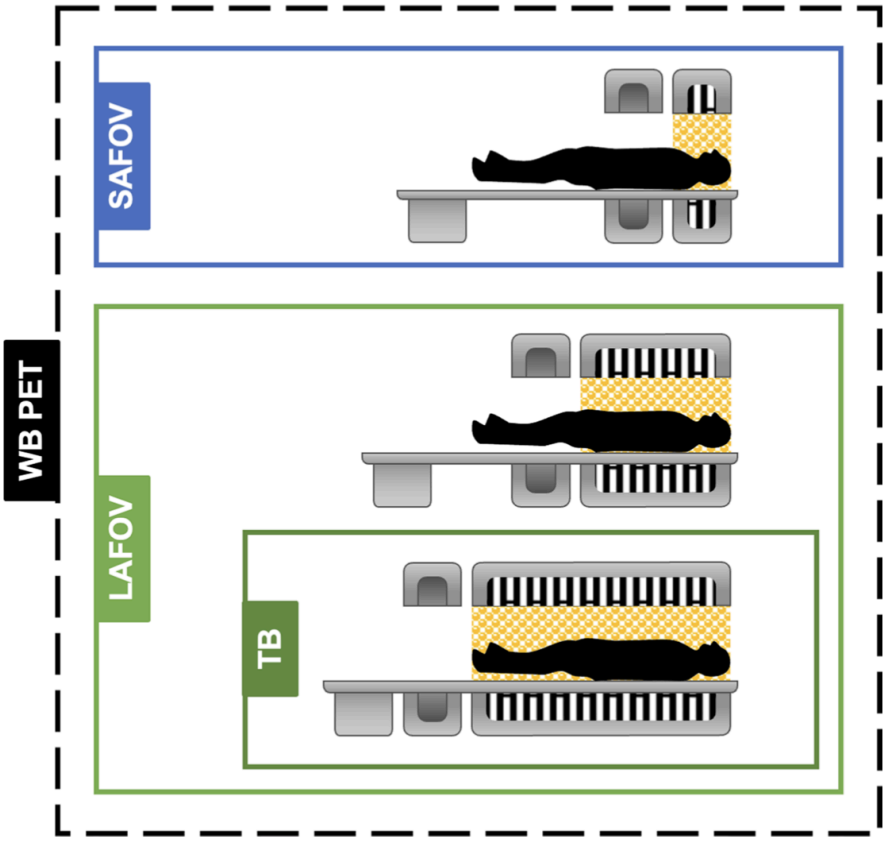

Figure 3.4: Graphic representation of the axial field-of-view of several PET/CT scanners, based on the clinical classification. SAFOV: short axial field of view. LAFOV: long axial field of view. TB: total body [9].

3.3.1 State-of-the-Art performances

Sensitivity and Spatial resolution

One of the main advances introduced by LAFOV PET/CT systems is their significantly enhanced sensitivity, achieved through extended AFOV, which provides a larger axial acceptance angle for the detecting coincidence photons. LAFOV scanners can measure a higher coincidence photon count rate per unit of injected activity than conventional SAFOV PET/CT systems. Better count statistics and increased sensitivity enable the development of customised clinical protocols for LAFOV systems, optimising the balance between injected tracer activity, PET acquisition time and image quality [22]. As mentioned in Section 3.3, using smaller scintillation crystals with cross-sectional dimensions of less than 4x4 m^2 enables the detection system to achieve a higher spatial

resolution. This technological advancement allows for sharper and more detailed images, enhancing lesion detection and diagnostic accuracy while reducing false positives [20].

Lesion detectability

Even though sensitivity and spatial resolution are two distinct parameters that are affected by different technological factors (the reduction in detector crystal size and the extension of the axial field of view, respectively), when combined, these significantly improve lesion detection capabilities in LAFOV PET/CT systems. The inability to detect metastatic tumours smaller than 5 mm represents a significant limitation of conventional FDG-PET/CT scans, primarily attributable to their reduced spatial resolution and low sensitivity. In contrast, LAFOV PET/CT systems have been shown to be particularly effective in the detection of micrometastases and low-density tumours. One of the key advantages of LAFOV systems is the significantly elevated SNR observed in the reconstructed images, which contributes directly to improved diagnostic accuracy. This enhanced SNR enables more accurate identification of small lesions, even in critical anatomical regions, such as near the diaphragm, where respiratory movements are significant. In addition, the extended axial coverage of LAFOV scanners allows for comprehensive whole-body imaging in a single acquisition, facilitating the detection of metastatic spread to more distal regions, including the extremities. Furthermore, the extended AFOV facilitates extensive scanning, enabling the detection of metastases in distant body regions, such as the limbs. In certain oncological cases, such as renal carcinoma or sarcomas, where there is a higher probability of distant metastases, this is a significant benefit [23].

Acquisition time

The expansion of the body volume scanned in a single acquisition results in a significant reduction in acquisition times, which is another important benefit. Recent research has revealed that the complete imaging procedure, including the patient's arrival and exit from the acquisition room, can be completed within approximately ten minutes using this technology. It is evident that this reduction in scan duration offers several clinical advantages. In addition to reducing respiratory motion-related artefacts, this method also minimises the impact of other patients' involuntary movements, such as bowel or bladder movements. This reduces the possibility of anatomical mismatch with the related CT acquisitions [7].

Furthermore, in certain patient populations, such as paediatric patients, patients affected by dementia, or those with neuromotor disorders, the reduction in scan time could potentially reduce or even remove the necessity for sedation. This improvement in clinical workflow efficiency is attributable to a reduction in the need for post-procedural monitoring and recovery, as well as a decrease in overall examination time [22].

Effective dose

Recent studies have shown that the high sensitivity of LAFOV systems allows for a significant reduction in patient's radiotracer dosage without a substantial decrease in diagnostic image quality. This reduction in dosage offers novel opportunities, particularly within clinical settings where the reduction of radiation exposure is critical, such as in pregnant women or paediatric patients. Particularly in paediatric patients, it is crucial to minimise radiation exposure, given the increased sensitivity of developing tissues and the potential for ionising radiation to induce secondary neoplasms. These concerns are further supported by the existing literature, which establishes a correlation between early exposure to ionising radiation and an elevated risk of juvenile leukaemia.

A recent study involving 100 paediatric patients has shown that the TB uEXPLORER system can be used to perform half-dose PET protocols, with additional reductions down to 1/20 of the usual reference dose, while preserving diagnostically acceptable image quality. This would result in the effective dose of a paediatric PET scan being reduced to a level that is significantly lower than current guidelines, ranging between 0.18 and 0.26 mSv, as outlined in [10]. As reported in a separate investigation involving 18 children, the lower limit for injected activity for delayed total-body PET with 18F-FDG could be reduced to 0.5 MBq/kg without any significant impact on image quality [10]. The findings were further supported by a simulation research study that utilised the uEXPLORER TB PET system on a 12-year-old paediatric cancer patient. The study demonstrated that the elevated SNR of TB PET allowed for image quality to be maintained at 0.5 MBq/kg, even increased noise levels resulting from reduced injected activity, as illustrated in Figure 3.5 [22, 9].

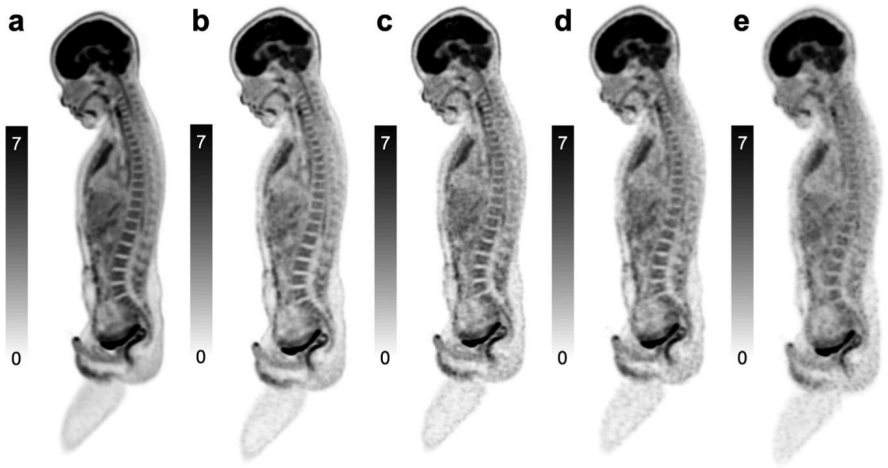

Figure 3.5: Low-dose [^{18}F]FDG images from a total-body PET scan of a 12-year-old patient with lymphoma. Sagittal PET-only images illustrate simulated dosage reductions: (a) 4 MBq/kg, (b) 1 MBq/kg, (c) 0.5 MBq/kg, (d) 0.25 MBq/kg, and (e) 0.125 MBq/kg. Image noise increases noticeably at lower activity levels [10].

From an operational perspective, the reduced radiotracer dosage in LAFOV PET systems offers several advantages, particularly in terms of enhancing radiological safety for medical personnel and hospital infrastructures. The decrease in radiological exposure to medical staff, who come into contact with patients post-injection, enhances radiation protection conditions. Additionally, the structural configuration of PET facilities may be influenced by the adoption of reduced dosage. In particular, less stringent radiation shielding would be required in areas where patients wait and receive the radiotracer, potentially reducing construction and modification costs of these areas. From an economic perspective, the ability to administer a reduced quantity of radiotracer in each examination has the potential to optimise operational expenses related to the production and administration of radiopharmaceuticals. A reduction in the quantity of radiotracer per patient would allow for an increase in the number of examinations that could be conducted using the same production batch, as tracer production represents one of the most significant costs in nuclear medicine departments, especially in the oncologic field. This would result in a reduction in the cost per dosage administered and an optimisation of radiopharmaceuticals efficacy [24].

3.3.2 Main limitations

Despite the potential of these systems to bring significant benefits to molecular imaging, their adoption in clinical centers may still be limited by several constraints, in particular related to their high cost and infrastructure requirements. These factors may prevent their acquisition by hospitals and consequently slow down their diffusion in healthcare facilities. The main limitations and drawbacks associated with LAFOV PET/CT systems will be discussed below, starting with an economic analysis, followed by ethical considerations and concluding with an examination of the crucial role played by medical personnel during the entire scanning procedure.

Cost and infrastructure

The installation of LAFOV PET/CT systems represents a considerable economic and infrastructural challenge for healthcare facilities, both in terms of initial investment and long-term management. Indeed, the initial purchase of these devices requires significant financial resources, with costs often exceeding 5 million dollars, not to include ongoing maintenance, infrastructure customisation and system management. From an infrastructural perspective, the implementation of LAFOV PET/CT systems in clinical settings requires a careful reorganisation of hospital space to accommodate both the increased physical dimensions of the scanner and the increased patient throughput. It is generally recommended that the dedicated area should be a minimum of 10x5 m^2, although some studies report that the installation of LAFOV PET/CT systems may require up to 200 m^2 [25]. This could represent a critical limitation, particularly for small- and medium-sized hospitals or for healthcare settings in developing countries. Furthermore, the significant heat generated by these scanners during operation often requires dedicated cooling systems, such as water-based refrigeration units, adding to the complexity and cost of the installation. In addition to spatial constraints, the installation of LAFOV PET/CT scanners has specific technical requirements, such as an adequate power supply to support both the imaging system and the computing infrastructure required for image reconstruction and processing. The significant amount of data generated by each scan (approximately 40–50 GB per examination) requires healthcare facilities to implement advanced IT infrastructures capable of storing, processing and securely managing large amounts of data. This often necessitates the implementation of scalable and high-performance storage systems, which can result in a significant increase in operational costs over time and may require additional upgrades to the existing electrical and data network infrastructure. A further critical aspect to consider is

the management of patient areas. The higher throughput associated with these scanners requires adequately sized waiting, changing and reception rooms. To ensure an efficient workflow and compliance with radiological safety regulations, previous studies suggest the availability of at least six dedicated rooms for patient management, including preparation and changing facilities [26, 25, 24, 27].

Ethical and affordability constraints

From an ethical perspective, the introduction of LAFOV PET/CT systems raises significant concerns regarding the potential risk of exacerbating global health inequalities. While developed countries are expected to benefit from enhanced diagnostic efficiency and image quality, low- and middle-income countries risk being further marginalised due to limited access to advanced imaging technologies. The World Health Organization (WHO) has reported that access to PET scanners is highly unequal across different regions. The data shows that just 3% of upper-middle-income countries and 4% of lower-middle-income countries have at least one PET scanner per million inhabitants. This is in strong contrast to the 29% of high-income nations that have access to such technology. Thereby, the considerable costs and demanding infrastructural requirements of LAFOV PET/CT systems have the potential to exacerbate this technological divide. Furthermore, the availability of radiopharmaceuticals, which are essential for PET imaging and require specialised equipment such as cyclotrons, remains a major barrier in resource-limited settings. These resources are often scarce or entirely absent in countries with limited healthcare infrastructure, making access to PET imaging, and particularly to LAFOV systems, even more challenging [28, 29].

Patient positioning and the role of medical personnel

The introduction of LAFOV PET/CT systems not only implies significant economic and infrastructure investments, but also profoundly impacts the operational management of diagnostic procedures, requiring a reorganisation of workflows and a greater involvement of specialised medical personnel. Patient positioning has become more critical to the PET scan workflow in LAFOV systems. Although positioning issues affect both LAFOV and SAFOV systems, LAFOV systems' significantly faster acquisition times shift the balance. As scanning speeds up, the time spent positioning the patient accounts for a comparatively larger portion of the overall procedure duration. Ensuring correct patient positioning is essential to provide full coverage of the anatomical regions of interest and to minimise artefacts caused by involuntary movement. This process

often requires longer preparation times and the involvement of more medical personnel. In particular, radiographers and nuclear medicine physicians must have advanced skills, not only in patient management, but also in the use of positioning tools and immobilisation systems specifically designed for LAFOV imaging. Moreover, the operational complexity of these systems is further increased by the integration of advanced positioning technologies, such as laser guidance systems, optical sensors, and 3D tracking solutions. While these technologies can contribute to improving the precision of patient alignment, their correct use requires dedicated training and constant supervision by highly qualified personnel. In conclusion, the clinical integration of LAFOV PET/CT systems requires not only technological adjustment, but also a significant effort involving the employment and training of specialised medical personnel capable of managing the complexity of these devices and ensuring optimal patient care throughout the diagnostic procedure.

4

Walk-Through PET scanner

As outlined in Chapter 3, despite notable advancements in wide AFOV systems, such as LAFOV PET/CT and TB PET scanners, designed to acquire whole-body images in a single slice acquisition to address limitations of earlier SAFOV PET/CT scanners, constraints related to the conventional cylindrical geometry of these systems persist. As previously discussed, although the scan times have been significantly reduced through the adoption of long AFOV and one-shot imaging techniques, the time required for medical personnel to instruct patients and position them accurately within the scanner remains substantial. This not only increases the demand for specialised medical personnel in the examination room, resulting in higher operational costs, but also contributes to greater radiological exposure for personnel, due to extended proximity to the radioactive patient. Moreover, the cylindrical structure of the scanner and the circular gantry geometry necessitate a large number of detectors and silicon photomultipliers to achieve adequate body coverage and acquire a good quality image. It is particularly significant to note that the electronics associated with these systems represent the main cost items, in addition to installation and maintenance costs. The combination of these factors has resulted in the widening of two distinct gaps: a technological gap, defined by the disparity between the increasing demand for PET imaging and the limited performance capabilities of current systems in terms of time; and an economic gap, driven by the discrepancy between the rising need for PET examinations and the limited number of clinical and research institutions able to afford such costly technologies. According to an article published by Global Banking and Finance Review, the molecular imaging market is set to expand at a compound annual growth rate (CAGR) of approximately 11.3% between 2021 and 2031, reflecting the robust expansion within this sector [30]. This trend not only underscores the increasing importance of molecular imaging in the early cancer detection and evolution of personalised therapeutic approaches, but also highlights the urgent need to address key limitations, such as high development and

service costs and low patient throughput, which have the potential to compromise the sector's future expansion. In response to these challenges, the Medical Imaging and Signal Processing (MEDISIP) research group at the Ghent University is developing a new PET scanner model with a novel design, inspired by the concept of flat panel scanners introduced in the airports for passenger security screening [31].This new system, known as the Walk-Through PET, proposes a paradigm shift in scanner geometry and workflow. The concept behind the new scanner model and the current mock-up design is illustrated in Figure 4.1.

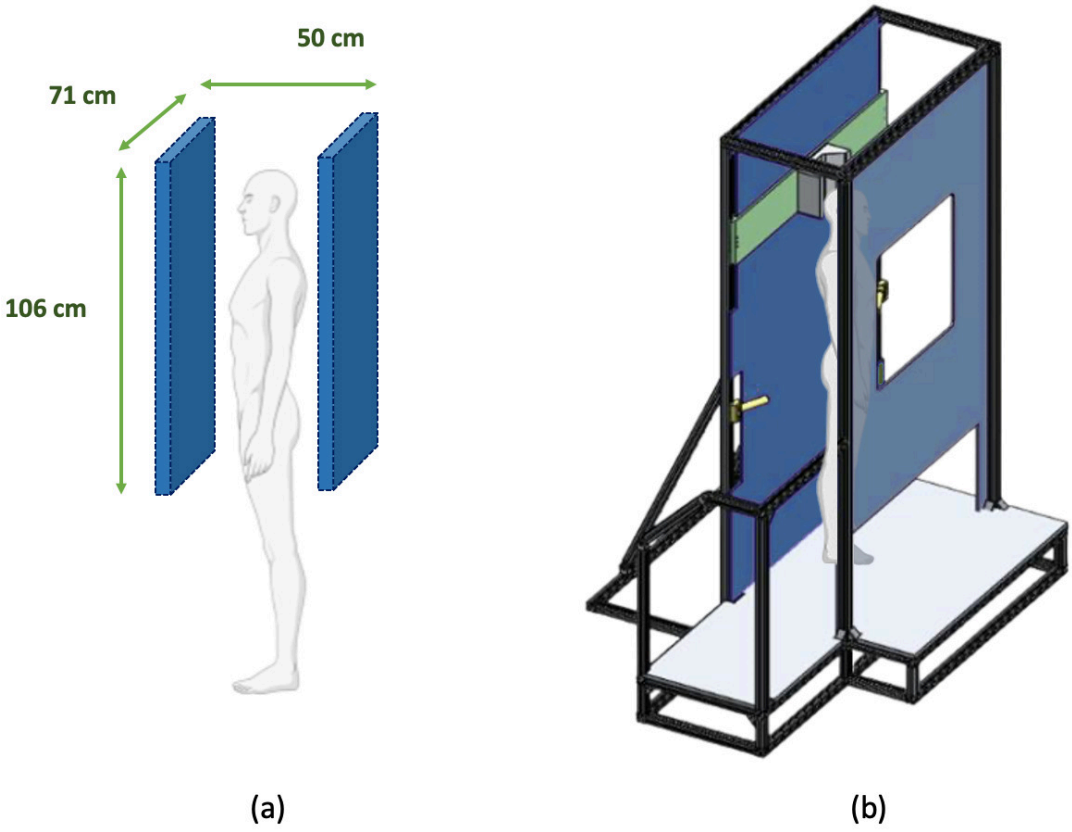

Figure 4.1: (a) The Walk-Through PET concept with panel dimensions. (b) Current design of the Walk-Through PET mock-up, including ergonomic components such as headrest and handlebars to provide enhanced patient support.

A detailed analysis of this system under development is presented in Chapter 4. Starting from the design concept, the mock-up's components will be described, concluding with a discussion of the main structural and technological innovations that overcome the limitations of conventional PET scanners. The chapter also addresses the current

limitations of the novel system and the ongoing research efforts aimed at overcoming them in future work.

4.1 Design concept and current mock-up system

4.1.1 Flat panel design

The primary practical throughput limitation of TB-PET systems is the requirement to position the patient in a supine position on the bed, a process that is both time-consuming and constrained by the lack of specialised medical personnel required to perform it effectively. To this end, a new design model has been developed. This new design allows patients to remain in an upright position during the acquisition phase, eliminating the need for a bed to be integrated into the scanner. The newly developed system, known as Walk-Through PET (WT-PET), derives inspiration from the security screening procedures employed in airports, which make use of millimetre wave scanners and planar radiography. These technologies have demonstrated a high level of efficiency in terms of throughput, as they can scan multiple subjects per minute. The WT-PET scanner is composed of two detector panels that are positioned vertically, 50 cm apart. Each detector panel measures 71 centimetres in width and 106 centimetres in height. During the scan, the patient is asked to stand still between the two panels. The dimensions of the panels were initially determined by referring to the anthropometric data reported in the volume *'Body Space: Anthropometry, Ergonomics, and the Design of Work'*, with the objective of developing a device that is aligned with the characteristics of the user and the task to be performed [31]. The result was a system that had been designed according to a patient-centred approach. The aim of this design was to optimise the patient experience and diagnostic performance. Guided by a clinical rather than purely research-based objective, it was decided to restrict the axial field-of-view (AFOV) of the scanner from the head to the proximal portion of the thighs, thus including the entire torso. This axial extension, equal to 106 cm, was defined with the aim of maximising the system's efficiency in cancer diagnosis, as it allows the inclusion of the organs with the highest incidence of cancer, according to data from the World Cancer Research Fund (2020) [32]. The WT-PET system could also facilitate whole-body imaging through continuous vertical movement of the detector panels, enabling scanning of the lower limbs without the need for patient repositioning or the use of additional mobile components.

4.1.2 Detector choice

The latest design allows for 12x14 detectors per panel, each consisting of a 50x50x16 m^3 monolithic LYSO scintillation block, coupled to an 8x8 array of 6x6 m^2 SiPMs [31]. In addition to the innovative structural design, a key factor in the overall improvement in performance, in terms of cost, sensitivity and spatial resolution, was the decision to replace traditional pixelated scintillator crystals with monolithic crystals. In the majority of clinical PET/CT systems currently in use, detectors consist of pixelated scintillator crystals, typically made of LYSO or BGO, with dimensions of 3–4 m^2 and a thickness of approximately 20 mm. Despite their well-established use, these configurations are limited in their capacity to provide information on DOI and to ensure high overall (2D) spatial resolution. However, monolithic detectors represent a highly promising alternative. In contrast to pixelated detectors, where each module consists of a matrix of scintillating crystal pixels coupled directly to an array of SiPMs, monolithic detectors employ a single, continuous scintillating crystal block, which is also coupled to a matrix of SiPMs. This new type of detector offers enhanced performance, particularly in terms of better spatial resolution and the ability to extract DOI information. The latter function is enabled by the fact that the scintillation light, no longer constrained by the pixel size as in pixelated detectors, can spread within the block and be analysed in its spatial distribution, thereby providing information regarding the depth of interaction and favouring a higher positioning resolution. The WT-PET configuration currently utilises monolithic LYSO crystals with dimensions of 50x50x16 m^3. Figure 4.2 depicts a schematic representation of monolithic LYSO detectors used for WT-PET vertical panels.

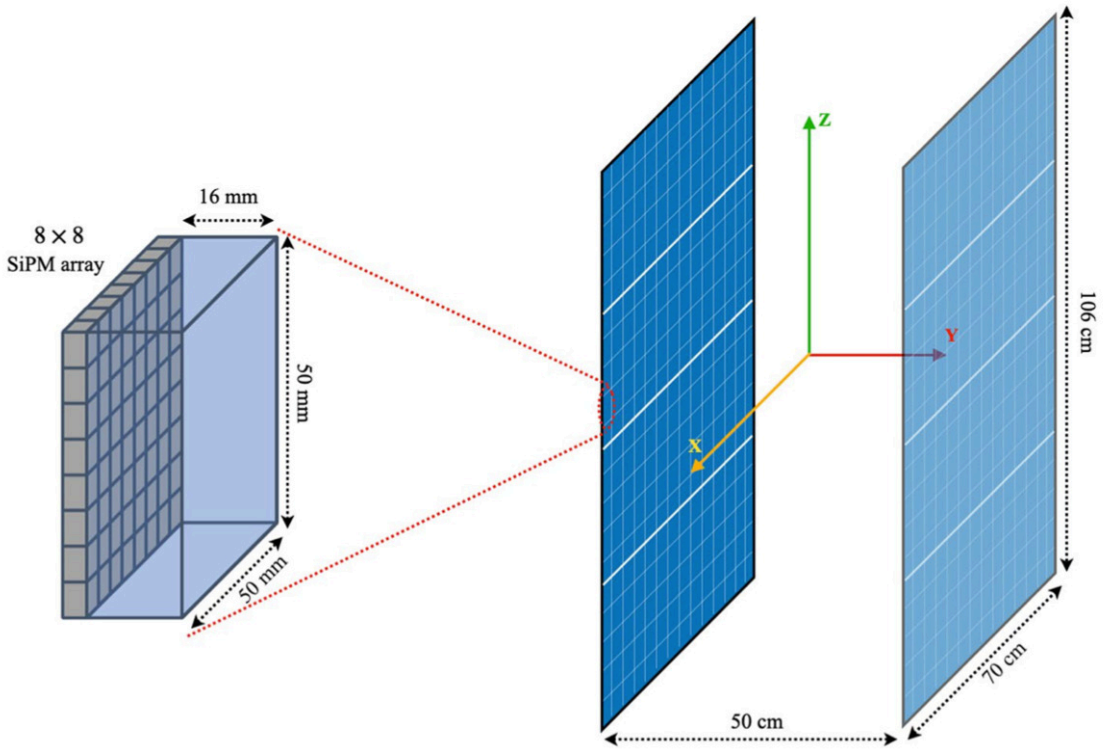

Figure 4.2: A schematic representation of an 8x8 SiPM array connected to a single LYSO monolithic detector (left). Each of the two flat panels that make up the scanner is composed of 14x20 monolithic detectors (right) [11].

It is notable that the adoption of these detectors, which exhibit a spatial resolution close to 1 mm, results in an overall system spatial resolution of approximately 2 mm [1]. The use of monolithic detectors also allows the detector panels to be positioned as close as possible to the patient. While this was not a possibility with pixelated detectors, due to the resultant high parallax error, since monolithic detectors have DOI capabilities, this is no longer a significant issue for them. This approach has been demonstrated to significantly enhance the sensitivity of the system, thereby increasing the probability of detecting annihilation events [31]. Another improvement, although is relatively minor compared to the others benefits offered by monolithic detector technology, is the partial reduction in the effect of photon acollinearity, which is achieved indirectly through improved spatial resolution. Using monolithic detectors allows the panels to be positioned closer to the patient, reducing the distance that annihilation photons must travel, thereby reducing the impact of photon acollinearity on the overall imaging performance [31, 1].

Another fundamental aspect of the design is the choice of LYSO crystals, which offer superior performance in the context of TOF technology, enabling greater effective sensitivity. This approach has been demonstrated to enable the preservation of comparable image quality while utilising half the number of detected events. With regard to TOF temporal resolution, researchers are currently aiming to achieve a TOF of approximately 300 ps. Furthermore, a 30-second acquisition time was hypothesized as a potential target for future PET scanning procedures, with the aim of increasing patient throughput in nuclear medicine departments. Currently, patient flow is significantly constrained by the positioning process within conventional PET scanners, which contributes to a total examination time of approximately 5 to 10 minutes in typical LAFOV systems.

4.1.3 Integration with stability support

While the patient's upright positioning has yielded numerous benefits, including simplified patient positioning, reduced reliance on medical staff in the scanning room, and enhanced patient throughput, recent studies on body motion have revealed that the novel positioning's method can introduce variability in movement, particularly in the shoulders and chest, when compared to the standard PET scanner. This phenomenon is likely attributable to the more open and less restrictive design of the WT-PET scanner [1]. For this reason, the current mock-up has been integrated with support elements aimed at increasing patient stability during the scanning phase, in order to reduce the consequent blurring effects on the acquired image. Firstly, the introduction of an ergonomic headrest to the back panel ensured greater patient stability. The equipment is affixed to a vertically adjustable structure, which can be adapted to each scan according to the patient's height. Secondly, handlebars were incorporated into the design. The primary function of these components is to provide enhanced support to the patient during the scan procedure. These are also adjustable according to the patient's height. Once positioned between the two panels of the mock-up scanner, the patient is asked to hold the two handles, and with the assistance of the medical technician, these are adjusted if they do not match the patient's height perfectly, in order to achieve maximum comfort and immobility during the 30-second examination. Finally, the patient's positioning is assisted by footprints that have been printed on the platform, thereby implicitly guiding him into the correct position. The primary objective of integrating these elements was to enhance patient composure during the scan, with the aim of minimising head and shoulder movement and ensuring the acquisition of superior quality images. Secondly, the objective is also to make the system as intuitive and user-friendly as possible, in

order to facilitate patient's comprehension of the examination at all stages, thus also reducing the involvement for medical staff in the scanning room.

4.2 Performance analysis: potential and strengths

4.2.1 High patient throughput

The WT-PET scanner, currently under development, has been designed to reduce the time required not only for the scanning process but for the entire clinical procedure, thanks to its novel upright configuration, flat panel detector design, and long AFOV. From a temporal perspective, it has been demonstrated that, by adopting an image acquisition time of 30 seconds, the total interval required between consecutive patients is limited to approximately 3–5 minutes [1]. This high efficiency enables a patient throughput estimated to be about 4–5 times higher than that of conventional PET/CT systems, with the potential to scan up to 100 patients in a standard working day [33]. This is particularly significant given the current clinical environment, which is marked by a constantly rising need for PET scans.

4.2.2 Smaller footprint

The compact and vertically oriented design of the WT-PET system is another relevant feature. This design leads to a significantly smaller installation footprint than traditional LAFOV systems, which usually require a dedicated area of approximately 35–40 m^2. The mock-up's actual dimensions are 2.3 meters high by 2 meters wide by 1.5 meters deep [1] . This makes it possible to redesign the clinical setting more effectively. For example, in a floor plan of 6.5x5 m^2, the space previously allocated to the scanning room alone could instead accommodate a waiting area, a preparation room, and the acquisition area, thereby improving both workflow and logistical comfort for clinical personnel and patients, as illustrated in Figure 4.3 [31].

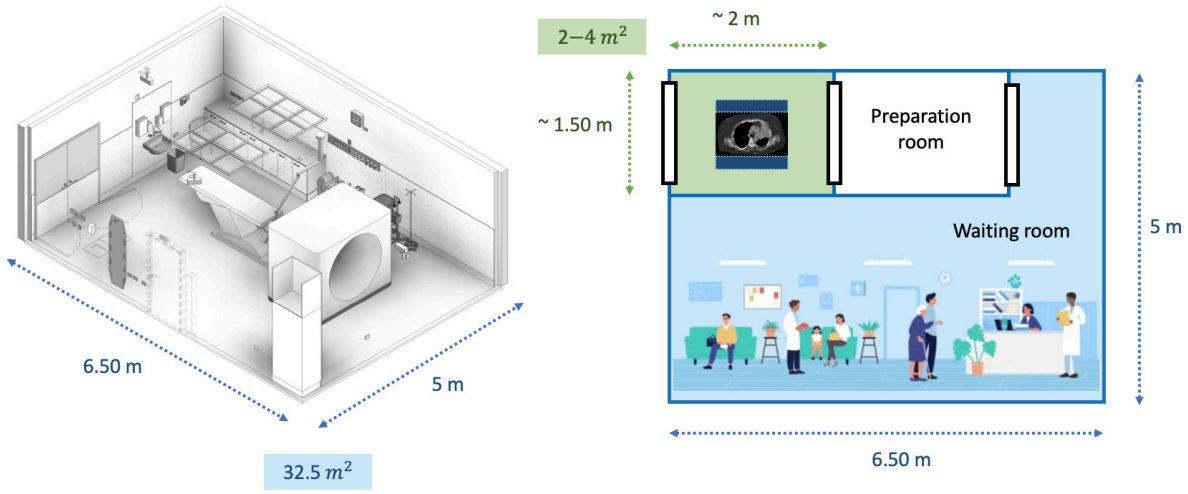

Figure 4.3: (a) Traditional PET/CT scanners require a large installation footprint. (b) The compact design of the WT-PET scanner enables more efficient use of space, allowing the PET/CT scanning room to be reconfigured into multiple functional areas, such as imaging, preparation, and waiting rooms.

4.2.3 Cost-effectiveness

In addition to enhancing image quality, the use of monolithic detectors together with the flat-panel design has enabled more effective utilization of the detectors. A comparison of the Siemens Vision Quadra system with the new WT-PET revealed that, with an equivalent AFOV of 106 cm, the novel flat panel model enables a 1.9-fold reduction in the number of detectors utilised, while preserving a sensitivity that is comparable to the conventional model [31]. This reduction is all the more significant when one considers that scintillator crystals, the SiPMs and associated electronics currently account for approximately 70% of the total cost of a PET scanner [31]. It is evident that the financial savings resulting from the utilisation of a reduced number of detectors are of considerable significance. It is first necessary to consider that conventional PET systems with an AFOV between 15 and 25 cm have an indicative cost of between 2 and 3 million euros. In comparison, TB-PET scanners, capable of covering up to 1–2 metres of the patient's body, can cost between 8 and 10 million euros, due to the large detection surface and the complexity of the electronics required. The WT-PET system, on the other hand, has been shown to offer an economically sustainable solution, with an estimated cost of around 4-5 million euros, while ensuring the same AFOV [32]. This

reduction therefore represents a highly advantageous opportunity for hospitals and research centres with limited financial resources, as it offers high-quality diagnostics at a significantly more affordable cost.

4.3 Main limitations

Despite significant performance improvements, WT-PET is still in the developmental stage and has certain limitations that need to be resolved. These issues are not only attributable to upright patient positioning during acquisition, but also to the system's unique geometry. Sections 4.3.1 and 4.3.2 will analyse in detail the main limitations currently associated with this novel scanner model.

4.3.1 Standing position and motion artefacts

Recent studies conducted by the MEDISIP research group at Ghent University have demonstrated that patients in a standing position could exhibit greater mobility than those in a lying position, resulting in lower image quality for PET scans. In addition to the increased sensitivity to motion artefacts, another inherent limitation of this scanner design is its unsuitability for certain patient populations, such as those who are bedridden or have reduced mobility. Such patients must therefore continue to rely on conventional PET systems for their examinations. As previously discussed in Section 2.3.5, during a PET acquisition, there is frequent exposure to both voluntary and involuntary, physiological and non-physiological patient movements. Such movements have the potential to compromise image quality to a significant level, with the resultant effects including blurring or contrast reduction of the lesion. This, in turn, can lead to inaccuracies in the definition of regions of interest (ROIs) and in the absolute quantification of standardised uptake values (SUVs) [1]. These artifacts, that are a well-known issue in conventional PET systems, in WT-PET become especially noticeable due to its improved spatial resolution (approximately 2 mm), which allows even the smallest details to be reproduced [1]. A recent advancement in this field has been enabled by the integration of ergonomic support components within the mock-up, including a headrest and handle bars. These elements have contributed to enhancing patient stability during the 30-second scan time, thereby improving comfort. Previous motion studies have shown that standing motion is comparable to that observed in the supine position within a conventional scanner [1].

4.3.2 Others

Among the additional limitations, which are primarily related to the practical and structural aspects of the new WT-PET model, it is important to mention also the potential loss of detectable events during acquisition. In contrast to cylindrical geometry scanners, which ensure 360° patient coverage, the WT-PET system is characterised by a physical opening of approximately 50 cm between the front and back panels. This open space causes an interruption in angular coverage, resulting in the loss of some projection angles. The detectors integrated into the vertical panels are only able to sample a limited angular range. This feature may result in the loss of some coincident events and the introduction of artefacts in the final image, potentially compromising image reconstruction. However, good TOF resolution can help mitigate these artefacts, thereby improving the overall diagnostic quality and reliability of the reconstructed image. A further structural limitation is attributable to the geometric mismatch between the WT-PET system and current CT scanners. In this regard, the MEDISIP research group at Ghent University is working specifically on the development of an innovative CT scanner design that can be coupled with WT-PET. The proposal entails a novel rectangular CT geometry, capable of scanning and acquiring 3D tomographic images during vertical translation movement [34]. This work thus opens up new possibilities for the development of a hybrid Walk-Through PET-Computed Tomography (WTPET-CT) design.

5

Animated 3D video guide for WT-PET scanner

Based on the knowledge acquired in the previous sections, this chapter introduces one of the main objectives forming the core of the thesis project, along with the methodology adopted for its development. It concerns the optimisation of the patient positioning phase that precedes the actual WT-PET scan. In order to achieve this objective, a 3D animated video guide has been developed with the intention of providing patients with clear and comprehensive instructions on the main preliminary steps to be taken, from correct positioning between the panels to the adjustment of the ergonomic components integrated into the system. The aim of this study is to reduce the workload on medical personnel, who is still heavily involved in these phases, while simultaneously speeding up the patient preparation procedure. This would result in a potential increase in patient throughput compared to the positive results already achieved with the introduction of the WT-PET prototype. This chapter will provide a detailed and structured description of the development process that led to the final animated 3D video guide, illustrating all the stages involved, from the initial design steps to the final implementation. The materials, software and tools used, as well as the methods for the integration of the scenes and frames produced, will also be analysed.

5.1 Identification of the key steps in patient preparation and positioning

The design of the video guide constituted the most time-consuming and technically challenging phase of the entire thesis project. A significant amount of time was invested in the preliminary planning stage, during which a detailed analysis was conducted of the

novel WT-PET scanner concept and the acquisition mechanism on which it is based. Particular attention was given to the main steps required for patient preparation and positioning, with the aim of creating a concise yet effective audiovisual product capable of providing all the necessary instructions for correct, almost autonomous positioning. First of all, it is useful to specify at which stage of the clinical pathway this video guide will be integrated. As instructional material, it will be shown to the patient, assisted by the medical technician, before entering the scanning room. The latter will be available to provide clarification and explanations in case of any doubts or difficulties in understanding the content. Based on this, the four main steps on which the video guide has been structured are outlined below.

5.1.1 Step 1: Initial positioning

The video begins with the patient entering the scanning room and being guided to stand between the two vertical panels of the mock-up, located on the platform. Here, the subject is asked to assume a comfortable and stable posture, starting with the correct positioning of the feet on the footprints marked on the platform, as shown in Figure 5.1.

Figure 5.1: Correct foot placement on the platform.

5.1.2 Step 2: Headrest adjustment

The second phase is one of the most crucial steps, as it establishes the foundation for ensuring optimal image quality. In this step, the patient is guided to check the height of the headrest, a support located on the back panel that can be adjusted vertically. Since the headrest height may not always be suitable for every patient, the medical technician will assist by adjusting it as needed. This ensures that the patient's head is

correctly positioned within the designed cavity. Figure 5.2 provides a visual illustration of this crucial step.

Figure 5.2: Headrest adjustment.

This procedure is adopted to minimize movement during the scan. However, it is crucial that a sufficient level of comfort is maintained: the head support must not exert excessive pressure, as this could cause discomfort and lead to patient motion during image acquisition.

5.1.3 Step 3: Handlebars adjustment

Once the headrest has been adjusted, same will be done for the handlebars. The current mock-up system includes adjustable handles located on either side of the back panel, supported by a mechanism that enables vertical movement according to the patient's height. The patient is asked to grip them tightly to ensure overall stability. Again, the technician's assistance may be required to ensure correct position, as depicted in Figure 5.3.

Figure 5.3: Handlebars adjustment.

5.1.4 Step 4: Scanning instructions

Once the correct position has been assumed, we move on to the description of the fourth and final step. This phase is directly linked to the second objective of the thesis. In this fourth step, the video guide will explain to the patient how the actual PET scan will take place, showing the projection of the 30-second timer video onto the front panel. Figure 5.4 provides a clear illustration of this final step.

Figure 5.4: Conclusive instructional scene.

This will guide the patient through the scan, asking him to remain as still as possible and to stare at a static red dot projected in the center of the screen, which has been introduced to reduce upper body motion. Finally, the patient will receive a visual notification informing him that the scan has been successfully completed. This will be followed by

an instruction to exit the platform.

5.2 Scripting: defining content and accessibility

Once the steps had been defined, we moved on to the scripting phase. This step played a pivotal role in the learning process, as it transformed the previously identified steps into verbal instructions, thereby providing essential support for the user's comprehension. The text that accompanies the video helps to make the message more direct, clear, and effective. Accessible language was chosen, avoiding technical terms and preferring simple and short sentences instead. A calm and reassuring tone was chosen with the aim of inspiring tranquillity in a potentially stressful clinical environment. Another significant aspect was determining the overall duration of the video guide, which was essential for properly calibrating the pace of the script. After several trials, a duration of ~2 minutes was determined to be optimal, allowing for pauses between sentences and ensuring good comprehensibility for patients. In order to make the product as applicable and usable as possible on a large scale, a series of accessibility strategies were adopted. Firstly, British English was chosen as the language for the initial version, as it is widely understood internationally. In addition, the structure of the script itself has been designed to include patients with sensory disabilities. For patients with hearing impairments, the script has been converted into subtitles synchronized with the video scenes to ensure clear understanding, even without audio. Furthermore, a descriptive audio track has been integrated to facilitate access for visually impaired or blind users. The online platform *Voicebooking* was used to create the voiceover. This is an online platform designed to generate AI audio tracks from written texts, with the option to adjust tone, pace and pauses to achieve a realistic, natural and engaging result.

5.3 Storyboarding

Once the script was finalized, the next stage of the creative process began with the creation of the storyboard. This phase was necessary to translate the textual content into a visual product and is commonly used by animators and directors to preview the narrative organization of the video content. The storyboard, a sequence of drawings and sketches, aims to visually represent each scene described in the script, thereby providing a concrete first draft of how the images will be organized. The *OneNote* application, which is included in the Microsoft Office package, was utilized for this task.

The primary objective was to ensure effective and clear communication of the message for each scene. With regard to the stages involving the adjustment of ergonomic supports, such as the headrest and handlebars, the initial proposal was to utilize half-length shots to highlight on the scene the adjustment of both components, as can be observed in Figure 5.5.

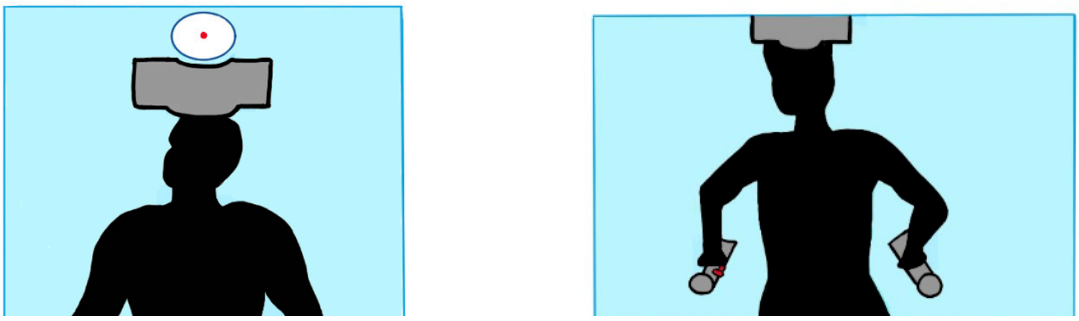

(a) (b)

Figure 5.5: Initial sketches produced during the storyboarding phase: (a) headrest adjustment, and (b) handlebars adjustment.

However, during the 3D modelling phase, it was decided to adopt closer shots, focusing directly on the areas of interest, such as the head and hands, to promote greater clarity and visual effectiveness. In Figure 5.6 some of the most significant drawings produced during this phase are shown.

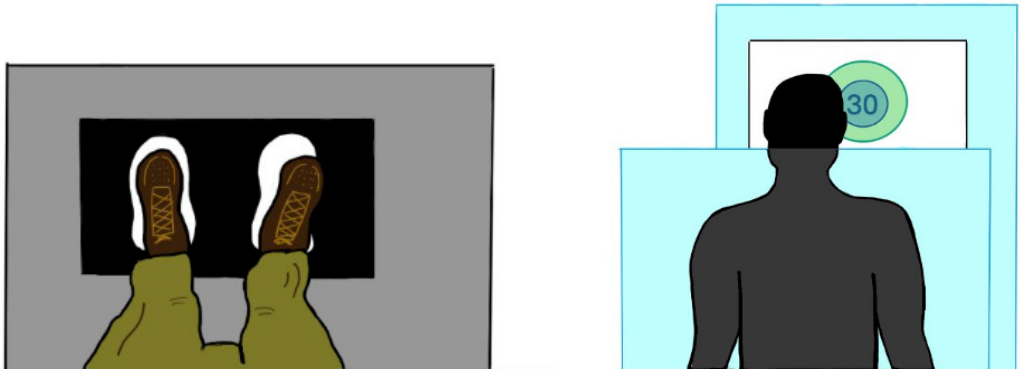

(a) (b)

Figure 5.6: Initial sketches produced during the storyboarding phase: (a) correct foot positioning, and (b) upright patient during a 30-second scan.

5.4 Planning and development of the 3D animation process

Initially, the focus was on 2D animation, employing the same technique as flipbooks. The concept involved the creation of a video animation consisting of a series of 2D drawings. The objective was to utilise video editing software to combine these sketches in a manner that would evoke the movement illusion, as observed in cartoons. However, it was decided to switch from 2D to 3D animation because of the advanced drawing skills required and the desire to produce a professional-quality video product for widespread use in nuclear medicine departments, more easily achievable with 3D design programmes. *Blender*, an open source 3D graphics software known for its exceptional multi-capabilities, was chosen after extended research and consideration of the resources available.

5.4.1 Blender: online open source platform for 3D design

Blender is a free and open-source platform, easily installable on devices with high technological performance. It supports the entire pipeline of 3D design, from modelling to post-production. This software allows the creation of 3D objects, environments and scenes by generating meshes (i.e. reticular structures) of simple volumes or surfaces, which can then be modelled into more complex shapes using sculpting techniques. Scenes can also be improved with realistic visual effects thanks to advanced lighting management. Regarding this, *Blender* supports different types of lights, including point lights, area lights and directional lights capable of simulating natural sunlight. Once the scene has been realized, the user can export a static image using the Render Image option, or simulate moving objects and characters using the rigging system. The latter allows for easier animation, which can thus be rendered in video format using the Cycles rendering engine. Another significant feature, which has also been used in this thesis project, is the integration of the Video Editing tool. Since animation, of any duration, is based on a sequence of frames rendered in succession, this tool was used in the following case to select the frames relating to a specific scene and concatenate them, thus generating the final 3D animation.

5.4.2 WT-PET Scanner Design

The design process started with the development of the WT-PET model. The first model realized consists of multiple components: two parallel vertical panels with a grid integrated into each one to replicate the PET scanner detectors along the AFOV, a support for going onto the platform where the panels are placed, a platform with marked footprints, a headrest and a projector (see Figure 5.7). To make the scene more realistic, a prepared human model with robotic features, as shown in Figure 5.8, was imported from *Mixamo*, an online platform that offers a wide range of animated 3D characters. This character had a predefined walking animation, which was useful at the beginning for simulating patient's movement towards the scanner.

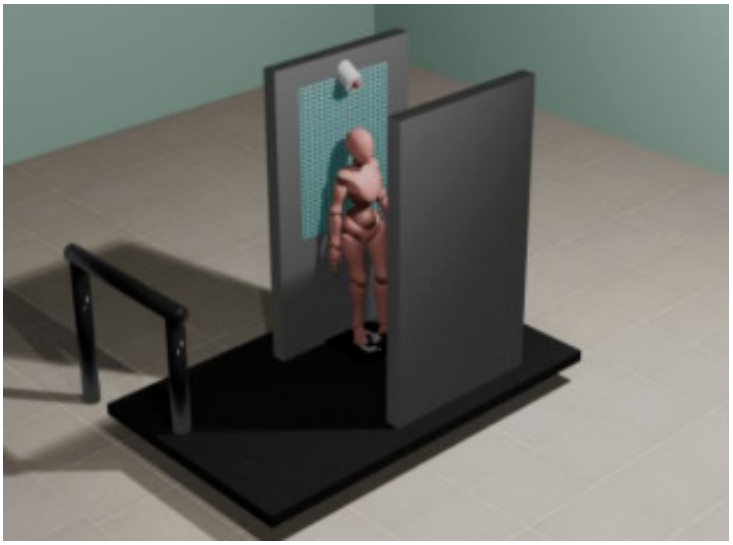

Figure 5.7: Top view of the initial scanner model.

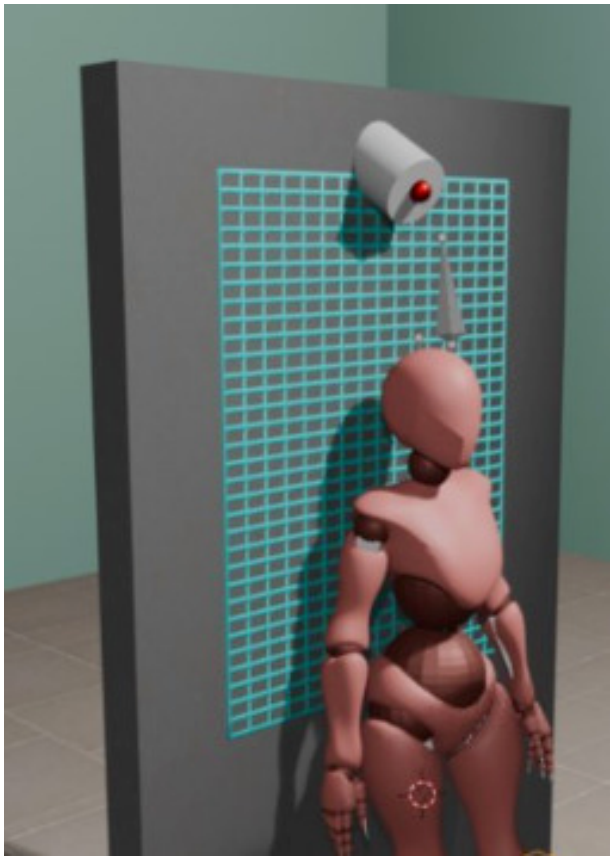

Figure 5.8: Close-up view of the human model positioned within the scanner.

5.4.3 Final Scanner and Environment Design

The next step involved refining the scanner and the environment design with the goal of closely replicating an actual hospital setting. Regarding the architecture of the scanner, many components were redesigned to replicate the real model as accurately as possible. The grids were removed and handlebars were added, along with a mounting system for each one on the back panel. Additionally, the side panels were redesigned to reflect the envisioned geometry of the scanner, which is no longer perfectly straight but features a trapezoidal shape on the sides. The final scanner model can be visualized in Figure 5.9.

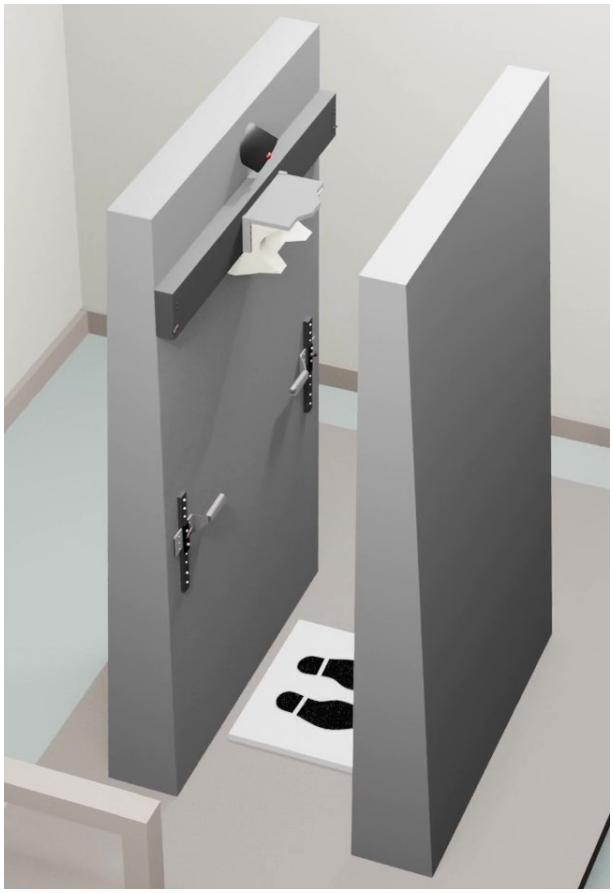

Figure 5.9: Final WT-PET scanner design.

As for the architectural design of the scene, the environment was divided into two distinct areas. The scanning room was placed next to a separate room for the medical technician. This design choice enabled the introduction of a dual perspective into the video guide, allowing the user to observe the scene from both the patient's and the medical personnel's points of view (see Figure 5.10). To further enhance realism, various props were integrated into the technician's room. These included a printer, a computer, and a work chair, all imported from predefined 3D object platforms such as *Turbosquid*. Particular attention was also paid to the use of lighting, in order to achieve greater overall realism.

(a) (b)

Figure 5.10: Dual-viewpoint scene layout showing (a) the medical technician's and (b) the patient's perspectives.

5.4.4 Human figures integration and Animation

We then proceeded with the integration of realistic human figures. To this end, the *MakeHuman Plugin* for *Blender* (MPFB) was utilised, an open-source 3D human character generator available online for free. This tool, which can be easily integrated into the Blender work environment, allows users to generate high-fidelity humanoid meshes in a few simple steps. The software supplies a highly extensive library of options that enables the user to customise the character's appearance, including height, ethnicity, gender, skin type, eyes, and numerous other morphological characteristics. A particularly useful feature is the automatic rigging tool, which attaches an articulated skeleton to the 3D character mesh, accelerating the animation workflow. The optional 'Rig helpers' parameter offers additional functions for simplified model manipulation, allowing the movement of limbs and joints using control nodes, thus allowing specific postures to be easily set. The integration of this tool represented a significant turning point in the production, as it enabled the animation phase to begin. As illustrated in Figure 5.11, manual rigging enabled us to define specific poses, such as the medical technician seated at the desk in an operational stance and the patient correctly positioned within the scanner waiting for the scan.

(a) (b)

Figure 5.11: Manual rigging results: (a) technician seated in the control room in an operational stance, and (b) patient correctly positioned between the two panels of the scanner.

The human body's animation proved to be very time-consuming, as even a few seconds of smooth animation necessitated frame-by-frame adjustments to the character's posture. To simplify the process, an alternative approach was adopted: a video guide composed of short static scenes, where characters remain still and dynamism can be achieved through camera movements.

5.4.5 Camera movements and Final Rendering

The approach adopted to choose the most suitable camera movements was to immerse in the 3D environment, imagining how a director would move the camera to capture each scene in the clearest and most expressive way possible. Following a series of trials, two primary shots were identified as being most effective in directing the user's attention.

Panoramic environmental shot

This shot was employed to provide the user an overview of the space, thereby ensuring a clear idea of the operating environment. For instance, it was used in the opening scene, where the mock-up is presented for the first time inside the scanning room, and in the final scene, with the patient correctly positioned within the scanner. The camera was positioned in a strategic location inside the room, in a corner, with the lens

oriented downwards, and with a rotational movement of approximately 180°. This made it possible to simulate a continuous panoramic shot.

Zoom in and out

This optical movement, achieved without physically moving the camera but by changing the focal length of the lens, has been widely used to draw the user's attention to specific details. For instance, the technique of zooming in was employed to focus on patient's feet during the positioning phase on the marked footprints, or to focus on patient's hands when the handlebars were held. This movement was achieved by starting from a wider shot and gradually narrowing the field of view. In contrast, the zoom-out technique was employed in scenes where the intention was to start with a detail and gradually expand to include the entire human figure. This approach was used in different sequences such as the ones showing the adjustment of the headrest and handlebars.

Render Images

The only instance where camera movement was not used was in Step 1, previously described in Section 5.1.1, which shows the subject entering the scanning room and stepping onto the platform. To represent the walking motion in a simpler and less time-consuming way, the ”Render Image” technique was applied: four static frames were acquired in sequence with a fixed camera. Once we got the frames, they were placed side by side using a video editing program to create an illusion of the movement. After defining the camera movements, the rendering phase for each scene was carried out within *Blender*.

Rendering process

A pivotal decision was to switch from the Cycles rendering engine to *Extra Easy Virtual Environment Engine* (EEVEE). Although Cycles offers higher visual quality, it proved to be too time-consuming for even short scenes. EEVEE, on the other hand, provided a good balance of quality and speed thanks to several tests and optimizations of rendering settings. Figure 5.12 shows the high quality achieved post-rendering using EEVEE.

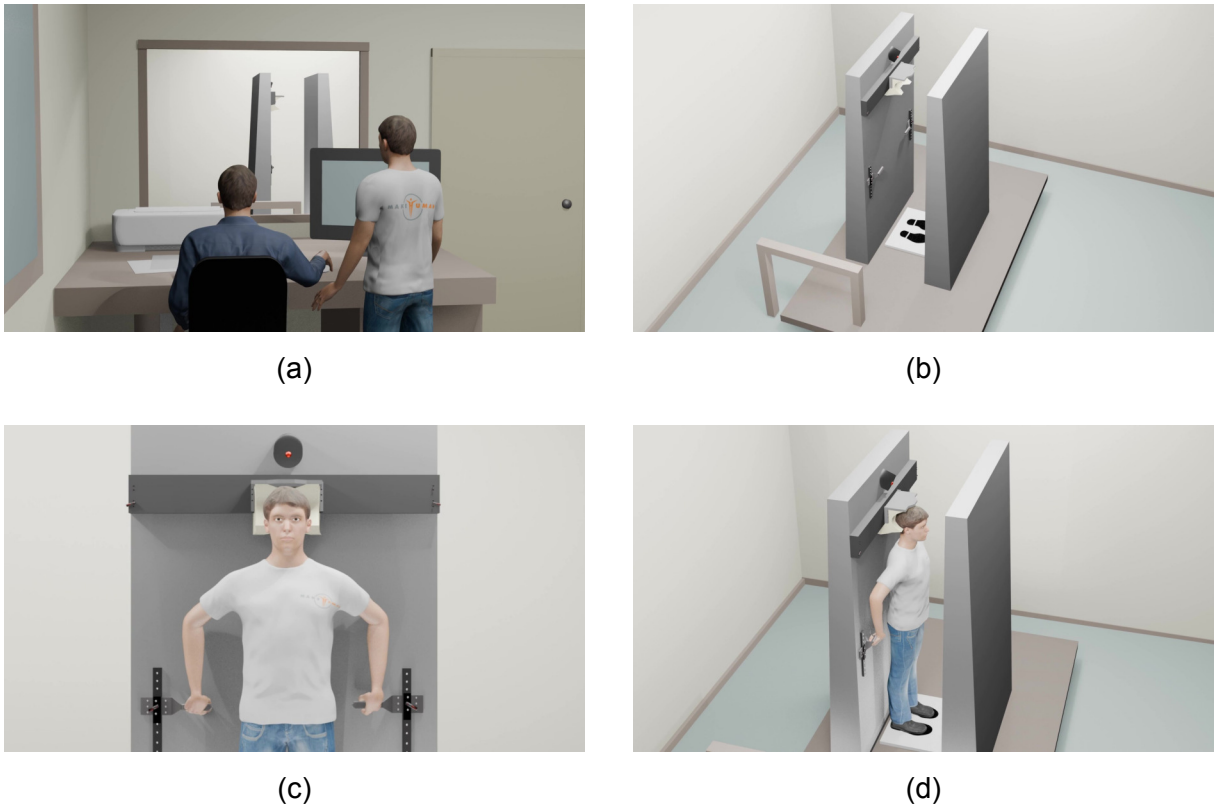

(a) (b)

(c) (d)

Figure 5.12: Selected final scenes rendered with EEVEE and featured in the current 3D animated video guide: (a) introductory scene, (b) initial overview of the WT-PET scanner, (c) final patient positioning, and (d) concluding scene prior to the scan.

5.5 Video editing

The final step of the videoguide involved the video editing to assemble and graphically refine the scenes into a single professional product. For this tasks, we used *CapCut*, an intuitive and powerful platform suitable for both video editing and image design. A visual representation of the graphical interface used for this work phase is illustrated in Figure 5.13.

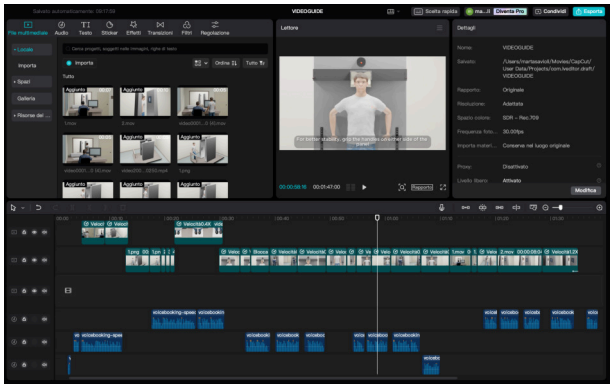

Figure 5.13: CapCut graphical interface.

In the following stage of the project, the narrative structure was defined, dividing the content into macrosections, and introductory titles were added for each part. The purpose of this was to provide the user with a clear overview of the main four steps of the clinical procedure, as shown in Figure 5.14.

(a)

(b)

(c)

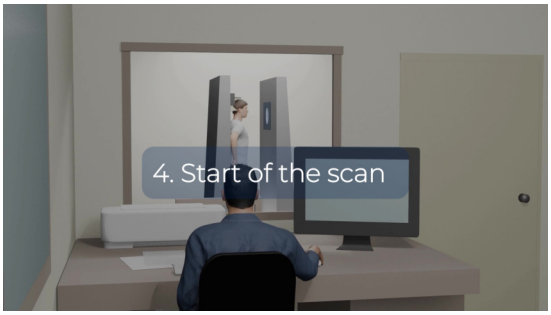

(d)

Figure 5.14: The four key steps in patient preparation and positioning: (a) Step 1 – initial positioning, (b) Step 2 – headrest adjustment, (c) Step 3 – handlebars adjustment, and (d) Step 4 – start of the scan.

The title chosen for the video guide was: *'Walk-Through PET: an Intuitive Video Guide for the Scan'*. To enhance visual fluency between scenes, dynamic transitions such as zooms and fades were integrated, while icons and arrows were strategically positioned throughout the video to direct the user's attention to the key elements of the scene, as illustrated in Figure 5.15. The addition of these graphic elements aims to make the guide clearer, more intuitive, and engaging. In order to enhance accessibility, particularly for users with hearing impairments, the automatic subtitling tool incorporated into the software was used. This enabled the text to be perfectly synchronised with the voiceover previously recorded.

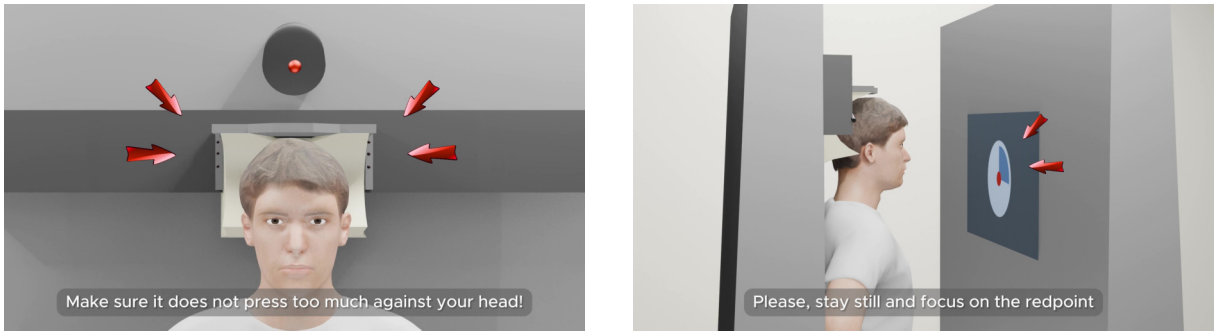

(a) (b)

Figure 5.15: Visual warnings integrated into the 3D animated video guide: (a) potential pressure from the headrest during positioning, and (b) focus on the central red dot during the scanning procedure.

The video guide, which has a duration of 1 minute and 49 seconds in total, is currently a prototype. In the future, the effectiveness and clarity of the content will be evaluated through tests with volunteers. The purpose of these tests is to evaluate how effectively the content may help patients better understand the clinical procedure in a more autonomous way. This, in turn, could reduce the need for constant assistance from medical personnel in nuclear medicine departments during PET examinations. A further development planned is the adaptation of the video guide into other languages, such as Dutch and French, with a view to improving accessibility, particularly among

elderly patients who are often unfamiliar with English.

5.6 Results

This section presents a selection of keyframes from the current prototype of the animated 3D video guide. The content is divided into six main sections: the introductory scenes, the scenes corresponding to Steps 1 through 4, and the concluding scene. Figure 5.16 provides an overview of the keyframes featured in the current version of the video guide.

Cover of the animated 3D video guide.

Providing the patient with scanning instructions following the video guide in the medical technician's room.

Initial overview of the WT-PET mock-up in the scanning room.

Step 1 display.

The patient steps onto the platform and positions himself between the two panels of the WT-PET mock-up.

Correct foot positioning on the marked footprints.

2 Headrest adjustment

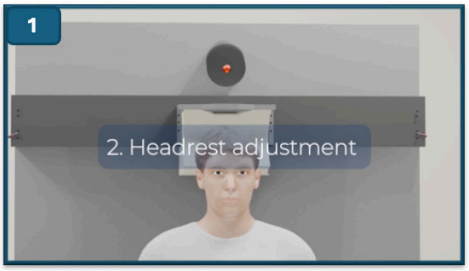

Step 2 display.

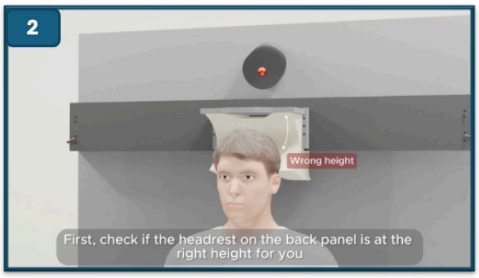

Headrest height check.

Headrest adjustment supported by medical technician.

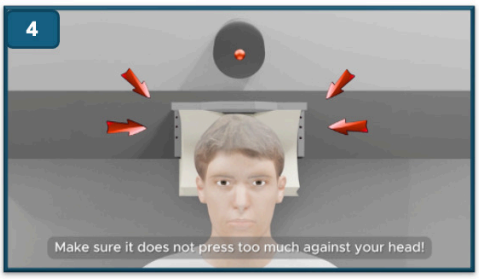

Checking the pressure exerted by the headrest on the patient's head.

3 Handlebars adjustment

Step 3 display.

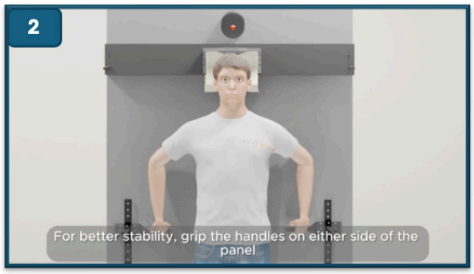

Gripping handles for greater postural stability.

Handlebars adjustment supported by medical technician.

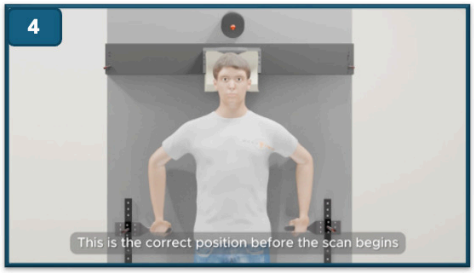

Correct final position.

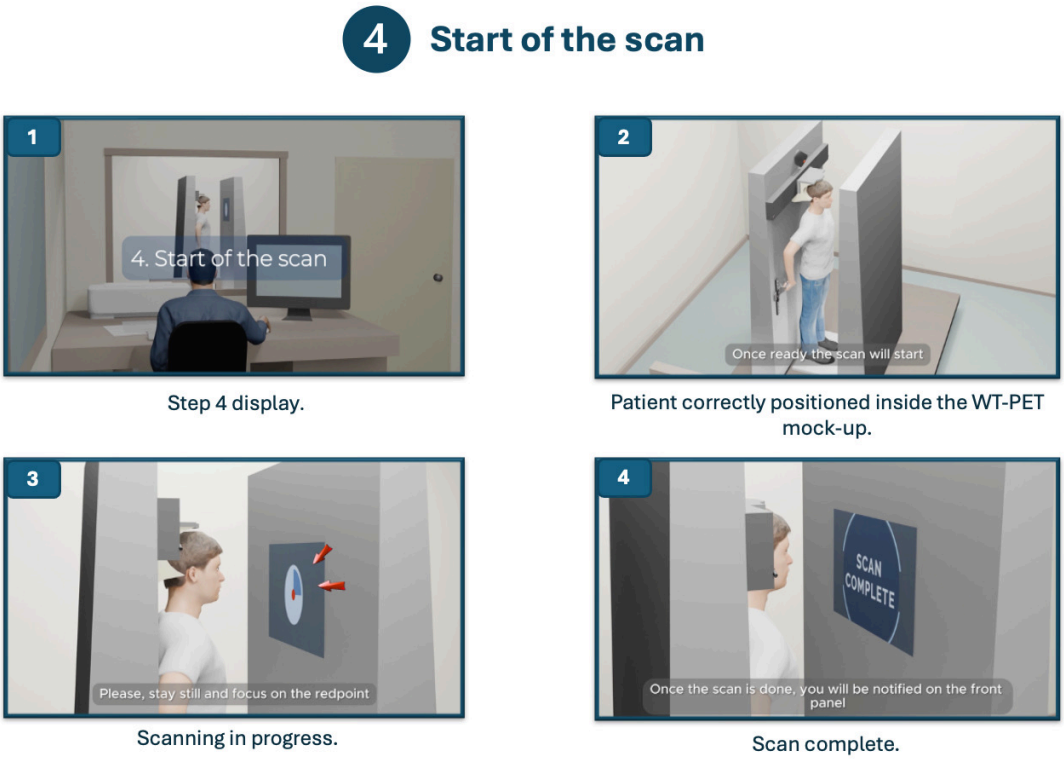

Figure 5.16: Overview of the keyframes featured in the current animated 3D video guide.

6

30-second Timer Video

Chapter 6 is entirely dedicated to the second objective of this thesis project, which involves the development of a 30-second timer video that can be integrated into the scanner model. This audio-visual content has been designed to improve the performance of the WT-PET scans by encouraging patients to maintain a high level of attention and focus during the 30 seconds of the examination. The objective is to achieve enhanced stability, particularly in the upper body motion, thereby optimising image quality and diagnostic accuracy. The idea for this project was proposed at the conclusion of a recent study made on the evaluation of rigid and non-rigid motion during normal breathing and breath-hold conditions [1]. This study was conducted on a group of eighteen volunteers within the dual flat panel Walk-Through Total Body PET (WT-TB-PET) [1]. The feedback collected demonstrated an evident necessity to incorporate a visual element into the existing system, with the objective of guiding the subject during the scan and encouraging him to stay still. In addition to the intention of reducing movement, the aim is also to make the experience more controlled, pleasant, and less perceptible in terms of time duration, thanks to the addition of an engaging audio-visual stimulus.

6.1 Design and Development of the 30-second Timer Video

6.1.1 Scripting

The development of the 30-second timer video began with the scripting phase. An additional goal was to ensure that the content remains as autonomous and self-sufficient as possible. For this reason, short introductory and concluding sentences were integrated alongside the timer video, presented as on-screen text. A critical constraint

considered from the outset was the limited duration of each PET acquisition, which is 30 seconds, as well as the necessity to maintain the high patient throughput enabled by the new WT-PET scanner prototype. In response, the total duration of the video was limited to approximately one minute, with the remaining 30 seconds dedicated to short sentences introducing the patient to the procedure. On the other hand, the final scenes were designed to clearly communicate the end of the scan and invite the patient to leave the platform. As for the video guide, the scripting phase was supported by the AI *Voicebooking* platform. In order to facilitate accessibility for patients with visual or hearing impairments, a synchronised audio track was produced for each text scene and incorporated into the video. The first version was produced in English using a male voice with a British accent. Subsequently, full adaptations were developed in French and Dutch, including both translation of the script and the recordings of the voiceover.

6.1.2 Timer design

The graphic design production was not organised according to the chronological sequence of the scenes; rather, it was structured based on the relevance of the individual elements to be developed. In response to this, we decided to start with the 30-second timer design. For this task we used *Wave.video*, an online platform known for its use in video marketing and equipped with features adapted for the development of the desired visual timer. A predefined layout available on the platform was utilised to develop a circular timer that rotates clockwise. In comparison to the other video scenes, this one necessitated a considerably greater number of aesthetic graphic revisions, following a trial and error approach. One of the primary considerations concerned the most effective visual representation of the timer, with particular attention to the colour palette, taking into account that it would be projected onto a vertical panel in front of the patient, estimated to be dark grey with a metallic finish. A series of comparative tests were conducted, initially with a dark (grey) background and subsequently with a light (white) one. Figure 6.1 shows a series of tests that were carried out to arrive at the final design.

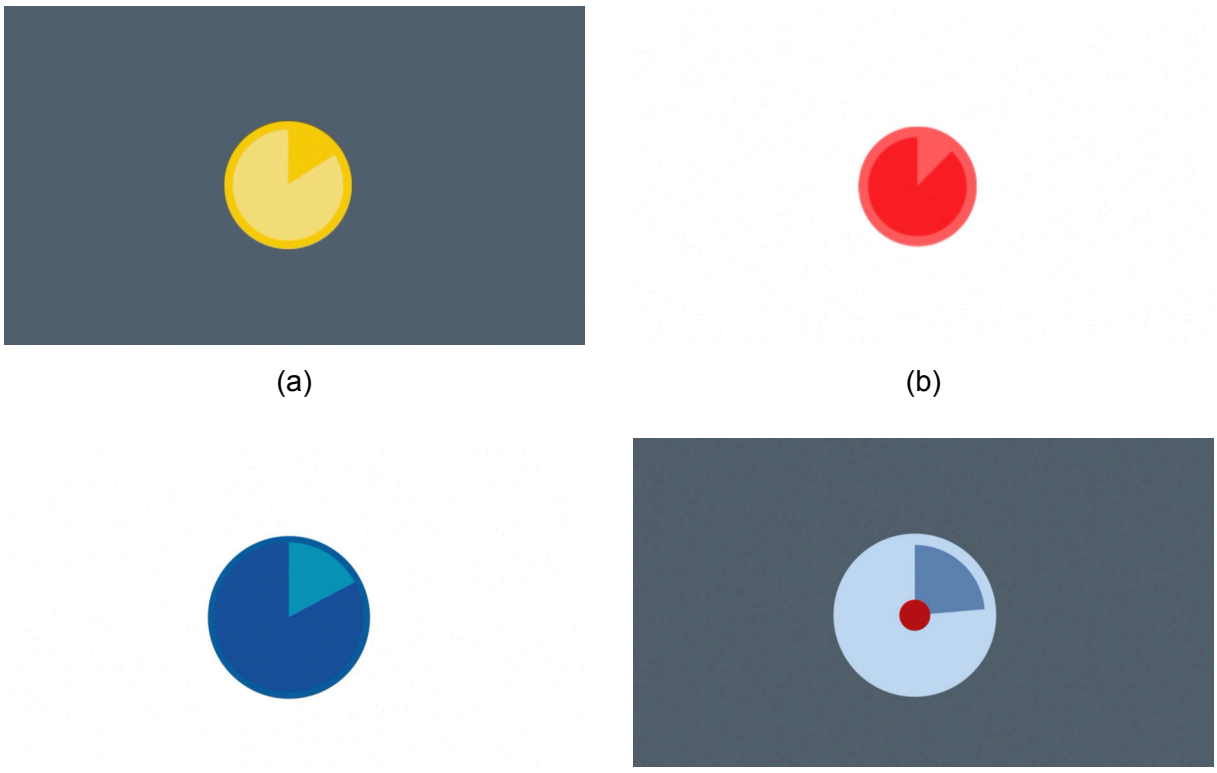

(a) (b)

(c) (d)

Figure 6.1: A series of tests conducted on the 30-second timer design: (a) yellow timer on a dark grey background, (b) red timer on a white background, (c) blue timer on a white background, and (d) final 30-second timer video design.

In each case, the colour scheme of the timer was also adapted: for example, a variant with a yellow timer on a grey background was tested (Figure 6.1a), designed to attract more visual attention; then, a configuration with a red timer on a white background (Figure 6.1b) with more compact dimensions, was evaluated to emphasise the contrast and the focus on the circle. The final choice was guided by two main considerations. On the one hand, it was considered important to avoid a sharp contrast between the video background and the projection panel in order to ensure consistent colour continuity. Furthermore, we want the content to look professional and appropriate for a hospital environment. It was therefore decided to implement a dark grey background to ensure visual continuity with the metal panel, a circular blue timer with a light blue element below to enhance contrast, and a small, centred red focal point to stimulate visual focus. Shades of blue and light blue were finally chosen due to their typical association to the healthcare field and feelings of calm and tranquillity. The dimensions of each element have been specifically designed to ensure both aesthetic consistency

and optimal readability, even for patients with visual impairments, considering the distance between the vertical panels of 50 cm. Figure 6.2 provides a visual representation of the video timer's projection within the WT-PET mock-up, along with the projector's mounting position. The timer displayed is a preliminary version that was utilised during the testing phase. It does not represent the final timer video design.

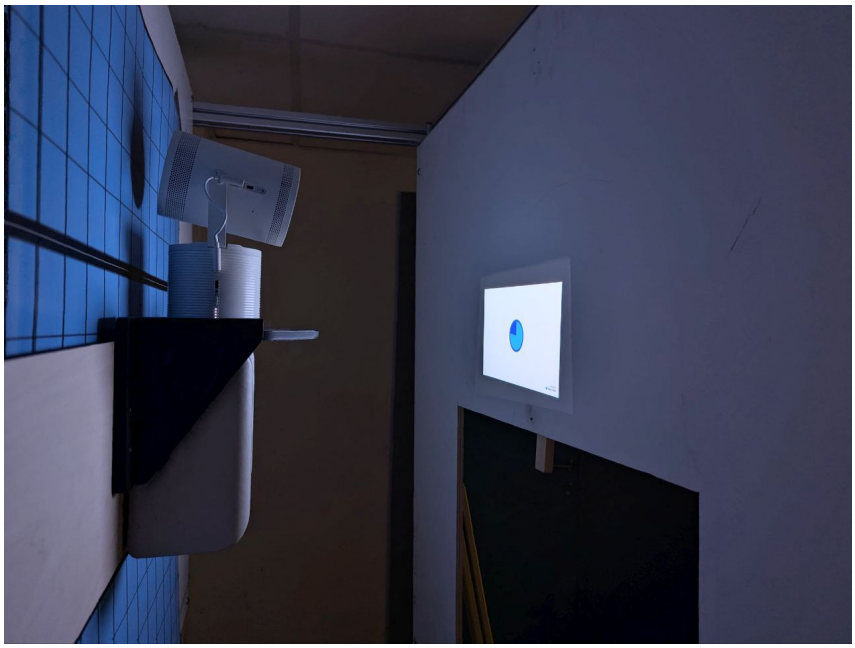

Figure 6.2: Display of the 30-second timer video inside the WT-PET mock-up using the Samsung's *The Freestyle – Second Generation* projector.

6.1.3 Instructional text scenes

We then moved on with the production of the opening and closing instructional scenes of the video. The objective was to design visually effective and minimalist content. To achieve this, we used *FlexClip*, a free online video editing platform, selected on the basis of its ease of use and the variety of tools offered for inserting text, images, and high-quality animations. Text instructions were added on a circular coloured background, in line with the aesthetic already defined for the timer. The text was created using simple capital letters in Raleway font, with bold type used for keywords such as *GET READY*, *FOCUS* and *RED POINT* in order to draw visual attention to the key steps. In order to enhance fluidity between scenes, graphic transitions have been incorporated. These transitions have been intentionally designed to be simple, with the objective of avoiding excessive dynamism that could potentially distract the viewer. Figure 6.3 illustrates

some of the introductory and concluding sequences integrated into the timer video, developed in accordance with the graphics and colour palette that have been adopted.

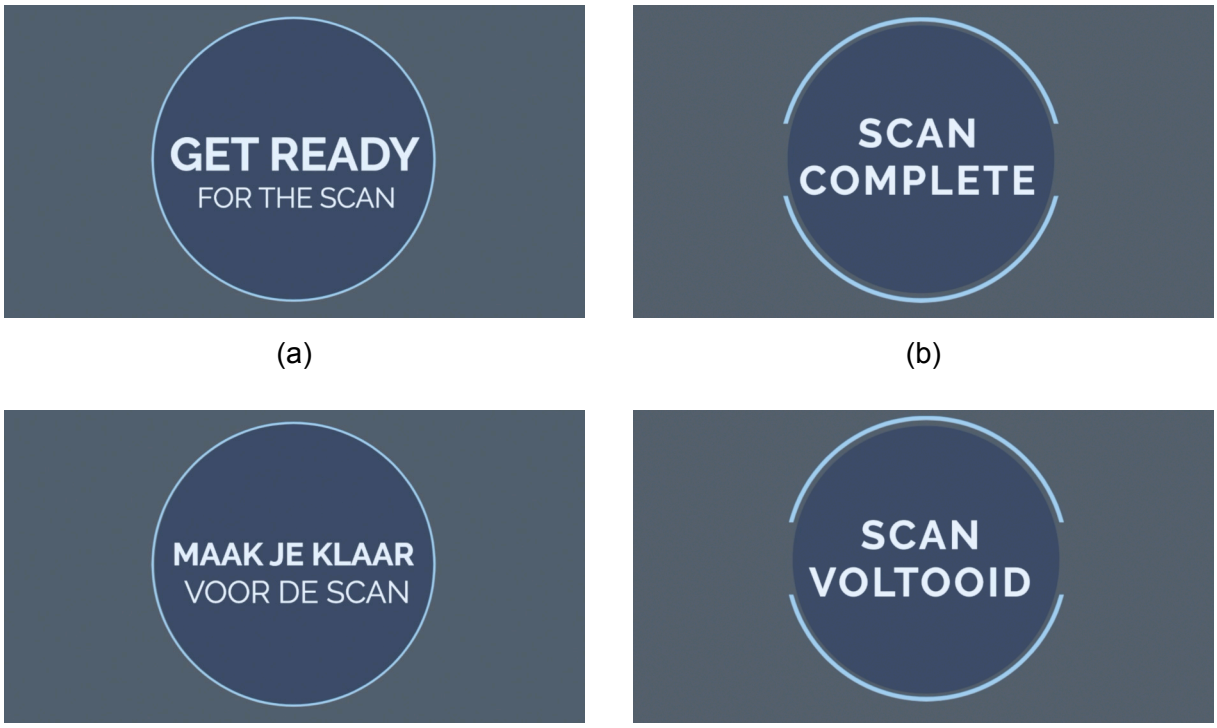

(a) (b)

(c) (d)

Figure 6.3: Addition of instructional text scenes: (a) English version of the initial instruction, (b) English version of the concluding instruction, (c) Dutch version of the initial instruction, and (d) Dutch version of the concluding instruction.

Finally, to give the patient a greater sense of being guided, a 3-second countdown was incorporated between the introductory scenes and the start of the timer. Each second is accompanied by a beep sound, designed to implicitly prepare the patient for the start of the examination.

6.1.4 Video editing

Once the production of the individual scenes was concluded, we moved on to the final video editing process. The elements were imported into the *iMovie* software, where the sequences were arranged in chronological order. Particular attention was paid for optimising the duration of each scene and defining the pauses between them. The audio component was then inserted and synchronised with the respective video scenes.

Furthermore, beep sounds were incorporated to accompany the initial 3-second countdown and to alert the user to the conclusion of the 30-second scan. These sounds were selected and imported from online sources. Figure 6.4 represents the *iMovie* working screen that enabled the final realisation of the timer video.

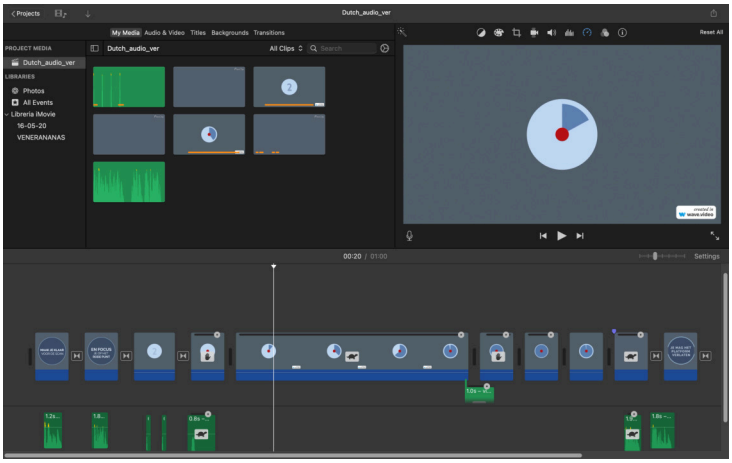

Figure 6.4: Final video editing process using iMovie.

6.2 Results

This section presents all the keyframes that make up the 30-second timer video, shown in both the English (Figure 6.5) and Dutch (Figure 6.6) versions.

Figure 6.5: Overview of the keyframes featured in the English version of the 30-second timer video.

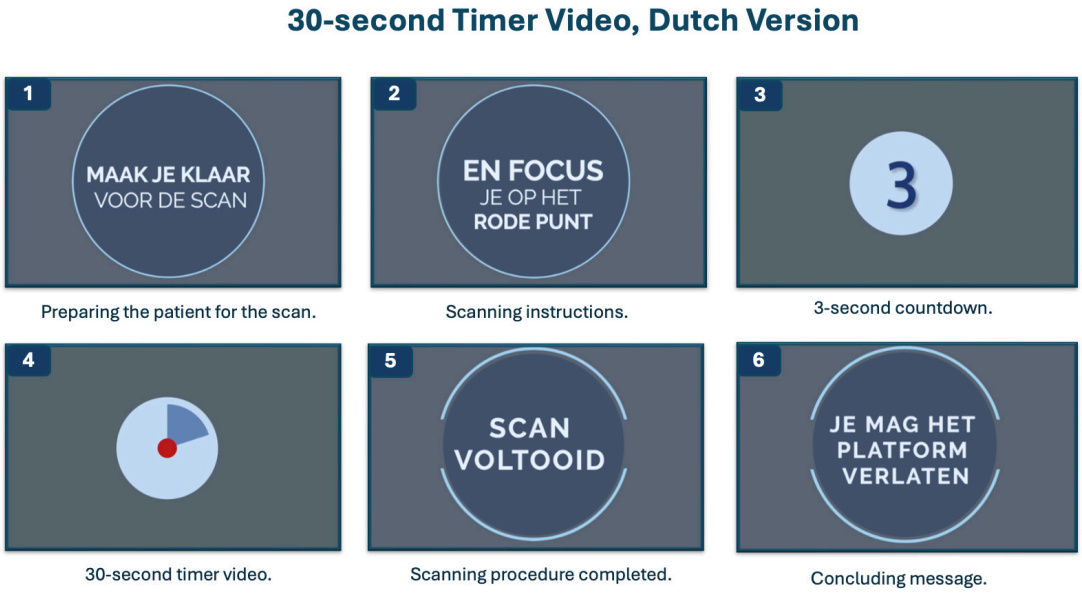

Figure 6.6: Overview of the keyframes featured in the Dutch version of the 30-second timer video.

7

Motion Study

7.1 Materials and Methods

At the end of the 30-second timer video production, an experimental study was designed and conducted with the objective of evaluating its effectiveness in terms of patient understanding and focus, assessing the degree of motion reported by the patient during a 30-second scan. The experiment, conducted in the research laboratory, involved the integration of the video into the WT-PET system employing the *"Freestyle – Second Generation"* projector supplied by Samsung. The study was conducted on a total of thirty-one healthy volunteers and was structured according to two different experimental conditions (Study Design 1 and Study Design 2), each corresponding to a specific video sequence. In order to detect upper body motion during the PET scan simulation, five passive infrared markers were applied to the head, shoulders, chest, and abdomen. The three-dimensional coordinates of each marker were acquired in real time throughout the scan using the *Orbbec Femto Mega* depth camera. The collected data were then processed using image processing techniques, including thresholding and connected component analysis.

7.1.1 Participants

Thirty-one healthy volunteers participated in this experimental study with the aim of assessing the degree of motion during a simulated PET acquisition performed inside the WT-PET mock-up [1]. The study involved two different sequences of a 30-second timer video projected onto the front vertical panel of the mock-up. In order to compare the effectiveness of each of the two different video sequences, the initial sample, consisting of thirty-one participants, was divided into two groups: twenty subjects took part in Study Design 1, while the remaining eleven were assigned to Study Design 2. Before

the start of each session, participants were provided with detailed information about the research objectives and the procedure to be followed, with particular emphasis on the importance of maintaining the most stable position possible during the entire simulation. Afterwards, each participant signed an informed consent form, thereby certifying that they had full understanding of the purpose of the study, the data privacy policies, and the potential risks [1].

7.1.2 Video Projection System

To display the video timer within the WT-PET mock-up, Samsung's *The Freestyle – Second Generation* projector was selected following a comparative evaluation of various models. The choice was guided by the need for high-quality audiovisual output in a confined space, as the distance between the two panels of the mock-up is approximately 50 cm, with the patient positioned in between. These spatial constraints required a compact, lightweight device capable of delivering clear visual content. *The Freestyle* fulfilled these requirements, offering compact dimensions (140 × 243 × 137 mm), a total weight of only 1.4 kg (including packaging), and an integrated support suitable for placing it on the headrest. Its installation ensures that no direct weight is applied to the patient, thanks to a support system connecting the headrest to the back panel. Additional features, such as a 180° projection angle and an automatic image optimisation system, allow the device to project correctly without manual adjustment. Figure 7.1 provides two views of the Samsung's *The Freestyle – Second Generation* projector: a side view (Figure 7.1a) and a top view (Figure 7.1b).

(a) (b)

Figure 7.1: Samsung The Freestyle – Second Generation projector: (a) side view and (b) top view.

7.1.3 Study design

The motion study was structured according to two primary objectives, which guided the decision to divide the experimental design into two different conditions. The first objective was to evaluate the effectiveness of the video timer in improving patient's attention and focus levels during the scan. These effects were measured indirectly through the analysis of body motion. The main aim of the study was to compare the condition in which the patient observed the video timer with that in which no video was projected on the panel. The second objective was to investigate whether adding an audio track to the video timer could enhance the patient's sense of guidance compared to using the visual timer alone. It was hypothesised that this multi-sensorial experience could positively influence attention, focus and, consequently, reduce movement during the scan. To this end, upon achieving the final version of the video timer with audio track, a second version without audio was exported using the video editing software *iMovie*.

Study Design 1

A total of twenty volunteers participated in Study Design 1. Each test required a time slot of approximately fifteen minutes per participant. The tracking procedure was executed by using the *Orbbec Femto Mega* depth camera that was installed at the top of the front panel, with the lens oriented towards the subject. After correctly positioning the five passive infrared markers, participants were guided towards the WT-PET mock-up, where a preliminary adjustment of the ergonomic components (such as headrest and handlebars) was carried out to ensure maximum comfort, stability, and support during the scan. The adjustments were adapted to the height and subject's posture. Once the setup phase was complete, participants were instructed to maintain as stable position as possible for the entire duration of the procedure, with their head comfortably positioned within the headrest cavity and their hands firmly grasping the handlebars, as illustrated in Figure 7.2.

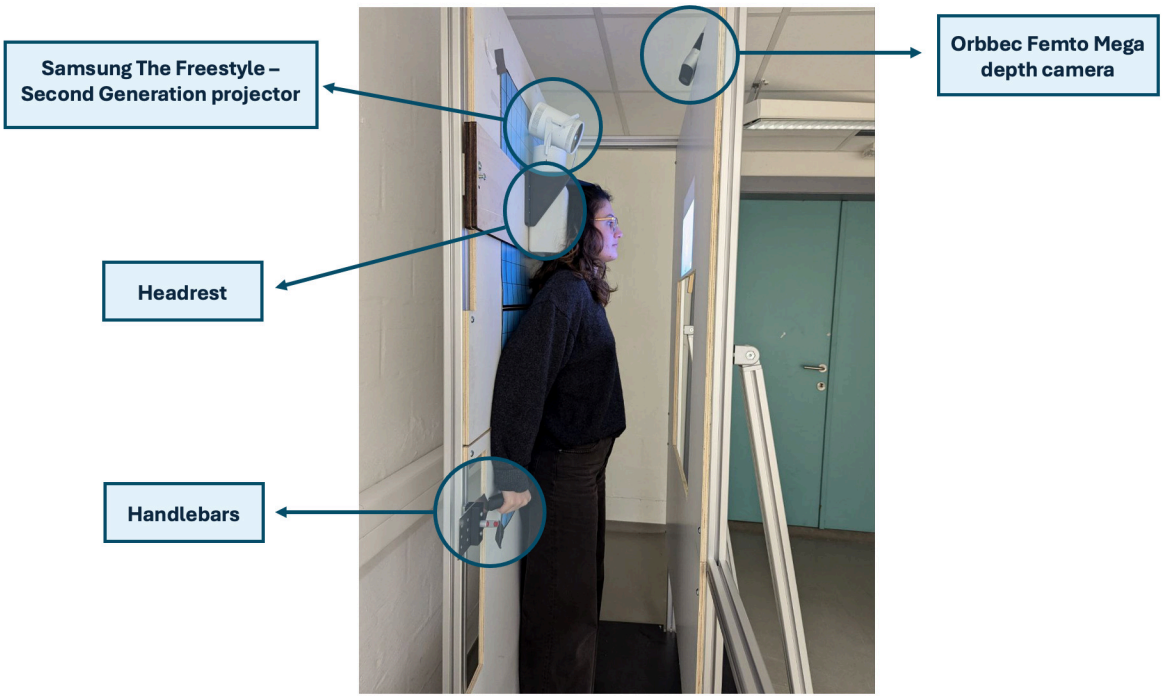

Figure 7.2: Final setup with the patient correctly positioned within the mock-up. It includes ergonomic supports, such as the headrest and handlebars, and employes two main devices: Samsung's The Freestyle Second Generation projector for video timer projection, and the Orbbec Femto Mega depth camera for motion tracking.

In Study Design 1, each participant was subjected to a visual sequence consisting of four consecutive recordings lasting 30 seconds each, separated by brief technical breaks to verify correct data acquisition. The sequence was as follows:

1. No video display;
2. Video timer display without audio;
3. Video timer display with audio;
4. No video display again;

This configuration was designed to assess the impact of different audiovisual conditions on participant response. In particular, the decision to include a final recording without video again aimed to evaluate potential adaptation to the visual stimulus over time. In order to prevent prolonged immobility from having a negative effect on the most recent acquisitions (due to fatigue or stiffness), participants were advised to move or briefly

leave the scanner between recordings. Upon conclusion of the sequence and confirmation of the correct data recording, the participant was asked to leave the platform and provide brief subjective feedback on three aspects:

- whether they perceived an enhanced level of concentration while viewing the video with the central red dot compared to the condition without visual stimulus;
- whether they noticed any differences between the recordings with and without audio track;
- whether they had any suggestions or changes to propose regarding the graphics or audio of the videos shown.

Study Design 2

The same experimental procedure was also applied in Study Design 2, conducted on the second group of eleven participants. The only difference between Study Design 1 and Study Design 2 was the sequence of visualizations adopted, which was modified to test the effectiveness of the video order. It involved three consecutive recordings:

1. Video timer display with audio;
2. Video timer display without audio;
3. No video display;

A particular feature of Study Design 2 was the inclusion of a Dutch version of the video timer, created with the specific purpose of enabling the eleventh participant, who was not an English speaker, to fully understand the instructions, thus ensuring uniformity of the experimental conditions.

7.1.4 Motion tracking and Data Processing

In both Study Design 1 and Study Design 2, the *Orbbec FemtoMega* depth camera was utilized to capture the 3D coordinates of five infrared (IR) markers strategically placed on specific anatomical points such as head, left and right shoulders, chest, and abdomen. From the video recordings of each participant, three distinct image types (RGB, Depth, and Infrared) were extracted using a dedicated image processing pipeline. To enhance marker's visibility and separate each of them from artifacts and background noise, the IR images underwent an additional pre-processing steps [1].

IR Image Pre-processing and 2D Centroid Detection

The IR images were processed using standard image analysis techniques to prepare them for subsequent analysis, such as thresholding and connected component analysis. Through the application of the first technique, we were able to reach a contrast enhancement between IR markers and background, converting each IR image in a binary image. The second technique was then used to better visualize and then label each marker in the binary image. To precisely localize each marker, a moment-based method was adopted. In particular, image moments were computed. These statistical features describe the spatial distribution of pixel intensities within a given region. The zero-order moment M_{zero} captures the total area of a binary region, while the first-order moments (M_{12} and M_{21}) represent the intensity-weighted coordinates along the x and y axes, respectively. Based on these values, the 2D centroid of each marker was computed, providing its precise location in the image plane [1]. Specifically, the x and y coordinates (c_x and c_y) were obtained by dividing the first-order moments (M_{12}, M_{21}) by the zero-order moment (M_{zero}), as expressed in Equations 7.1 and 7.2.

$$c_x = \frac{M_{12}}{M_{zero}} \tag{7.1}$$

$$c_y = \frac{M_{21}}{M_{zero}} \tag{7.2}$$

The entire image processing pipeline applied is illustrated in Figure 7.3.

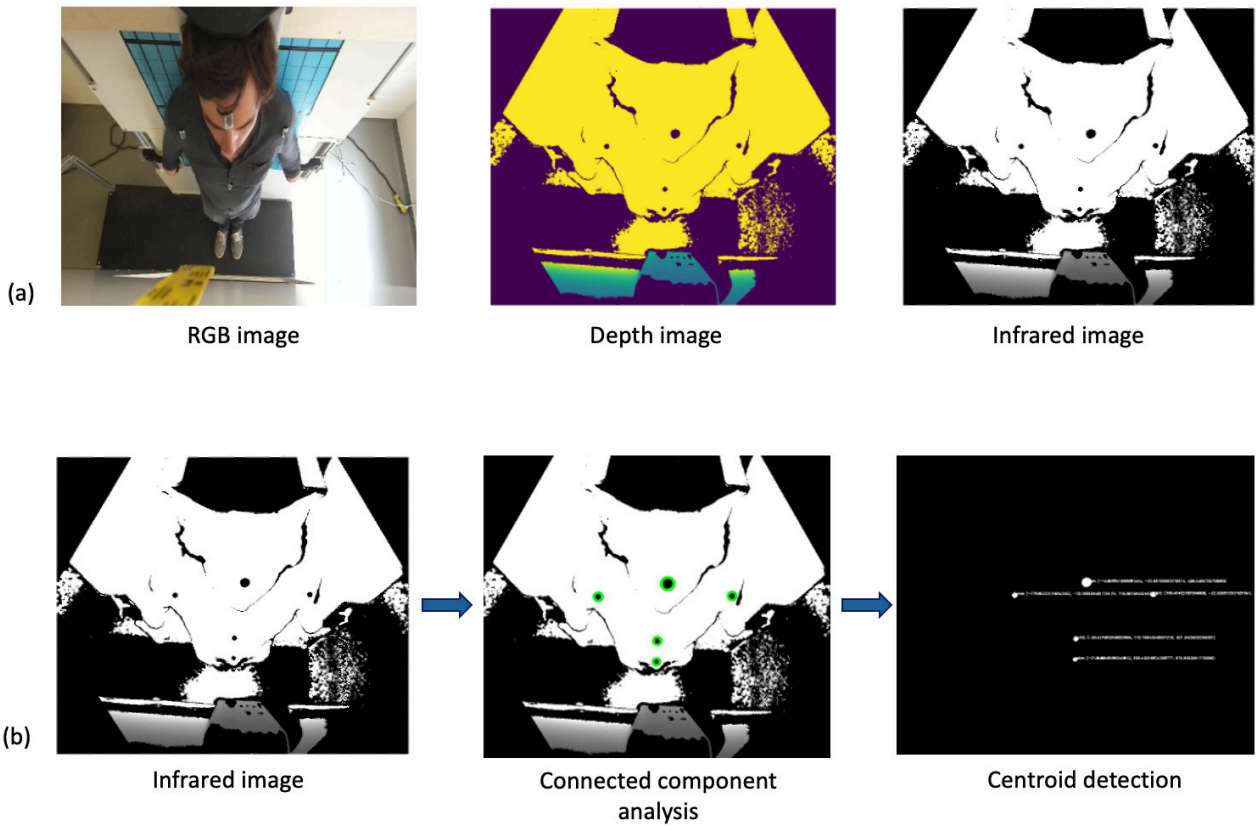

Figure 7.3: Image processing pipeline: (a) extraction of RGB, Depth, and Infrared images, and (b) pre-processing of the IR image and 2D centroid detection.

2D to 3D Coordinate Estimation

To determine the 3D spatial positions of the markers, the 2D centroids, previously obtained , were projected into 3D space using depth information from the depth camera. This process began by defining a square region, based on a predefined radius, around each 2D point. Then we proceeded with the evaluation of image pixels around each center point, calculating for each one the squared Euclidean distance from the centroid, within each neighborhood. Only those pixels that had positive values and were located within the specified distance from the center were considered for further analysis [1].

The mean of the valid depth values in the selected neighborhood was then computed in order to proceed with the 3D transformation. By applying the camera's intrinsic parameters (specifically the focal lengths and the principal point) and using the average depth value previously defined, the original 2D coordinates were transformed into 3D

spatial coordinates, expressed in millimeters within the camera coordinate system [1]. The equations used for this transformation, corresponding to the x, y and z axes, are taken from a recent quantitative analysis [1] computed on patient motion in WT-PET scanner and are shown in Equations 7.3 to 7.5:

$$x_{\text{mm}} = \frac{(x - c_x)}{f_x} \cdot \mu_{\text{depth}} \tag{7.3}$$

$$y_{\text{mm}} = \frac{(y - c_y)}{f_y} \cdot \mu_{\text{depth}} \tag{7.4}$$

$$z_{\text{mm}} = \mu_{\text{depth}} \tag{7.5}$$

The resulting 3D coordinates are represented by $(x_{\text{mm}}, y_{\text{mm}}, z_{\text{mm}})$, the 2D image coordinates are (x, y, z), and the principal point and focal length of the camera are defined by (c_x, c_y) and (f_x, f_y), respectively [1].

Transformation to World Coordinate system

Once the 3D spatial coordinates were defined, another conversion was applied to move these points in a world coordinate system. This coordinate transformation method is based on the application of a 4x4 homogeneous transformation matrix (T), obtained through the combination of a rotation matrix (R) and a translation vector (t). While the vector t defines the camera's position within the world coordinate system, the matrix R defines its orientation within the same system.

In Equation 7.6, extracted from the following reference [1], the T matrix is shown:

$$T = \begin{bmatrix} R & t \\ 0 & 1 \end{bmatrix} = \begin{bmatrix} r_{11} & r_{12} & r_{13} & t_x \\ r_{21} & r_{22} & r_{23} & t_y \\ r_{31} & r_{32} & r_{33} & t_z \\ 0 & 0 & 0 & 1 \end{bmatrix} \tag{7.6}$$

where t is the 3 × 1 translation vector, R is the 3 × 3 rotation matrix, and T is a homogeneous transformation matrix [1]. To finally compute the transformation, each initial 3D point, shown in Equation 7.7, was implemented with an additional fourth row representing an homogeneous coordinate, following the same method used in a recent quantitative analysis computed on patient motion in the WT-PET scanner [1]. The final result is shown in Equation 7.8.

$$\text{point}_{\text{initial}} = \begin{bmatrix} x \\ y \\ z \end{bmatrix} \tag{7.7}$$

$$\text{point}_{\text{hom}} = \begin{bmatrix} x \\ y \\ z \\ 1 \end{bmatrix} \tag{7.8}$$

This addition was necessary for allowing the multiplication between the transformation matrix T and the 3D point, in order to obtain the final transformed one. The process described above is shown in Equations 7.9, which is cited from the following source [1].

$$\text{point}_{\text{trans}} = T \times \text{point}_{\text{hom}} = \begin{bmatrix} r_{11} & r_{12} & r_{13} & t_x \\ r_{21} & r_{22} & r_{23} & t_y \\ r_{31} & r_{32} & r_{33} & t_z \\ 0 & 0 & 0 & 1 \end{bmatrix} \begin{bmatrix} x \\ y \\ z \\ 1 \end{bmatrix} \tag{7.9}$$

7.1.5 Motion evaluation

To quantify the degree of motion for each marker during the simulated WT-PET scan, two main statistical parameters were calculated: the average absolute deviation and the Euclidean distance.

Average absolute deviation

The Average Absolute Deviation (AAD) was computed separately for the X, Y, and Z sets of coordinates. This metric provides a measure of variability by capturing how much each marker's point deviates, on average, from the mean position along each axis. For every marker, the AAD was calculated by taking the absolute difference between each recorded coordinate and the mean value of that coordinate across the entire sequence. These absolute deviations were then averaged on the total number of coordinate values to obtain a single value for each axis (x,y and z). The process described above is shown in Equations 7.10 to 7.12 , for each coordinate x,y and z. The Equations 7.10 to 7.12 are taken from [1]:

$$\text{AAD}_x = \frac{1}{n} \sum_{i=1}^{n} |x_i - \mu_X| \tag{7.10}$$

$$\text{AAD}_y = \frac{1}{n}\sum_{i=1}^{n}|y_i - \mu_Y| \tag{7.11}$$

$$\text{AAD}_z = \frac{1}{n}\sum_{i=1}^{n}|z_i - \mu_Z| \tag{7.12}$$

where x_i, y_i, and z_i represent each coordinate value; $X = \{x_1, x_2, x_3, \ldots, x_n\}$, $Y = \{y_1, y_2, y_3, \ldots, y_n\}$, and $Z = \{z_1, z_2, z_3, \ldots, z_n\}$ represent the set of coordinate values, n defines the total number of coordinate and μ_X, μ_Y, and μ_Z represent the mean values of the coordinates [1].

Euclidean distance analysis

To further quantify the overall motion of each marker in 3D space, the Euclidean distance from the mean position was computed. For each time instant during the scan, the distance between the current 3D marker position and its mean position over each recording was calculated. These distances were then averaged across the full recording session, yielding a single representative motion value for each marker. By repeating this process for all participants, it was possible to compare the degree of motion for each marker under different study conditions. The equation used to calculate this statistical parameter is defined in Equation 7.13, as outlined in [1]:

$$d = \sqrt{(x - \mu_x)^2 + (y - \mu_y)^2 + (z - \mu_z)^2} \tag{7.13}$$

7.2 Results

The findings presented in Section 7.2 are organized into two primary categories. Sections 7.2.1 through 7.2.4 provide a detailed quantitative analysis of the markers' displacement across the various recording sessions. Given that the study was conducted under two different experimental conditions, analyses were carried out independently for Study Design 1 and Study Design 2, taking into account the order in which audiovisual stimuli were administered to each participant. Section 7.2.5, instead, focuses on a qualitative analysis based on participants' feedback. It includes comments and impressions gathered from all 31 participants after the final recording, providing insights into their subjective experiences of the procedure.

7.2.1 3D Motion Profiles

For each participant, the transformed 3D markers' coordinates were plotted as a function of time over the 30-second duration of each recording. Each plot reflects markers' displacement, decomposed into its three spatial components, thereby enabling a clear interpretation of motion in 3D space. Following the standard anatomical coordinate system, each axis in the 3D motion profiles corresponds to a specific direction of movement recorded during the 30-second scan of a single participant. The x-axis represents lateral (side-to-side) movement, the y-axis captures anterior-posterior (front-to-back) displacement, and the z-axis reflects vertical motion. This analysis enhanced a detailed visualization of marker dynamics, providing more profound insights into upper body motion and a more precise interpretation of movement patterns across different anatomical points. The analysis was performed for both Study Design 1 and Study Design 2. The results obtained for one participant are illustrated in Figures 7.4 (Study Design 1) and Figure 7.5 (Study Design 2).

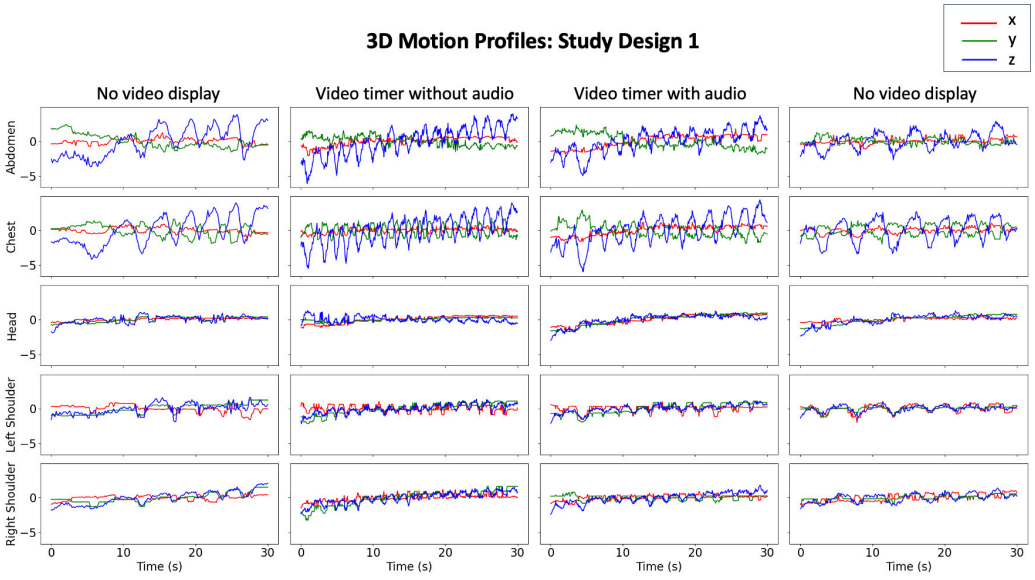

Figure 7.4: 3D motion profiles of a single participant from Study Design 1. Each plot shows the displacement of a marker placed on a specific anatomical point, recorded over a 30-second scan. A total of four recordings were performed as part of Study Design 1. The marker's displacement is represented along the three spatial coordinates (x, y, z), corresponding respectively to lateral (x), antero-posterior (y), and vertical (z) movement. Each axis is color-coded as follows: red for the x-axis, green for the y-axis, and blue for the z-axis.

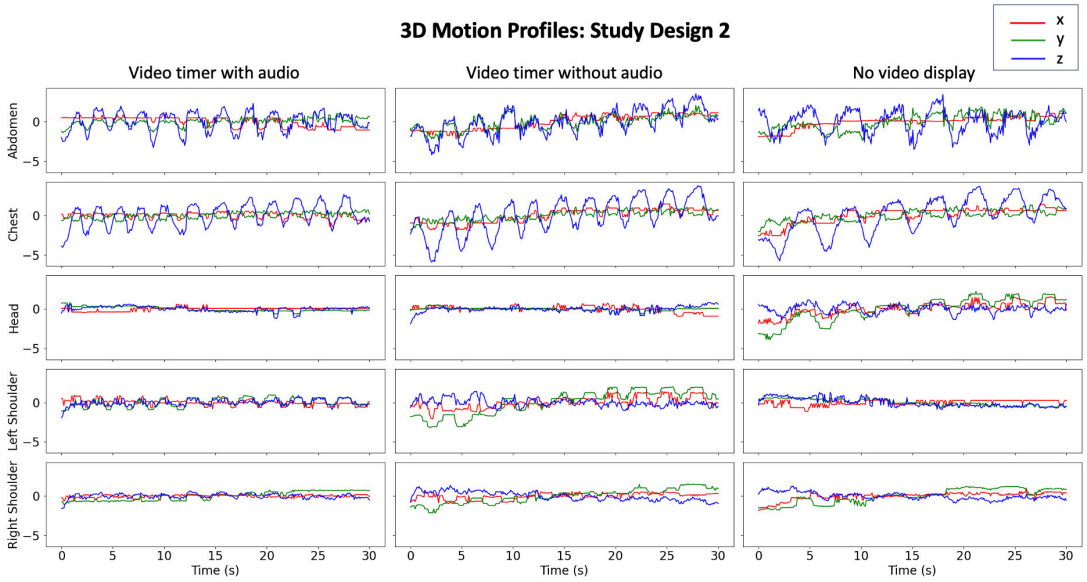

Figure 7.5: 3D motion profiles of a single participant from Study Design 2. Each plot shows the displacement of a marker placed on a specific anatomical point, recorded over a 30-second scan. A total of three recordings were performed as part of Study Design 2. The marker's displacement is represented along the three spatial coordinates (x, y, z), corresponding respectively to lateral (x), anteroposterior (y), and vertical (z) movement. Each axis is color-coded as follows: red for the x-axis, green for the y-axis, and blue for the z-axis.

7.2.2 Average Absolute Deviation

For both recording sequences tested in Study Designs 1 and 2, the Average Absolute Deviation (AAD) was computed for each marker based on the mean values for all subjects, as illustrated in Tables 7.1 and 7.2. This dispersion metric is indicative of the mean deviation of the motion data for the x,y and z coordinates of each marker from the corresponding mean value. The two experimental designs can be compared to evaluate the effects of different stimulus conditions and their presentation order on subject-to-subject variability in body motions.

Table 7.1: Average Absolute Deviation (mm) for each anatomical marker and spatial coordinate (X, Y, Z) across the four recording conditions evaluated in Study Design 1.

Marker	Coordinate	No video display (mm)	Video timer without audio (mm)	Video timer with audio (mm)	No video display again (mm)
Head	X	0.24 ± 0.2	0.31 ± 0.1	0.40 ± 0.4	0.34 ± 0.3
	Y	0.44 ± 0.2	0.49 ± 0.2	0.52 ± 0.3	0.49 ± 0.3
	Z	0.26 ± 0.1	0.33 ± 0.1	0.39 ± 0.2	0.36 ± 0.3
Left Shoulder	X	0.32 ± 0.2	0.34 ± 0.2	0.40 ± 0.2	0.37 ± 0.2
	Y	0.38 ± 0.2	0.44 ± 0.2	0.46 ± 0.1	0.43 ± 0.2
	Z	0.54 ± 0.5	0.60 ± 0.3	0.74 ± 0.5	0.60 ± 0.2
Right Shoulder	X	0.28 ± 0.1	0.33 ± 0.2	0.43 ± 0.2	0.35 ± 0.1
	Y	0.39 ± 0.2	0.49 ± 0.3	0.46 ± 0.3	0.41 ± 0.2
	Z	0.51 ± 0.3	0.72 ± 0.6	0.77 ± 0.5	0.66 ± 0.7
Chest	X	0.44 ± 0.3	0.49 ± 0.4	0.55 ± 0.3	0.55 ± 0.6
	Y	1.12 ± 0.7	1.02 ± 0.5	1.18 ± 0.7	1.01 ± 0.4
	Z	0.62 ± 0.3	0.60 ± 0.2	0.66 ± 0.3	0.55 ± 0.2
Abdomen	X	0.44 ± 0.2	0.60 ± 0.3	0.68 ± 0.4	0.56 ± 0.4
	Y	0.92 ± 0.4	0.90 ± 0.3	0.93 ± 0.4	0.87 ± 0.3
	Z	0.93 ± 0.4	0.93 ± 0.4	1.08 ± 0.9	0.91 ± 0.4

Table 7.2: Average Absolute Deviation (mm) for each anatomical marker and spatial coordinate (X, Y, Z) across the three recording conditions evaluated in Study Design 2.

Marker	Coordinate	Video timer with audio (mm)	Video timer without audio (mm)	No video display (mm)
Head	X	0.22 ± 0.1	0.26 ± 0.1	0.30 ± 0.2
	Y	0.34 ± 0.1	0.43 ± 0.3	0.45 ± 0.1
	Z	0.27 ± 0.2	0.28 ± 0.3	0.37 ± 0.3
Left Shoulder	X	0.25 ± 0.1	0.34 ± 0.1	0.29 ± 0.1
	Y	0.32 ± 0.1	0.33 ± 0.1	0.36 ± 0.1
	Z	0.48 ± 0.2	0.54 ± 0.3	0.50 ± 0.3
Right Shoulder	X	0.21 ± 0.1	0.30 ± 0.1	0.28 ± 0.0
	Y	0.37 ± 0.2	0.46 ± 0.3	0.36 ± 0.1
	Z	0.50 ± 0.3	0.57 ± 0.2	0.48 ± 0.2
Chest	X	0.29 ± 0.1	0.39 ± 0.2	0.35 ± 0.2
	Y	1.09 ± 0.4	1.13 ± 0.4	1.17 ± 0.4
	Z	0.50 ± 0.1	0.53 ± 0.1	0.56 ± 0.2
Abdomen	X	0.41 ± 0.2	0.51 ± 0.2	0.47 ± 0.3
	Y	1.13 ± 0.4	1.13 ± 0.4	1.14 ± 0.6
	Z	0.94 ± 0.5	0.93 ± 0.4	1.00 ± 0.4

7.2.3 Euclidean Distance Analysis

The third measurement was computed to make a comparison of the average motion (mm) across the five labeled anatomical points, organized along the x-axis, under different recording conditions. To facilitate this comparison, grouped bar charts were generated, where the height of each bar represents the extent of motion for each infrared marker. For each Study Design, the number of bars per marker position corresponds to the number of recordings performed by each participant, and, as before, each bar is color-coded, following the same color scheme applied in the previous analysis. Standard deviation is illustrated by error bars, included in the plot to show variability between subjects under each condition. The results of this analysis are presented in Figure 7.6 for Study Design 1 and Figure 7.7 for Study Design 2.

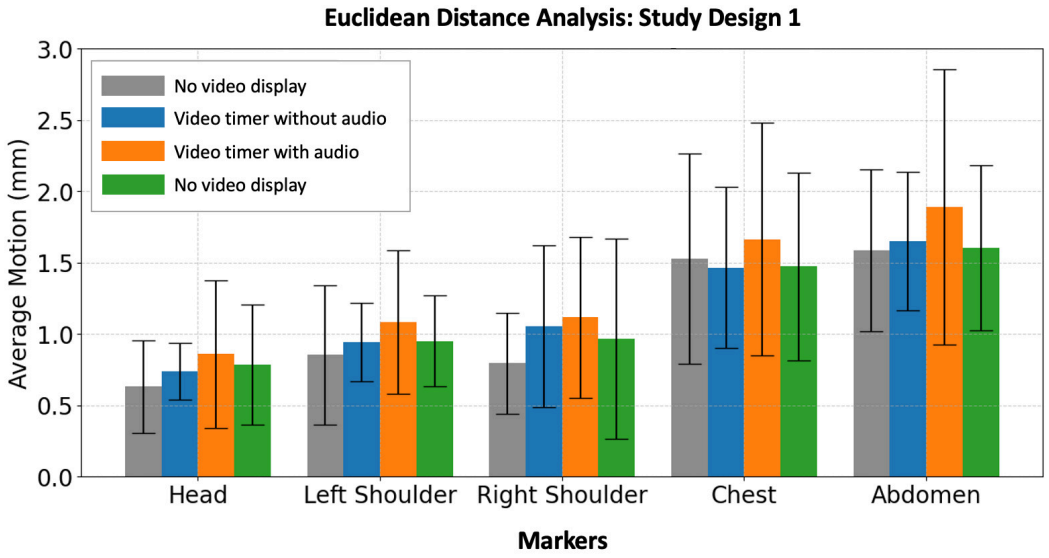

Figure 7.6: Average Euclidean distance (mm) for each marker under four recording conditions in Study Design 1. Each anatomical point is represented by four bars, each with a different color code based on the stimulus administered: grey for no video display, blue for video timer without audio, orange for video timer with audio, and green for no video display.

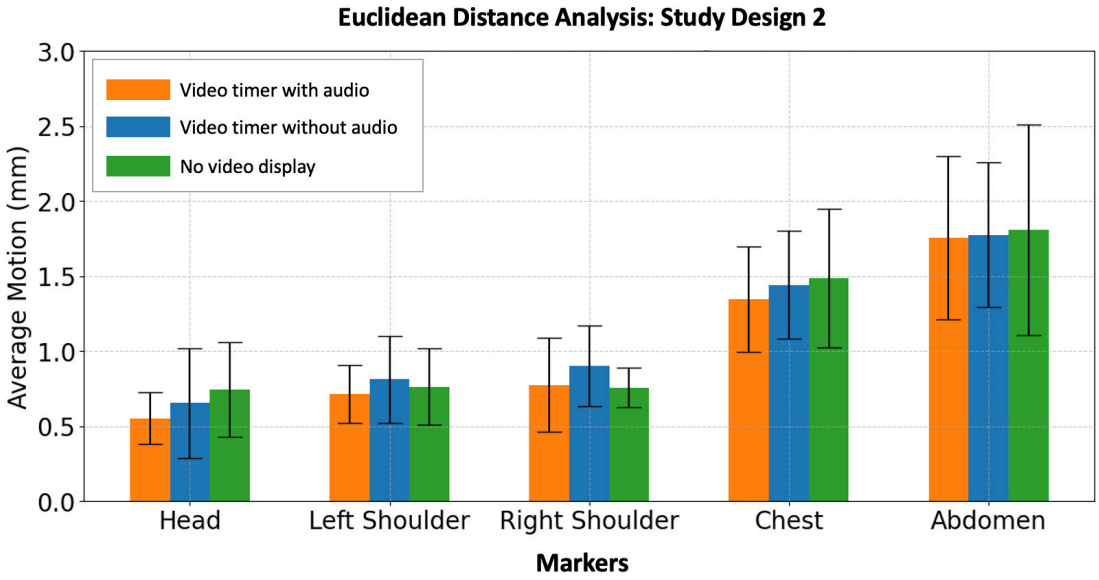

Figure 7.7: Average Euclidean distance (mm) for each marker under three recording conditions in Study Design 2. Each anatomical region is represented by three bars, each with a different colour code based on the stimulus administered: orange for video timer with audio, blue for video timer without audio, and green for no video display.

The potential impact of visual and auditory stimuli on participants' motion can be evaluated through this analysis. The comparison between Study Design 1 and Study Design 2 provides valuable information on the effect of the type of stimulus administered on participants' attention, as well as on the temporal order in which it is administered within the protocol.

7.2.4 Participant Motion Variability

To identify motion patterns across participants, scatter plots were generated using motion data collected during each recording session from both Study Design 1 and Study Design 2. Motion values (expressed in millimeters) are plotted according to the anatomical regions where markers were placed. For each region, the number of clusters reflects the number of recording conditions conducted for each Study. Each cluster contains data points, and each point represents each participant. As shown in Figure 7.8, Study Design 1 involved twenty participants. Accordingly, for each anatomical region, four clusters of twenty data points are displayed, each distinguished by a different color

representing one of the four recording conditions.

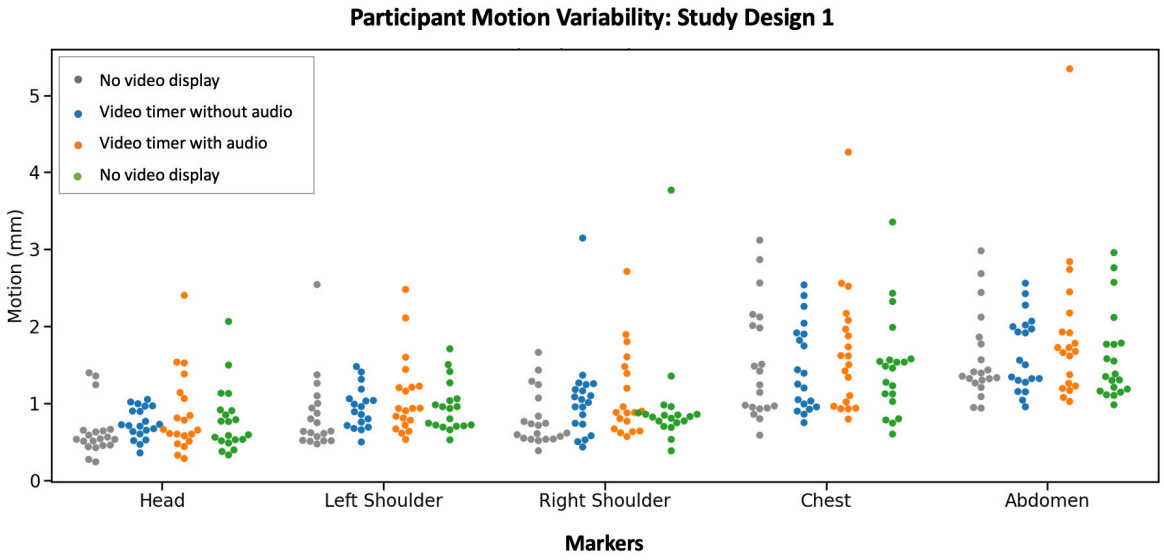

Figure 7.8: Analysis of motion variability on a set of 20 participants who took part in Study Design 1. Four different recording conditions are represented, each one marked by a different colour: no video display (grey), video timer without audio (blue), video timer with integrated audio track (orange) and no video display again (green).

Figure 7.9, on the other hand, presents the results obtained from Study Design 2, which involved eleven participants subjected to three different recording conditions.

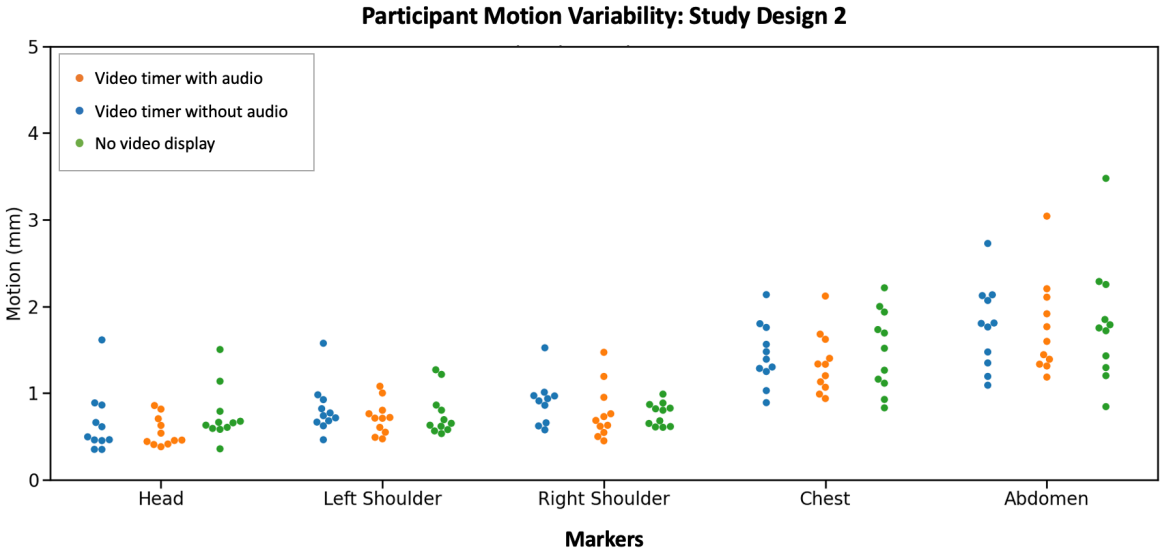

Figure 7.9: Analysis of motion variability on a set of 11 participants who took part in Study Design 2. Three different recording conditions are represented, each one marked by a different colour: video timer display with audio (orange), video timer without audio (blue), and no video display (green).

7.2.5 Participants Feedback

Following the final recording session, participants from both Study Design 1 and Study Design 2 were invited to provide feedback on their overall experience during the scanning procedure. Two considerations were given particular attention in the evaluation process. The first focuses on participants' perceived level of attention during the video timer projection, as compared to the recording session conducted in the absence of visual stimuli. The second focuses on the sense of guidance and concentration perceived when the timer video was accompanied by audio, in contrast to the timer video projected without sound. Furthermore, participants were encouraged to propose potential improvements to the video content, including modifications to the audio components, colour schemes, or textual elements.

Figure 7.10 presents a comparative assessment, in percentage terms, of the recording conditions most preferred by participants across both studies.

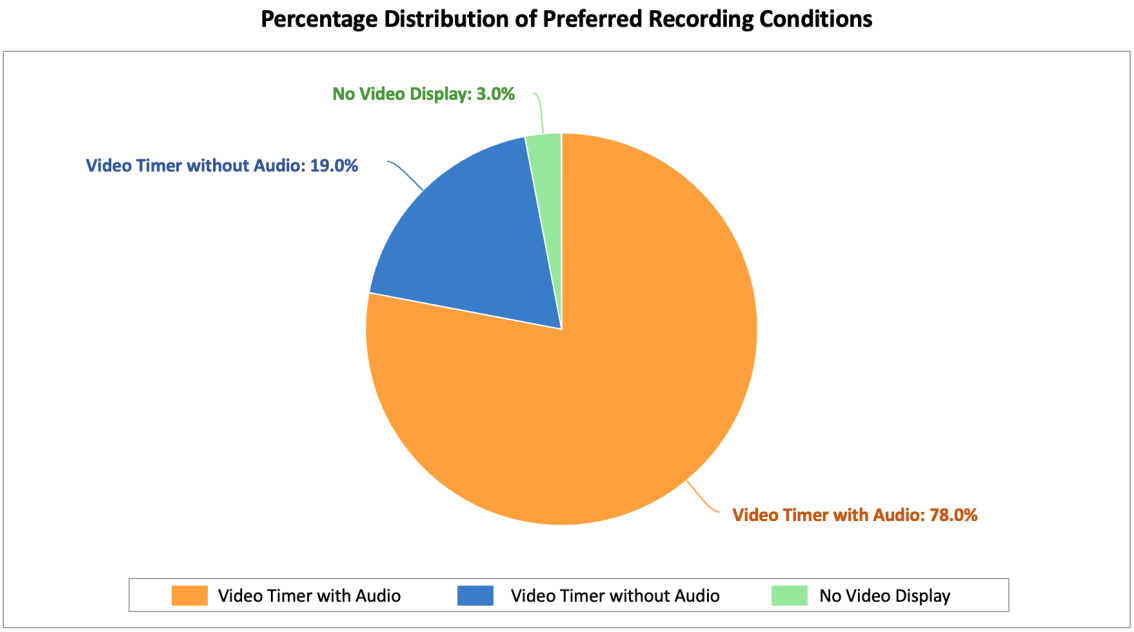

Figure 7.10: Percentage distribution of participants' preferences across different recording conditions in Study Design 1 and Study Design 2.

As illustrated in Figure 7.10, 78% of participants expressed a clear preference for the video timer with an integrated audio track. The primary reasons provided for this preference are outlined below:

- the presence of audio was found to enhance the sense of guidance, thereby improving participants' comprehension of the steps to be performed. Communication was perceived as both simple, effective, and immediately impactful;
- the integration of the audio track was considered useful especially for visually impaired people, improving accessibility to the examination;
- when combined with audio, the timer video altered participants' subjective time estimation, resulting in a perceived reduction in duration and an improved mental experience throughout the examination;

The option of the timer video without audio track was selected by 19% of the participants. The following reasons have been given for this preference:

- the absence of audio was not perceived as a disadvantage by some participants, who did not feel it was necessary to maintain concentration;

- it has been reported that the audio was sometimes experienced as a potential source of stress or anxiety during the scanning;
- it was noted by other participants that there were no significant differences between the two versions of the timer video with and without audio. However, the visual timer and the central red point designed for maintaining focus and stability were identified as beneficial, in contrast to the absence of visual stimuli;

Of the 31 participants, only one expressed a preference for no visual stimuli, finding the video projection too close and potentially distracting.
Suggestions and improvements collected at the end of each exam are listed below:

- extend the use of the audio track to include the 30 seconds of acquisition to ensure greater continuity between the pre-, during and post-scan phases;
- insert relaxing background music during the scan to create a calmer and more positive atmosphere;
- introduce a voice guide to inform the user about the elapsed time, thereby increasing patient's awareness;
- reduce the size of the central red dot to facilitate better visual focus;

7.3 Discussion

The motion analysis was structured around three principal areas of investigation.

The primary objective of the present study was to evaluate the effectiveness of the 30-second timer video, which was displayed in front of the participant during the WT-PET simulation. The investigation focused on determining whether the visualisation of a fixed red dot at the center of the screen could serve as a focal point, thereby enhancing visual attention and reducing involuntary movements compared to a baseline condition in which the simulation was performed without visual stimuli.

Subsequently, an enhanced version of the original setup was evaluated through the integration of an audio track synchronised with the video timer. The objective of this audiovisual configuration was to investigate the hypothesis that multisensory stimulation would enhance participants' perception of time, sense of stability, and level of concentration. Finally, the potential impact of stimulus administration order within the

recording session was evaluated, investigating the possible occurrence of bias in the study due to fatigue, loss of concentration, or postural adaptation.

The following discussion will be structured in line with the logical approach adopted in the analytical process. It initiates with the analysis of the data from Study Design 1, whose results did not align, as expected, with the initial hypotheses. The discussion then proceeds to the analysis of results of Study Design 2, which exhibited trends more consistent with the initial expectations and the feedback provided by participants. To conclude, a comparison is presented between the initial recording condition of Study Design 1 and 2. The purpose of this comparison is to provide clarification and confirm the influence that the order in which stimuli are administered exerts on the participants' motion.

7.3.1 Impact of stimuli on participants stability in Study Design 1

The results of Study Design 1 demonstrate that the administration of a visual stimulus (video timer without audio) did not result in a significant improvement in postural stability, as illustrated in Figure 7.6. This outcome diverges from the initial hypothesis. The mean Euclidean distance computed across five passive infrared markers (head, shoulders, chest, abdomen) did not demonstrate any statistically significant motion reduction relative to the baseline condition (no video display), with the exception of a slight motion reduction in chest (-0.06 mm). In contrast, the right shoulder exhibited a notable increase in movement (+0.26 mm).

The subsequent addition of an auditory stimulus (video timer with audio) did not result in any improvements in participants' stability. On the contrary, all anatomical markers exhibited an increase in mean Euclidean distance (+0.07 mm to +0.24 mm), with the most pronounced displacements observed at the chest and abdomen. This effect is likely attributable to a greater influence of diaphragmatic breathing. It is important to note that, despite the objective data indicating an increase in instability and lack of concentration in the subject, 78% of participants expressed a subjective preference for the audiovisual condition, considering it clearer and more intuitive. In contrast, only 3% of participants favored the baseline condition.

This discrepancy between subjective perception and objective performance suggests that the video timer with audio, while perceived as more engaging, may lead to greater inter-subjective variability in postural response. This is confirmed by the widening of the standard error bands depicted in Figure 7.6, and further supported by the scatter plot in

Figure 7.8, particularly in conditions involving the administration of stimuli (video timer with and without audio), with some particularly marked outliers in chest, abdomen, and shoulders.

7.3.2 Impact of stimulus delivery order

A significant element in the interpretation of the results is the potential bias that may have been introduced by the sequence in which the stimuli were administered. The audiovisual condition in Study Design 1 was always shown as the third recording after at least two minutes of standing upright position. This period included time for instructions, tests, and intermediate breaks. It can be hypothesised that fatigue, loss of attention, or postural adaptation may have negatively influenced the subject's performance during this condition.

In contrast, Study Design 2 presented the 30-second timer video with audio to each participant first. Under this condition, opposite results were observed: postural stability improved compared to the visual-only condition, with a reduction in mean Euclidean distances ranging from 0.07 mm to 0.13 mm, and a decrease in inter-subject variability, as shown in Figure 7.7. This finding is further supported by the lower AAD values observed in the video timer with audio condition when administered during the initial recording session (Study Design 2), as reported in Table 7.2. This reduction indicates greater effectiveness in limiting body motion variability, suggesting that the order in which the stimulus is presented influences the participant's attention response. Furthermore, the scatter plot in Figure 7.9 demonstrates a more compact distribution of data points during the audiovisual condition, suggesting a more consistent response across participants. These results lend support to the hypothesis that while the audiovisual stimulus does indeed improve postural stability, the order in which it is presented has a significant impact on its effectiveness. The results demonstrate that the audiovisual stimulus performs optimally when employed as the initial condition, a phenomenon that is likely attributable to reduced fatigue and enhanced attentional capacity.

To further support this hypothesis, a direct comparison was conducted between the first recordings from Study Designs 1 and 2. Figure 7.11 visually compares the average motion (mm) observed during the initial no-video display condition in Study Design 1 with the first video timer with audio condition in Study Design 2.

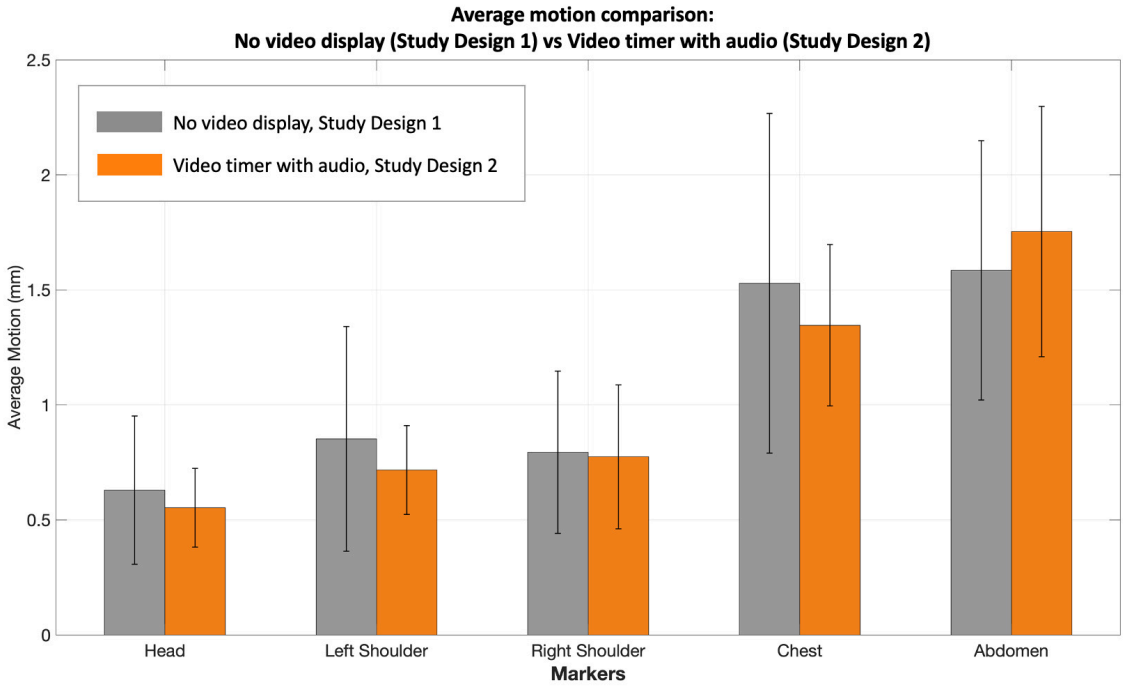

Figure 7.11: Comparison of Average Motion (mm) for each anatomical marker between the first recordings of Study Design 1 and Study Design 2. Each marker is represented by two bars, corresponding to different stimulus conditions: grey indicates the baseline condition (no video display, Study Design 1), while orange represents the audiovisual condition (video timer with audio, Study Design 2). This comparison illustrates the effect of stimulus type on postural stability at the initial recording stage.

In this comparison, four out of five anatomical markers showed reduced movement in the audiovisual condition (–0.06 mm to –0.18 mm), with a slight increase observed only at the abdominal marker (+0.16 mm). The results reinforce the hypothesis that the presentation of the audiovisual stimulus at the initial recording stage may promote greater focus and physical stability. The observed phenomenon, without considering stimulus order or adaptation to the task, lends further support to the hypothesis that the timer video with audio is the most effective tool among those tested. Therefore, the data obtained in Study Design 1 must be interpreted with caution: the apparent decline in performance during the audiovisual condition seems more attributable to temporal factors and postural fatigue than to the intrinsic ineffectiveness of the audiovisual stimulus itself. This analysis highlights the critical influence of the order in which stimuli are administered, confirming that it constitutes a significant source of bias that can have a substantial impact on study outcomes.

7.3.3 Impact of diaphragmatic breathing

The analysis of 3D markers' motion profile, illustrated in Figures 7.4 and 7.5 for a single participant, reveals significant variability across both experimental designs, with the most notable fluctuations observed in the chest and abdomen. The most pronounced oscillations along the y-axis outline a cyclical pattern consistent with the physiology of diaphragmatic breathing, characterised by periodic expansions and contractions of the abdominal wall. This interpretation is further supported by the average motion values of the corresponding markers, presented in Figures 7.6 and 7.7, and by the analysis of the AAD values reported in Tables 7.1 and 7.2, in which the anatomical points in question exhibit the highest AAD values for the y coordinate (anterior-posterior direction). In both Study Design 1 and Study Design 2, the chest and abdomen consistently exhibited a greater range of movement compared to the other anatomical regions analyzed.

Conversely, the markers applied to the head and shoulders exhibit a significant decrease in motion, consistent with the expectation of greater stability in upright positioning. The head, in particular, exhibits minimal displacement, likely due to the integration of the headrest within the WT-PET mock-up, which provides additional mechanical support.

This comparison highlights how the combination of audiovisual stimuli introduced during the initial acquisition results in the lowest recorded mean head displacement (0.55 mm), representing the most significant reduction in head motion across the entire sample.

7.3.4 Comparison with literature

To objectively quantify the reduction in upper body motion observed in the present study, a comparative analysis was conducted using data from a previously published study [1]. That study, involving twenty healthy volunteers under both normal and controlled breathing conditions, evaluated postural stability across three different PET scanner systems: (1) an initial prototype of the WT-PET scanner, (2) the current mock-up equipped with an integrated headrest and hand supports, and (3) a conventional PET scanner, the Siemens Biograph mCT scanner, used at the Department of Nuclear Medicine, Ghent University.

In order to ensure consistency and comparability, the present analysis focused specifically on comparing the mean Euclidean distance values recorded under the *Video timer with audio* condition in Study Design 2 of this work with those reported in Study 2A of [1], as both studies employed the same WT-PET mock-up configuration.

Table 7.3 presents a summary of the comparative data, offering a quantitative perspective on the improvements in postural stability achieved through audiovisual stimulation.

Table 7.3: Comparison of Average motion (mm) $\pm$ Standard Deviation between video timer with audio experimental condition in Study Design 2 and experimental measurements conducted at normal breathing and breath-hold conditions taken from [1]. For each marker position, the best result in terms of average motion is shown in bold.

Study condition	**Head**	**Left Shoulder**	**Right Shoulder**	**Chest**	**Abdomen**
Normal breathing	1.03 ± 0.6	1.12 ± 0.4	1.15 ± 0.5	1.99 ± 0.8	2.42 ± 1.1
Breath-hold	0.81 ± 0.4	1.04 ± 0.4	0.92 ± 0.3	$\mathbf{1.33 \pm 0.7}$	$\mathbf{1.67 \pm 1.1}$
Video timer with audio	$\mathbf{0.55 \pm 0.2}$	$\mathbf{0.72 \pm 0.2}$	$\mathbf{0.78 \pm 0.3}$	1.35 ± 0.4	1.75 ± 0.5

As shown in Table 7.3, a comparison between the average motion observed under normal breathing conditions, without any external stimulus, as reported in [1], and the results obtained from the most effective experimental condition in the present study (video timer with audio under normal breathing), reveals a clear improvement in postural stability.

Specifically, average head motion was reduced by approximately 47%, decreasing from 1.03 mm to 0.55 mm. Similarly, the left and right shoulders exhibited reductions of 36% and 32%, respectively. These improvements were accompanied by lower standard deviation values, indicating a more consistent effect across participants. These findings support the original hypothesis: the integration of a visual timer with synchronized audio and a fixed focal point leads to significantly enhanced postural stability when compared to a standard PET acquisition protocol.

Further comparison with the breath-hold condition examined in [1], in which participants suspended breathing for 30 seconds, also highlights the effectiveness of the audiovisual stimulus. Although the reduction in motion is less dramatic than in the previous comparison, the video timer with audio condition still achieved superior results for the head and shoulder markers. This suggests that the attention and stability induced by a well-designed audiovisual stimulus can even exceed the biomechanical effect of temporary respiratory suspension in certain upper body regions.

With regard to the chest and abdominal markers, the video timer with audio condition also demonstrated a reduction in average movement, although less marked than at

the anatomical points previously mentioned. This outcome was predictable, given the physiological prevalence of respiratory motion in these regions. In contrast to the effects on the head and shoulders, the chest and abdomen are more directly impacted by diaphragmatic breathing. This phenomenon is more effectively regulated under the parameters of a breath-hold protocol. This observation is consistent with the periodic motion patterns that were discussed earlier and visualised in the 3D motion profiles in Figures 7.4 and 7.5.

In conclusion, the utilisation of an audiovisual stimulus, such as a 30-second video timer with an integrated audio track, is a promising and clinically sustainable approach to enhancing patient stability, particularly in the upper body. This tool could be effective in avoiding the discomfort and compliance challenges associated with prolonged apnea, offering a non-invasive, patient-friendly, and repeatable method to enhance motion stability.

8

Concluding Remarks

This thesis investigated two of the primary challenges that still represent a significant limitation for the implementation of the novel Walk-Through PET scanner: the need for constant assistance from medical personnel during the patient positioning phase and the considerable upper body motion observed during upright scanning procedures. To address these issues, two interactive audiovisual products were developed: a 3D animated video guide and a 30-second timer video (with and without audio). While the former has finished the development and production stage, the latter was further validated through an experimental motion study conducted on a sample of 31 participants. This study evaluates the effectiveness of the timer video, with a visual focal red point and audio track integrated, in enhancing postural stability during the upright scan simulations conducted in the WT-PET mock-up.

Although the order in which the stimuli were administered influenced the experimental results, this factor does not represent a limitation in clinical practice. In an actual PET examination, the patient undergoes a single scan, which can be set directly to the optimal condition identified from this study. The data collected demonstrate that the video timer with audio, when presented as the initial condition, is the most effective tool for promoting postural stability during a WT-PET scan simulation. A direct comparison between the initial recordings of both Study Design 1 and 2 confirms the superiority of the latter, thus validating its integration into clinical protocols. This finding is further validated by comparison with the data reported in the study [1], especially under normal breathing condition.

Therefore, the results demonstrated the impact of the audiovisual stimulus in reducing upper body motion. This was evidenced by a 47% decrease in average head motion (from 1.03 millimetres to 0.50 millimetres), as well as a 36% and 32% reduction in right and left shoulder mobility, respectively. Moreover, the timer video with audio also out-

performed conventional controlled breathing techniques, underscoring its potential as a valid alternative to more invasive or complex procedures used to limit patient movement, such as apnoea.

However, further analysis revealed that, although participant average motion values were lower than the spatial resolution of the scanner (2 mm), which is undoubtedly beneficial, the chest and abdomen remain the areas most prone to respiratory artefacts (1.35 mm and 1.75 mm, respectively, in the *video timer with audio* condition). Based on these observations, to address this critical issue, the integration of audiovisual stimuli with a breathing control protocol, such as the one already tested and validated in the study cited, could be considered in order to combine the benefits of both techniques across all monitored anatomical areas.

Additional improvements in abdominal image quality could involve the integration of motion correction algorithms directly into the current WT-PET system and the design of new adjustable support components, such as the existing headrest, to enhance stability at the thoracic level. One potential application of this concept, which could represent a functional evolution of the WT-PET design, is the creation of a support structure with a cavity to accommodate the patient's torso, adaptable to the chest morphology and optimised for use in the upright position. However, it should be noted that this solution would require an additional manual adjustment step during patient positioning, potentially impacting the high patient throughput. Considering that one of the primary objectives of the MEDISIP group's proposal for an innovative vertical panels scanner is to optimise the daily patient flow, it will be essential to evaluate through new experimental studies how much this additional support improves effectiveness without compromising overall operational efficiency.

In conclusion, the 30-second timer video developed in this thesis represents a significant contribution towards improving the usability and efficiency of the current WT-PET prototype. The outcomes lay the foundation for future system optimisation, promoting its large-scale adoption in clinical settings.

In the future, it will be essential to assess the effectiveness and clarity of the 3D animated video guide as a supportive tool for patients during the preparation phase prior to scanning. This audiovisual product, designed to visually and clearly illustrate the four steps patients should autonomously carry out inside the scanner, represents a potentially innovative solution to reduce the workload and stress experienced by medical personnel in nuclear medicine departments. By promoting greater patient autonomy in understanding positioning instructions, this approach not only improves clinical ef-

ficiency but also contributes to a smoother and faster scanning procedure. Once the steps are understood, patients are able to replicate them quite independently within the vertical panel scanner, thereby minimizing downtime and the need for constant technician intervention. The combination of a more intuitive scanner system and the instructional video guide may therefore lead to significant positive outcomes, such as an increase in patient throughput, ultimately contributing to a more efficient and sustainable clinical workflow.

9

Ethical Reflections

This study was conducted in full compliance with established ethical guidelines for research involving human participants. All 31 healthy adult volunteers who participated in the study signed a written consent form prior to the start of the research activities. This consent form was obtained only after participants were thoroughly informed about the study's purpose, the procedures involved, how their data would be handled, and their right to withdraw at any time without consequence.

To ensure privacy protection, motion data were anonymized at the time of recording. No personally identifiable information was collected, stored, or reported. Although a depth camera was used to capture movement, no video was shared. Visual data were used exclusively for the extraction of anonymous numerical information relating to the movement of the markers. This information was then analysed and presented in the thesis through the use of graphs and tables. This choice is indicative of an ethically conscious approach that respects the privacy of the participants.

The recruitment process was conducted in accordance with principles of fairness and impartiality, ensuring that no form of discrimination based on gender, ethnicity, or other personal characteristics occured. Particular attention was given to inclusivity and equity in access to the study. A concrete example concerns a participant who was involved in Study Design 2 and who was not fluent in English. To facilitate complete comprehension of the instructions and procedures, a second version of the 30-second timer video was produced in Dutch. Furthermore, all information about the study's procedure was translated in Dutch with the assistance of an external collaborator to ensure that the subject was able to make an informed and voluntary decision to participate. This approach is indicative of a strong commitment to accessibility and respect for linguistic diversity, in accordance with the ethical principle of respect for the person.

Participants were not exposed to any physical risks, as the activities involved only walk-

ing inside the WT-PET scanner mock-up and independently positioning themselves within it, without the use of invasive instruments. Five passive motion-tracking markers were applied externally to each participant using adhesive, ensuring a completely non-invasive procedure.

Special ethical considerations were also applied to the development of the audiovisual tools, namely the video guide to assist patients in positioning themselves more independently within the scanner and the 30-second timer video. The animations in the 3D video guide have been created in a neutral, clear, and inclusive manner, with the intention of avoiding explicit references to gender, ethnicity, or body shape. Furthermore, in order to facilitate accessibility to a wider audience, subtitles, high-contrast images, and explanatory audio tracks have been included in both videos, with particular attention also paid to possible sensory disabilities (visual and auditory).

In conclusion, this study highlights the importance of responsible, inclusive, and privacy-conscious design in scientific research involving human subjects. Each stage of the project, from data collection to the production of digital materials, was methodically designed to guarantee respect for the individual, fairness of access, and the protection of sensitive information.

References

[1] R. Aziz, J. Maebe, F. M. Muller, Y. D'Asseler, and S. Vandenberghe, "Quantitative analysis of patient motion in walk-through pet scanner and standard axial field of view pet scanner using infrared-based tracking," *EJNMMI physics*, vol. 11, no. 1, p. 99, 2024.

[2] R. B. Workman Jr and R. E. Coleman, "Fundamentals of pet and pet/ct imaging," in *PET/CT: Essentials for Clinical Practice*. Springer, 2006, pp. 1–22.

[3] T. G. Turkington, "Introduction to pet instrumentation," *Journal of nuclear medicine technology*, vol. 29, no. 1, pp. 4–11, 2001.

[4] R. Lecomte, "Novel detector technology for clinical pet," *European journal of nuclear medicine and molecular imaging*, vol. 36, pp. 69–85, 2009.

[5] M. M. Khalil, Ed., *Basic Science of PET Imaging*, 1st ed. Cham, Switzerland: Springer, 2017.

[6] W. Sureshbabu and O. Mawlawi, "Pet/ct imaging artifacts," *Journal of nuclear medicine technology*, vol. 33, no. 3, pp. 156–161, 2005.

[7] W. V. Vogel, S.-d. Boer, M. Milou, S. M. Jansen, E.-J. Rijkhorst, B. de Wit-van der Veen, B. van der Hiel, A. J. Braat *et al.*, "Clinical benefits of lafov pet/ct in growing demand for molecular imaging," pp. 1–4, 2025.

[8] S. Vandenberghe, P. Moskal, and J. S. Karp, "State of the art in total body pet," *EJNMMI physics*, vol. 7, pp. 1–33, 2020.

[9] C. Mingels, F. Caobelli, A. Alavi, C. Sachpekidis, M. Wang, H. Nalbant, A. R. Pantel, H. Shi, A. Rominger, and L. Nardo, "Total-body pet/ct or lafov pet/ct? axial field-of-view clinical classification," *European journal of nuclear medicine and molecular imaging*, vol. 51, no. 4, pp. 951–953, 2024.

[10] C. Mingels, K. J. Chung, A. R. Pantel, A. Rominger, I. Alberts, B. A. Spencer, L. Nardo, and T. Pyka, "Total-body pet/ct: Challenges and opportunities," in *Seminars in Nuclear Medicine*. Elsevier, 2024.

[11] M. Dadgar, J. Maebe, M. Abi Akl, B. Vervenne, and S. Vandenberghe, "A simulation study of the system characteristics for a long axial fov pet design based on monolithic bgo flat panels compared with a pixelated lso cylindrical design," *EJNMMI physics*, vol. 10, no. 1, p. 75, 2023.

[12] E. M. Rohren, T. G. Turkington, and R. E. Coleman, “Clinical applications of pet in oncology,” *Radiology*, vol. 231, no. 2, pp. 305–332, 2004.

[13] J. S. Karp, S. Surti, M. E. Daube-Witherspoon, and G. Muehllehner, “Benefit of time-of-flight in pet: experimental and clinical results,” *Journal of Nuclear Medicine*, vol. 49, no. 3, pp. 462–470, 2008.

[14] H. N. Wagner Jr and P. S. Conti, “Advances in medical imaging for cancer diagnosis and treatment,” *Cancer*, vol. 67, no. S4, pp. 1121–1128, 1991.

[15] J. Cardinale, M. Schäfer, M. Benešová, U. Bauder-Wüst, K. Leotta, M. Eder, O. C. Neels, U. Haberkorn, F. L. Giesel, and K. Kopka, “Preclinical evaluation of 18f-psma-1007, a new prostate-specific membrane antigen ligand for prostate cancer imaging,” *Journal of Nuclear Medicine*, vol. 58, no. 3, pp. 425–431, 2017.

[16] U. Hennrich and M. Eder, “[68ga] ga-psma-11: the first fda-approved 68ga-radiopharmaceutical for pet imaging of prostate cancer,” *Pharmaceuticals*, vol. 14, no. 8, p. 713, 2021.

[17] W. W. Moses and M. Ullisch, “Factors influencing timing resolution in a commercial lso pet camera,” *IEEE Transactions on Nuclear Science*, vol. 53, no. 1, pp. 78–85, 2006.

[18] C. L. Wright, K. Binzel, J. Zhang, and M. V. Knopp, “Advanced functional tumor imaging and precision nuclear medicine enabled by digital pet technologies,” *Contrast Media & Molecular Imaging*, vol. 2017, no. 1, p. 5260305, 2017.

[19] A. Z. Kyme and R. R. Fulton, “Motion estimation and correction in spect, pet and ct,” *Physics in Medicine & Biology*, vol. 66, no. 18, p. 18TR02, 2021.

[20] J. van Sluis, R. Borra, C. Tsoumpas, J. H. van Snick, M. Roya, D. Ten Hove, A. H. Brouwers, A. A. Lammertsma, W. Noordzij, R. A. Dierckx *et al.*, “Extending the clinical capabilities of short-and long-lived positron-emitting radionuclides through high sensitivity pet/ct,” *Cancer Imaging*, vol. 22, no. 1, p. 69, 2022.

[21] G. J. Cook, I. L. Alberts, T. Wagner, B. M. Fischer, M. S. Nazir, and D. Lilburn, “The impact of long axial field of view (lafov) pet on oncologic imaging,” *European Journal of Radiology*, p. 111873, 2024.

[22] A. H. Dias, K. F. Andersen, M. Ø. Fosbøl, L. C. Gormsen, F. L. Andersen, and O. L. Munk, “Long axial field-of-view pet/ct: New opportunities for pediatric imaging,” in *Seminars in nuclear medicine*. Elsevier, 2024.

[23] S. Katal, L. S. Eibschutz, B. Saboury, A. Gholamrezanezhad, and A. Alavi, “Advantages and applications of total-body pet scanning,” *Diagnostics*, vol. 12, no. 2, p. 426, 2022.

[24] R. J. Hicks, R. E. Ware, and J. Callahan, “Total-body pet/ct: pros and cons,” in *Seminars in Nuclear Medicine*. Elsevier, 2024.

[25] G. Liu, Y. Gu, M. Sollini, A. Lazar, F. L. Besson, S. Li, Z. Wu, L. Nardo, A. Al-Ibraheem, J. Zheng *et al.*, “Expert consensus on workflow of pet/ct with long axial field-of-view,” *European Journal of Nuclear Medicine and Molecular Imaging*, pp. 1–12, 2024.

[26] T. S. Martinez-Lucio, O. I. Mendoza-Ibañez, W. Liu, S. Mostafapour, Z. Li, L. Providência, G. S. de Souza, P. Mohr, M. M. Dobrolinska, B. van Leer *et al.*, “Long axial field of view pet/ct: Technical aspects in cardiovascular diseases,” in *Seminars in Nuclear Medicine*. Elsevier, 2024.

[27] R. H. Slart, C. Tsoumpas, A. W. Glaudemans, W. Noordzij, A. T. Willemsen, R. J. Borra, R. A. Dierckx, and A. A. Lammertsma, “Long axial field of view pet scanners: a road map to implementation and new possibilities,” *European journal of nuclear medicine and molecular imaging*, vol. 48, no. 13, pp. 4236–4245, 2021.

[28] H. C. Verduzco-Aguirre, G. Lopes, and E. Soto-Perez-De-Celis, “Implementation of diagnostic resources for cancer in developing countries: a focus on pet/ct,” *ecancermedicalscience*, vol. 13, p. ed87, 2019.

[29] L. Filippi, A. Dimitrakopoulou-Strauss, L. Evangelista, and O. Schillaci, “Long axial field-of-view pet/ct devices: are we ready for the technological revolution?” *Expert Review of Medical Devices*, vol. 19, no. 10, pp. 739–743, 2022.

[30] Global Banking & Finance Review. (2024) Global banking & finance review. [Online]. Available: https://www.globalbankingandfinance.com/

[31] S. Vandenberghe, F. M. Muller, N. Withofs, M. Dadgar, J. Maebe, B. Vervenne, M. A. Akl, S. Xue, K. Shi, G. Sportelli *et al.*, “Walk-through flat panel total-body pet: a patient-centered design for high throughput imaging at lower cost using doi-capable high-resolution monolithic detectors,” *European journal of nuclear medicine and molecular imaging*, vol. 50, no. 12, pp. 3558–3571, 2023.

[32] M. Dadgar, J. Maebe, and S. Vandenberghe, “Evaluation of lesion contrast in the

walk-through long axial fov pet scanner simulated with xcat anthropomorphic phantoms," *EJNMMI physics*, vol. 11, no. 1, p. 44, 2024.

[33] S. Vandenberghe, M. Abi Akl, N. Withofs, F. M. Muller, J. Maebe, M. Dadgar, S. Xue, K. Shi, G. Sportelli, and N. Belcari, "Efficient patient throughput and detector usage in low cost efficient monolithic high resolution walk-through flat panel total body pet," in *Total-Body PET 2022*, 2022, pp. 28–29.

[34] B. Vervenne, J. Maebe, and S. Vandenberghe, "Feasibility study of a rectangular ct geometry for high throughput total-body pet-ct," in *8th International Conference on Image Formation in X-Ray Computed Tomography*, 2024, pp. 272–275.